6th Conference on Impedance-Based Cellular Assays

IBCA

2025

September 17th – 19th, 2025
in Regensburg

Welcome to the
6th Conference on Impedance-Based Cellular Assays

Dear Participants of IBCA2025;

It is with great pleasure that we welcome you to the **6th Conference on Impedance-Based Cellular Assays**, hosted on the beautiful campus of the University of Regensburg. We are delighted to see almost 100 colleagues, researchers, and friends joining us from around the world to share their latest insights, exchange ideas, and strengthen the collaborative spirit that drives this exciting and rapidly evolving field.

This conference marks a special occasion, as it is the third time that Regensburg has the honor of hosting this meeting. Following our most recent IBCA gathering in Aachen in 2023, we are proud to continue the tradition of providing a dedicated platform for scientific exchange on impedance-based technologies and their applications in cellular research.

We are especially pleased to note the truly **international diversity of our participants**, who have traveled from many corners of the globe — including as far afield as **Argentina, Northern Scotland, Taiwan, and Canada**. This rich mix of perspectives and experiences will surely enhance the discussions and collaborations that emerge during our time together.

This year's meeting also offers us a moment of reflection. We remember with gratitude **Dr. Ivar Giaever**, one of the **inventors of impedance-based cellular assays**, whose pioneering work laid the foundation for the methods and applications that bring us together today. While we mourn his passing, we also celebrate his lasting scientific legacy, which continues to inspire innovation and collaboration across our community.

Over the coming days, you can look forward to a rich and stimulating program that includes **20 keynote presentations** from distinguished speakers, complemented by a wide range of contributions from participants across academia and industry in form of posters and short talks. Together, these presentations will highlight both fundamental advances and new applications, underscoring the growing impact of impedance-based approaches on cell biology, drug discovery, and biomedical engineering.

We would also like to take this opportunity to **express our sincere gratitude to the 12 companies and institutions supporting this conference through their generous sponsorship**. Each of these organizations plays an important role in advancing impedance-based cellular assays, and their contributions help us to create an inspiring environment for scientific exchange.

This meeting is also an opportunity to connect on a more personal level. We are pleased to invite you to two special social events: an informal **barbecue evening**, perfect for networking in a relaxed atmosphere, and the more festive **conference dinner at Regensburg's historic Salzstadl**, offering a memorable setting next to one of the city's most iconic landmarks, the stony bridge.

We sincerely thank all speakers, participants, and sponsors who have contributed to this conference. We wish you an inspiring and enjoyable time here in Regensburg - may it be filled with fruitful discussions, new perspectives, and lasting connections.

With warm regards,
Joachim Wegener and team

IBCA 2025 relies on the financial support of our sponsors. We gratefully acknowledge financial support by the companies and organizations listed below for providing the resources to organize this meeting. Thank you very much!!!

Applied BioPhysics

nanoAnalytics

nan]i[on

cellasys

scio spec

Amphasys

innoME

AXION BIOSYSTEMS
Imagine · Explore · Discover

DUNN

OLS
OMNI Life Science

Fraunhofer EMFT

REGENSBURGER UNIVERSITÄTS STIFTUNG HANS VIELBERTH

Scientific Program

Wednesday, September 17th 2025

Session 1		**Signal Transduction**
Chair:		**Joachim Wegener**
10:00 – 10:30		**Welcome**
10:30 – 11:00	**KN 1.1**	**Scott Boitano (Tuscon, USA):** Using Impedance in Asthma Drug Discovery: Protease-Activated Receptor-2 Antagonist Identification, Development and Application
11:00 – 11:30	**KN 1.2**	**Julia Erl (Regensburg, Germany):** Revealing Cellular Signaling Dynamics with Light-Activated Molecules: From Receptor Ligands to Second Messenger
11:30 – 11:45	**ST 1.1**	**Philipp Schwenk (Regensburg, Germany):** Correlation between label-free impedance analysis and Ca^{2+} fluorescence in vitro imaging
11:45 – 12:00	**ST 1.2**	**Michael Schaffer (Regensburg, Germany):** Dual Monitoring of impedance-based assessment of barrier function and NF-kB reporter signaling in Caco-2 intestinal inflammation model
12:00 – 13:00		**Lunch**
Session 2		**New Electrode Materials**
Chair:		**N.N.**
13:00 – 13:30	**KN 2.1**	**Kannan Balasubramanian (Berlin, Germany):** Soft Graphene Electrodes and Screen-Printed Carbon Electrodes for Monitoring Cell Adhesion Using Non-Faradaic Electrochemical Impedance Spectroscopy
13:30 – 14:00	**KN 2.2**	**Vivek Pachauri (Aachen, Germany):** Metal-Organic Frameworks based Electrochemical Interfaces for advanced Bioelectronics platforms
14:00 – 14:30	**KN 2.3**	**Stefanie Michaelis (Regensburg, Germany):** PEDOT/PSS as transparent, low cost electrode material for impedance-based cell analysis

Session 3		**Single Cell Analysis**
Chair:		**N.N.**
14:30 – 15:00	**KN 3.1**	**Sven Ingebrandt (Aachen, Germany):** Downscaling Electric Cell-substrate Impedance Sensing: What can transistor devices contribute?
15:00 – 15:30	**KN 3.2**	**Marco di Berardino (Lucerne, Switzerland):** Impedance Unplugged: Do Single Cells in Suspension Tell a Different Story?
15:30 – 15:45	**ST 3.1**	**Andreas Dietzel (Braunschweig, Germany):** Impedance flow cytometry for electrogenic microorganism
15:45 – 16:00	**ST 3.2**	**Osama Alalul (Braunschweig, Germany):** Biomechanics of single cells using a microfluidic device to correlate transients of flow impedance and electrical impedance
16:00 – 18:00		**Coffee & Poster Session 1**
18:00		**Barbecue at Venue**

Thursday, September 18th 2025

Session 4		**Epithelial Barrier Function**
Chair:		**Joachim Wegener**
08:30 – 09:00	**KN 4.1**	**Roisin Owens (Cambridge, UK):** Electrical impedance spectroscopy at the service of complex tissue models
09:00 – 09:30	**KN 4.2**	**Craig Simmons (Toronto, Canada):** Porous membrane electrical cell-substrate impedance sensing for barrier-on-chip modeling
09:30 – 09:45	**ST 4.1**	**Ina Carmans (Leuven, Belgium):** Combining TEER and high resolution spatial impedance mapping on porous MEA for improved in vitro barrier measurements
09:45 – 10:00	**ST 4.2**	**Rachana Archarya (Cambridge, UK):** A versatile, biomimetic, 3D electrochemical device for monitoring cell growth and epithelial barrier integrity
10:00 – 10:30		**Coffee & Refreshments**
Session 5		**Impedance Integration in Complex in vitro Models**
Chair:		**N.N.**
10:30 – 11:00	**KN 5.1**	**Peter Ertl (Vienna, Austria):** Vienna Calling - Innovations in Impedance-based analytical microsystems as advanced organs-on-a-chips
11:00 – 11:30	**KN 5.2**	**Massimo Mastrangeli (Delft, Netherlands):** Integrated sensing in microphysiological systems: the key role of microelectrode arrays
11:30 – 11:45	**ST 5.1**	**Tobias Naber (Regensburg, Germany):** Impedance-based monitoring of two cell monolayers co-cultured without physical contact (cis-TER)
11:45 – 12:45		**Lunch**

12:45 – 13:15	**KN 5.3**	**Pierre Bagnaninchi (Edinburgh, UK):** Towards 3D Cell Behavior Monitoring with advanced Electrical Impedance Tomography reconstruction
13:15 – 13:30	**ST 5.2**	**Babu Linkoon Meenaketan (Leuven, Belgium)** Advancing 3D impedance tomography for in vitro models

Session 6		**Monitoring Plasma Membrane Processes**
Chair:		**N.N.**
13:30 – 14:00	**KN 6.1**	**Anne-Kathrin Grimm (Regensburg, Germany):** A virus-free impedance platform to emulate virus-induced cell fusion
14:00 – 14:30	**KN 6.2**	**Ann-Sophie Kittel (Freiburg, Germany):** Monitoring of pore-forming toxin activity in live cells using high-throughput impedance assays

14:30 – 16:00	**Coffee & Poster Session 2**

16:00 – 18:00	**Sponsors´ Session**
16:00 – 16:10	AmphaSys AG (Sui)
16:10 – 16:20	Applied BioPhysics Inc. (USA)
16:20 – 16:30	Axion Biosystems Inc. (USA)
16:30 – 16:40	cellasys GmbH (G)
16:40 – 16:50	Dunn Labortechnik GmbH (G)
16:50 – 17:00	innoMe GmbH (G)
17:10 – 17:20	nanion Technologies GmbH (G)
17:20 – 17:30	nanoAnalytics GmbH (G)
17:30 – 17:40	OMNI Life Science GmbH (G)
17:40 – 17:50	Sciospec GmbH (G)

19:00	**Conference Dinner "Salzstadl Regensburg"**

Friday, September 19th 2025

08:30 – 08:45		**In Memoriam Ivar Giaever**
Session 7		**Advanced Analysis of Cell Dynamics**
Chair:		**Joachim Wegener**
08:45 – 09:15	**KN 7.1**	**Andreas Janshoff (Göttingen, Germany):** Cell-substrate-fluctuations enable fast and coherent collective migration
09:15 – 09:45	**KN 7.2**	**Abdul Barakat (Paris, France):** Monitoring of Cellular Spatiotemporal Dynamics via Machine Learning-Enhanced Electrical Impedance Spectroscopy
09:45 – 10:00	**ST 7.1**	**Bo Tang (Braunschweig, Germany):** Smart membrane: An on-chip cell sensor for monitoring barrier tissue supported by artificial neural networks
10:00 – 10:30		**Coffee & Refreshments**
Session 8		**Devices & Data Modelling**
Chair:		**N.N.**
10:30 – 11:00	**KN 8.1**	**Fabian Bonetto (Cuyo, Argentina):** A device to measure electrical impedance sensing: An objective device tool to discriminate dry eye, penfigoid and Sjogren diseases
11:00 – 11:30	**KN 8.2**	**Chun-Min Lo (Taipei, TW):** Cell–Electrode Models for Impedance Analysis of Epithelial and Endothelial Monolayers Cultured on Microelectrodes
11:30 – 11:45	**ST 8.1**	**Esteban Acerbo (Cuyo, Argentina):** Finite Difference Model Representing Cell Distribution in Monolayer
11:45 – 12:00	**ST 8.2**	**Uwe Pliquett (Heiligenstadt, Germany):** Concept for high channel systems for cell sensing
12:00 – 13:00		**Lunch Break**

Session 9		**Impedance-Based Phenotypic Assays**
Chair:		**N.N.**
13:00 – 13:30	**KN 9.1**	**Ziyu Gao (Aachen, Germany):** Impedance in real-time monitoring of trophoblast spheroid invasion dynamics and future applications
13:30 – 14:00	**KN 9.2**	**Arto Heiskanen (DTU, Denmark):** Impedance spectroscopy as a tool for real-time assessment of stem cell differentiation – a case study using neural stem cells
14:00 – 14:15	**ST 9.1**	**S. Knafl (Wien, Austria):** Impedance-guided Evaluation of Cancer Therapy: A new route for personalized medicine?
14:15 – 14:30	**ST 9.2**	**Sandra Friedrich (Regensburg, Germany):** Ready-to-use insect cell-based sensor for pesticide testing
14:30		**Farewell**

Oral Presentations

Using Impedance in Asthma Drug Discovery: Protease-Activated Receptor-2 Antagonist Identification, Development and Application

S. Boitano; T. Le, S. Gillman; H.V. Schiff; R. Plett; C. Weber and K.A. DeFea

University of Arizona, Tucson (United States)
sboitano@arizona.edu

Protease-activated receptor-2 (PAR2) is a G protein-coupled receptor associated with a variety of inflammatory diseases including asthma. PAR2 activation by proteases *in vivo* can elicit physiological or pathological responses that are mediated by β-arrestin/mitogen activated protein kinase (β-arrestin/MAPK) and/or Gq-protein/Ca^{2+} (Gq/Ca^{2+}) signaling. PAR2-dependent β-arrestin/MAPK signaling has been implicated in the development of several asthma associated indicators in pre-clinical animal models including airway hyperresponsiveness, inflammation and mucus overproduction. The multiple signaling pathways that follow PAR2 activation and the unique protease cleavage which elicits a “tethered ligand” result in uniquely difficult barriers to drug discovery. We have used impedance-based cellular screening as a primary assay to develop potent PAR2 agonists and efficacious PAR2 antagonists. PAR2 ligands that demonstrate reduction of impedance-based cellular response following activation by potent (e.g., 2-aminothiazole-LIGRL-NH_2) or natural (e.g., trypsin and elastase) PAR2 agonists are further evaluated for biased-ligand signaling *in vitro*. One full antagonist (C391) and three β-arrestin/MAPK-biased antagonists (C781, C937 and C957) have been moved to pre-clinical evaluation. Using a forced oscillation technique that requires impedance monitoring (flexiVent, SciReq, Canada), these four antagonists have been shown to be effective in preventing the development of airway hyperresponsiveness following allergen challenge of mice expressing mouse [1,2] and/or human PAR2 [3]. Impedance-based cellular assays provide a key resource in developing unique G protein-coupled receptor antagonists that can move forward in drug discovery.

References:

[1] S. Gillman, HV Schiff, M Kume, EC Sandoval, WP Pederson, RD Hellinger, T Le, BD Rivera, G Dussor, J Vagner, JG Ledford, TJ Price, KA DeFea and S Boitano. Acute allergen responses to human protease-activated receptor-2 is limited by the β-arrestin biased antagonist C781. *In review* 2025.

[2] CM Rivas, MC Yee, KJ Addison, M Lovett , K Pal, JG Ledford, G Dussor, TJ Price, J Vagner, KA DeFea, and S Boitano. Novel proteinase-activated receptor-2 (PAR2) antagonist C391 inhibits Alternaria-induced human airway epithelial signaling in vitro and asthma indicators in acute exposure murine models. *Br J Pharmacol* 2021.

[3] HV Schiff, CM Rivas, WP Pederson, EC Sandoval, S Gillman, J Prisco, M Kume, G Dussor, J Vagner, JG Ledford, TJ Price, KA DeFea, and S Boitano. β-arrestin-biased proteinase-activated receptor-2 antagonist C781 limits allergen-induced airway hyperresponsiveness and inflammation. *Br J Pharmacol* 180: 667-680, 2023

Revealing Cellular Signaling Dynamics with Light-Activated Molecules: From Receptor Ligands to Second Messenger

J. Erl[1]; C. Haag[1]; B. König[1]; J. Wegener[1,2]

[1] Faculty of Chemistry and Pharmacy, University of Regensburg, 93053 Regensburg (Germany)
[2] Fraunhofer Research Institution for Microsystems and Solid State Technology EMFT, Division Cell-Based Sensor Technology, 93053 Regensburg (Germany)
julia.erl@chemie.uni-regensburg.de

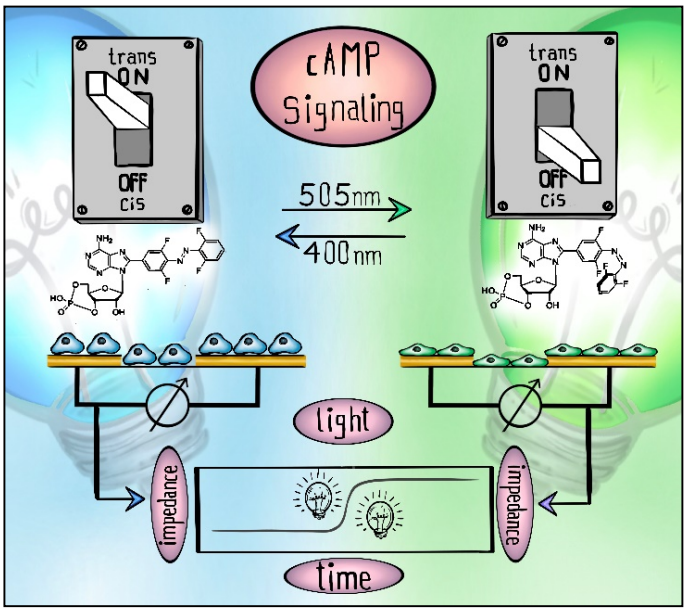

Figure 1. Schematic illustration of the measurement principle. Cells cultured on gold-film electrodes are stimulated with photochromic molecules, such as cAMP derivatives. Light-induced conformational changes in these molecules modulate cellular signaling, leading to alterations in cell shape that are detected as changes in the impedance signal.

Decoding the spatiotemporal dynamics of G protein–coupled receptor (GPCR) signaling remains a major challenge in cell biology. Classical pharmacological approaches often fail to capture the reversible and dynamic nature of these pathways. To overcome this, we employed photoresponsive molecules as optical triggers in combination with impedance-based readouts. At the receptor level, photoswitchable ligands for the neuropeptide Y4 receptor enabled precise, light-controlled GPCR activation. [1]

A novel two-electrode ECIS configuration further allowed localized stimulation within a single well and simultaneous monitoring of cellular responses. Downstream in the same pathway, photochromic derivatives of cyclic adenosine monophosphate (cAMP) were synthesized to directly modulate a key second messenger and assess its role in shaping signaling output. [2].

These optically controllable molecules, combined with real-time impedance measurements, provide unprecedented temporal and spatial resolution for dissecting GPCR-mediated signal transduction.

References:

[1] J. Erl, U. Wirth, S. Azzam, C. Höring, M. Skiba, R. Singh, K. Hochmuth, M. Keller, J. Wegener, B. König, *Angew. Chem. Int. Ed.* 62 (2023) e202215547.

[2] C. Haag, J. Erl, K. Helbig, J. Wegener, B. Koenig, *ChemRxiv*, (2024); 10.26434/chemrxiv-2024-cq5rz

Correlation between label-free impedance analysis and Ca^{2+} fluorescence *in vitro* imaging

P. Schwenk; J. Erl; A-K. Grimm; J. Wegener; J. Schlossmann

Department of Pharmacology and Toxicology, University of Regensburg, Regensburg (Germany)
philipp.schwenk@ur.de

There are several approaches for investigating and unraveling GPCR-dependent signaling pathways using cell-based assays. You can choose between label-based and label-free measurement methods. One of the more modern label-based fluorescence indicators is the popular and frequently used genetically encoded calcium indicator GCaMP [1], which can be utilized to measure intracellular Ca^{2+} levels. Since Ca^{2+} is a crucial second messenger involved in various cellular mechanisms and signaling pathways, the GCaMP sensor can be applied to investigate GPCR-dependent signaling cascades. In addition to label-based methods, label-free, non-invasive measurement methods can also be used to detect possible GPCR activation, such as by measuring impedance, also known as ECIS (electric cell-substrate impedance sensing). In the ECIS assay, any change in cell shape results in a change in the measured impedance [2]. Since GPCR activation can lead to a remodeling of the actin cytoskeleton [3], this label-free measurement method is also well-suited for investigating GPCR pharmacology. Although these two different measurement methods (GCaMP and ECIS) are often used independently, there are no scientific studies yet that use both assay approaches and investigate how and to what extent the results of these two methods correlate. If a strong correlation exists, combining Ca^{2+} fluorescence imaging with label-free impedance analysis has great potential for analyzing and deciphering GPCR signaling pathways more holistically, considering multiple perspectives. To investigate a possible correlation between the different approaches and their results, HEK293T cells were first transiently transfected with a plasmid of the Ca^{2+} sensor pN1-GCaMP6m-XC [4] and an empty vector, then incubated for 40–48 hours. The cells were subsequently preincubated with various inhibitors or chelators (FR900359 [Gq inhibitor], thapsigargin [SERCA inhibitor], BAPTA-AM [Ca^{2+} chelator], and Y-27632 [Rho kinase inhibitor]) at different concentrations before being stimulated with ATP to activate the GPCR signaling pathway. The measurement data of fluorescence and impedance signals were finally compared. In both label-based Ca^{2+} fluorescence imaging and label-free impedance analysis, the various inhibition approaches of the GPCR signaling pathway and changes in intracellular Ca^{2+} concentration after ATP stimulation are similarly well recognizable, making the results obtained highly consistent and reproducible. The combined use of Ca^{2+} fluorescence imaging and label-free impedance analysis thus offers enormous potential for analyzing and deciphering various GPCR signaling pathways more holistically, considering multiple perspectives.

References:

[1] Nakai, J.; Ohkura, M. and Imoto, K. A high signal-to-noise Ca2+ probe composed of a single green fluorescent protein. *Nat Biotechno*l **19**, 137–141 (2001).

[2] Lieb, S.; Michaelis, S. and Wegener, J. Label-free versus conventional cellular assays: Functional investigations on the human histamine H1 receptor. *Pharmacological Research* **114**, 13–26 (2016).

[3] Cotton, M. and Claing, A. G protein-coupled receptors stimulation and the control of cell migration. *Cellular Signalling* **21**, 1045–1053 (2009).

[4] Yang, Y.; Liu, N. and Liu, X. Improved calcium sensor GCaMP-X overcomes the calcium channel perturbations induced by the calmodulin in GCaMP. *Nat Commun* **9**, 1504 (2018).

Dual Monitoring of Impedance-Based Barrier Function and NF-κB Reporter Signaling in a Caco-2 Intestinal Inflammation Model

M. Schaffer and J. Heilmann

Department of Pharmaceutical Biology, University of Regensburg, Regensburg (Germany)
michael.schaffer@ur.de

Chronic inflammatory bowel disease (CIBD) is associated with factors such as the microbiome, genetics, and environmental influences. However, a dysregulated immune response, including cytokine signaling, and impaired intestinal barrier function are especially contributing to disease pathogenesis [1]. Besides interleukin-1β (IL-1β) and interferon-γ (IFN-γ), tumor necrosis factor-α (TNF-α) is particularly known for its critical role in regulating intestinal inflammation and is therefore a key target for biological therapies in CIBD [2]. However, TNF-α signaling in intestinal epithelial cells (IECs) is pleiotropic, contributing not only to pathological processes but also to the maintenance of intestinal homeostasis [3,4].
The transcription factor NF-κB is a key transducer of TNF-α and IL-1β signaling [5]. To monitor its activation over time, we developed a stable Caco-2 reporter cell line expressing a secreted luciferase. In combination with impedance spectroscopy, this system enables simultaneous monitoring of NF-κB activity and barrier function during cytokine-induced inflammation in a differentiated Caco-2 intestinal model (see Figure 1). Interestingly, IL-1β did not influence transepithelial electrical resistance (TEER), but increased NF-κB activation. While TNF-α alone had minimal impact on IEC barrier function, IFN-γ led to an initial TEER increase. Co-treatment revealed synergistic TEER breakdown after the initial increase. As NF-κB activity was not significantly altered by co-stimulation with IFN-γ, additional signaling pathways might be involved. Furthermore, IFN-γ stimulation was direction-independent, whereas TNF-α stimulation showed higher sensitivity of the basolateral membrane.
Our model provides valuable insights into cytokine-mediated responses of IECs, integrating intracellular signaling with functional readouts. A better understanding of these mechanisms may contribute to the development of more effective targeted therapies for CIBD.

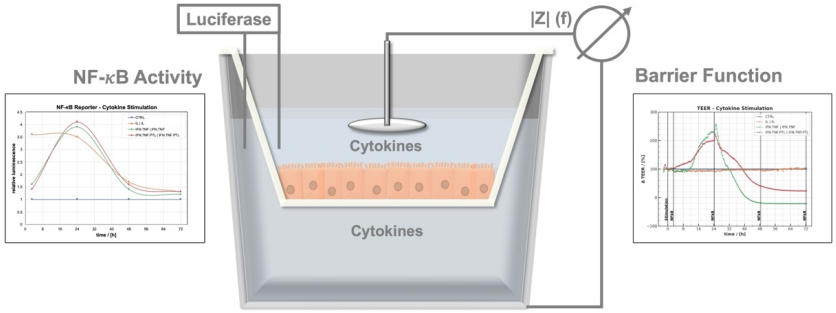

Figure 1: Dual monitoring of NF-kB activation by Caco-2 reporter cell line and impedance-based barrier function during cytokine-induced inflammation

References:

[1] J. Jang and S. Jeong, *BioChip Journal* 17 (2023) 403–430.
[2] M. Friedrich; M. Pohin and F. Powrie, *Immunity* 50 (2019) 992–1006.
[3] M. E. Delgado and T. Brunner, *Genes and Immunity* 20 (2019) 609–626.
[4] P. E. Dubé; S. Punit and D. B. Polk, *American Journal of Physiology-Gastrointestinal and Liver Physiology* 308 (2015) G161–G170.
[5] Q. Guo; Y. Jin; X. Chen; X. Ye; X. Shen; M. Lin; C. Zeng; T. Zhou and J. Zhang, *Signal Transduction and Targeted Therapy* 9 (2024) 53.

Soft Graphene Electrodes and Screen-Printed Carbon Electrodes for Monitoring Cell Adhesion Using Non-Faradaic Electrochemical Impedance Spectroscopy

E. Fuhry [1]; V. Guglielmotti [1,2]; T.J. Neubert [1]; M. Kuhl [1]; I. Wachta [1]; D. Pallarola [2]; J. Höök [1]; K. Balasubramanian[1]

[1]Dept. Of Chemistry, Humboldt-Universität zu Berlin, Germany; [2]Instituto de Nanosistemas, Universidad Nacional de General San Martin, San Martin, Argentina
nano.anchem@hu-berlin.de

Impedance sensors for detecting cell adhesion or cellular interactions are typically realized on hard substrates. Cells are known to interact with their microenvironment. Hence, the stiffness of the substrate where cells grow plays a crucial role in cell behavior, adhesion, growth and proliferation. [1]. Providing a substrate with a stiffness similar to the cellular microenvironment will help minimize deviations in the natural behavior of cells during the electrochemical measurements. Hence, impedance sensors on soft substrates are needed. Here, we present a soft biomaterial platform, wherein a soft elastic substrate made up of poly(dimethylsiloxane) (PDMS) is coated with a single graphene sheet as electrode material for the real-time detection of cell adhesion using impedance sensing. [2] While metal electrodes can also be realized on PDMS, we demonstrate using nanomechanical measurements, that the softness of PDMS is lost with deposited metal layers, due to the requirement of several nanometers of the metal. By contrast, the transfer of graphene as a single atomic layer on to PDMS brings a negligible increase in stiffness. Using such sensors, we have followed the adhesion of MCF-7 cancer cells to a soft graphene electrode in real-time using electrochemical impedance spectroscopy (EIS) in the absence of added redox probes (non-Faradaic). The EIS response can be correlated with different phases of cell adhesion on to the soft substrate.

One important challenge in monitoring cell adhesion using EIS is the understanding of the mechanism of the impedance response and its correlation with specific interfacial or cellular events. With this goal, we have used the sedimentation of silica beads on to a screen-printed carbon electrode as a model system for cell adsorption on to an electrode. Silica beads as models for cells is advantageous since they sediment rapidly on the electrode surface and their interaction is reversible and non-specific. Typically, in EIS the DC potential is left at open circuit or maintained at a constant value to measure the impedance response. We have introduced the DC potential as an additional variable and monitor non-Faradaic impedance as a function of the applied DC potential. Using this technique, referred to as Non-Faradaic Potentiodynamic EIS (NF-PDEIS) we demonstrate that the sensitivity towards interfacial processes in the impedance signal can be improved by choosing an appropriate potential. [3] Moreover, by elaborate modeling, we show that the non-Faradaic impedance is also able to detect changes in the point-of-zero-charge (pzc) and interfacial charge density. Using this model, the impedance response due to the adhesion of MCF-7 cells can be well-understood.

References:

[1] D.E. Discher, P. Janmey, Y-L. Wang, Tissue Cells Feel and Respond to the Stiffness of Their Substrate. *Science* 4 (2005) 310. 10.1126/science.1116995

[2] V. Guglielmotti, E. Fuhry, T.J. Neubert, M. Kuhl, D.Pallarola, and K. Balasubramanian, Real-Time Monitoring of Cell Adhesion onto a Soft Substrate by a Graphene Impedance Biosensor. *ACS Sensors* 4 (2024) e202400037. 10.1021/acssensors.3c01705

[3] E. Fuhry, V. Guglielmotti, I. Wachta, D.Pallarola, and K. Balasubramanian, Real-Time Non-Faradaic Potentiodynamic Impedance Sensing Using Screen-Printed Carbon Electrodes. *Analysis & Sensing* 9 (2024) 101-109. 10.1002/anse.202400037

Metal-Organic Frameworks based Electrochemical Interfaces for advanced Bioelectronics platforms

V. Pachauri

RWTH Aachen, Institute of Materials in Electrical Engineering 1, Aachen (Germany)
pachauri@iwe1.rwth-aachen.de

Living systems, such as cells, continuously interact with their surrounding environment, with the substrate playing a decisive role in regulating adhesion, proliferation, and overall cellular behaviour. Understanding and engineering cell–substrate interfaces are therefore critical not only for fundamental cell biology but also for emerging applications in bioelectronics, tissue regeneration, and implantable devices. Over the past several years, a variety of metal- and nanomaterial-based electrode arrays have been employed, offering distinct advantages for cell monitoring and stimulation. More recently, conductive organic polymers such as poly(3,4-ethylenedioxythiophene): polystyrene sulfonate (PEDOT: PSS) have become standard materials for biological interfaces, due to their reduced interfacial impedance and improved signal quality. However, issues such as intrinsic instability, electrochemical drift, and long-term degradation in aqueous environments significantly limit their reliability in sustained bioelectronic applications. While chemical and physical modifications provide incremental improvements, the demand for stable, high-performance biointerfaces remains largely unmet.

In this context, metal–organic frameworks (MOFs) have emerged as promising candidates in biomedical applications, including drug delivery, bioimaging, and cell-culture platforms. Recent studies demonstrate that MOF-based scaffolds, such as MIL-53(Al) films and ZIF-8–modified membranes, can enhance protein adsorption, cell adhesion, and proliferation, outperforming conventional substrates. Building on these findings, we introduce two-dimensional (2D) MOFs as active biointerfaces with distinct advantages over current nanomaterials for the fabrication of microelectrode arrays (MEAs) and transistor-based devices. Their tuneable structure and functionality also open opportunities for biosensing applications, including the detection of small molecules.

In this work, two BDC–NH_2–based 2D MOFs (Fe-MOF and Ni-MOF) were optimized for large-scale thin-film deposition on gold and silicon substrates using a layer-by-layer epitaxy approach. Cell-impedance spectroscopy was performed with PC-12 neuroblastoma cells, where Fe-MOF films demonstrated excellent electrochemical stability in culture media and strong biocompatibility, confirmed by proliferation and reactive oxygen species assays. Impedance measurements revealed clear signatures of cell adhesion, spreading, and proliferation over 24 h, underscoring the potential of MOF-based interfaces as stable, biocompatible, and functional platforms for cell studies and bioelectronic applications. These results highlight the promise of MOFs as next-generation materials for advanced cell biology and bioelectronics, while also pointing to remaining challenges regarding their stability in complex biological environments and cell-specific biocompatibility.

References:

[1] J.G. Miller, Living systems. I. The nature of living systems. Quad. Criminol. Clin. 1973, 48 (1), 63-91

[2] A. Kauth, J. Wegener, H. Jiang, V. Pachauri, S. Ingebrandt. PEDOT: PSS Electropolymerization Protocol for Microelectrodes Enabling Low-Cost Impedance-Based Cellular Assays. Applied Research 2025, 4, 1, e202400087

[3] Y. Li, B. Cui, et.al., Ion-selective organic electrochemical transistors: recent progress and challenges. Small, 18 (19) (2022), Article e2107413

[4] H. Jiang, Z. Gao, C. Lubrano, C. L. Bovio, H. Bommes, A. Kauth, L. Baumann, B. Cheng, D. Murugan, J. Knoch, R. Waser, S. Ingebrandt, F. Santoro, V. Pachauri*. Metal-organic frameworks as an active substrate for cell-interaction studies and cell-on-a-chip platforms, Biosensors and Bioelectronics X 2024, 19, 100487

PEDOT:PSS as transparent, low-cost electrode material for impedance-based cell analysis

S. Michaelis[1]; C. Götz[1,2] and J. Wegener[1,2]

[1]Fraunhofer EMFT, Division *Cell-Based Sensor Technology*, Regensburg (Germany)
[2]University of Regensburg, Regensburg (Germany)
stefanie.michaelis@emft.fraunhofer.de

Conducting polymers are increasingly integrated into everyday technologies and scientific equipment. Conventional electrode materials, such as gold or indium tin oxide, are progressively being substituted in certain applications, since conducting polymers combine low cost with advantageous material properties, such as mechanical flexibility, optical transparency, and favorable dielectric behavior. Among them, PEDOT:PSS exhibits the strongest potential for application in impedance-based cellular assays [1]. Its ability to disperse in aqueous media makes it compatible with scalable manufacturing approaches, including screen printing. When exposed to aqueous environments, PEDOT:PSS electrodes undergo swelling, which enhances the interfacial capacitance between electrode and electrolyte. This property renders PEDOT:PSS highly promising as a transparent transducing layer for impedance-based cell monitoring. The present work investigates PEDOT:PSS as an electrode material for impedance-based cell analysis as conducted in typical ECIS assays. Electrode arrays were fabricated through screen-printing, revealing considerable promise for commercial deployment. A performance comparison between screen printed PEDOT:PSS electrodes and conventional gold electrodes highlights both, advantages and limitations of this polymer material. Ongoing studies address diverse applications, with initial findings suggesting that the unique dielectric response of PEDOT:PSS provides enhanced sensitivity in probing cell-cell and cell-substrate junctions, thereby enabling impedance-based evaluation of cell types previously inaccessible by this technique. Furthermore, its low-cost production and facile processing may pave the way for mass scale industrial fabrication of electrodes, for instance, in reel-to-reel processes.

References:

[1] Michaelis, S., et al. *Applied Research* 4.1 (2025): e70004.

Downscaling Electric Cell-substrate Impedance Sensing: What can transistor devices contribute?

S. Ingebrandt

RWTH Aachen, Institute of Materials in Electrical Engineering 1, Aachen (Germany)
ingebrandt@iwe1.rwth-aachen.de

As an alternative to the classical Electric Cell-substrate Impedance Sensing (ECIS) with metal microelectrodes, electrolyte-gated field-effect transistor (FET) devices can be used. In this case, the transistor-transfer function (TTF) method is applied, where a sinosoidal stimulation voltage is provided to the reference electrode of the 3-electrode transistor configuration and the voltage response of the transistor together with its first transimpedance amplification stage is recorded. Similarly to classical impedance spectroscopy, TTF spectra are recorded representing the bandwidth of the device configuration.
This alternative method offers several advantages: First the input impedance of the transistor is not relevant in this configuration, since voltage changes at the transistor gate are directly transduced into current changes in the transistor channel. Second the transistor's direct current (DC) in its working point is much larger compared to classical currents in ECIS devices and hence much less prone to parasitic effects of the contact lines on chip and peripheral cables. The relevant alternating current (AC) information for cell impedance measurements is carried on top of this large DC current. Third transistor devices permit much larger integration density of many devices on one chip and individual devices can be miniaturized to cellular and even sub-cellular spatial resolution.
In this presentation, different transistor devices will be demonstrated, which were used for ECIS recordings from classical silicon-based ion-sensitive FETs [1, 2], planarized silicon FETs for migration studies [3], silicon nanowire FETs with scaling into the sub-micrometer range to polymer-based electrochemically gated transistor devices [4]. Different cell types from cell lines, primary neurons, heart muscle cells, individually acting immune cells down to erythorcyte ghost cell were utilized for ECIS with transistor devices.
It will be demonstrated that there is even more potential within these devices, if their ion-sensitivity is exploited or the electrochemical adhesion noise is analyzed as additional information relevant to cell adhesion [5].
As a conclusion, transistor devices for ECIS realized with different materials and device concepts offer exciting possibilities for the future of ECIS.

References:

[1] S. Schäfer, S. Eick, B. Hofmann, T. Dufaux, R. Stockmann, G. Wrobel, A. Offenhäusser and S. Ingebrandt, *Biosensors and Bioelectronics* 24 (2009) 1201-1208.
[2] A. Susloparova, D. Koppenhöfer, J. K. Y. Law, X. T. Vu and S. Ingebrandt, *Lab on a Chip* 15 (2015) 668-679.
[3] J.K.Y. Law, A. Susloparova, X.T. Vu, X. Zhou, F. Hempel, B. Qu, M. Hoth, F. Hempel, B. Qu, M. Hoth and S. Ingebrandt, *Biosensors and Bioelectronics* 67 (2015) 170-176
[4] F. Hempel, J.K.Y. Law, T.C. Nguyen, R. Lanche, A. Susloparova, X.T. Vu, and S. Ingebrandt, *Biosensors and Bioelectronics* 180 (2021) 113101.
[5] M. Voelker and P. Fromherz, Physical Review Letters 96 (2006) 228102.

Impedance Unplugged – Do Single Cells in Suspension Tell a Different Story?

M. Di Berardino

Amphasys AG, Technopark Lucerne, CH-6039 Root D4, Switzerland
marco.diberardino@amphasys.com

Electrical Cell Impedance Sensing (ECIS) has become a cornerstone technology for monitoring adherent mammalian and human cells in real time. However, its scope is inherently limited to cells that grow on surfaces. In contrast, Impedance Flow Cytometry (IFC) offers a fundamentally different approach: it analyzes individual cells in suspension, enabling high-throughput, label-free characterization at the single-cell level.

This talk introduces IFC to the ECIS community, highlighting the conceptual and technical differences between these two impedance-based methods. By comparing their working principles, we will explore how IFC complements ECIS — not only by extending impedance analysis to non-adherent cells, but also by unlocking new applications in both mammalian and microbial systems.

Selected case studies will illustrate how IFC can provide additional layers of insight, challenge existing assumptions, and open up new possibilities for cell-based assays. Whether as a complementary tool or a standalone platform, IFC invites us to rethink what impedance can reveal - when cells are no longer stuck to the surface.

Impedance Flow Cytometry for Electrogenic Microorganisms

M. Mozafari[1]; P. Erfle[1]; J. Block[2,3,4]; R. Krull[2,3,4]; A. Dietzel[1,4]

[1]Institute of Microtechnology, TU Braunschweig
[2]Institute of Biochemical Engineering, TU Braunschweig
[3]Braunschweig Integrated Centre of Systems Biology, TU Braunschweig
[4]Center of Pharmaceutical Engineering, TU Braunschweig
m.mozafari@tu-braunschweig.de

This study expands upon recent discoveries highlighting the important role of electrogenic gut bacteria [1]. The main objective is to develop and demonstrate impedance-based flow cytometry that can detect electrogenic microorganisms based on their electrical properties in real time and without markers with high precision. For this purpose, a microfluidic system was designed and manufactured. The system consists of a microchannel with three microelectrodes allowing differential measurements. The microchannel was structured on a glass wafer together with a thin PDMS layer using femtosecond laser ablation techniques, while co-planar microelectrodes were fabricated separately using gold and titanium via sputtering and photolithography. Both parts of the system were then aligned and sealed with a previously spin-coated PDMS layer (**Fig. Ia,c,d**). The impedance measurements were conducted using two microorganisms: *Escherichia coli*, a non-electrogenic model organism, and *Shewanella oneidensis*, a well-known electrogenic microorganism at 1MHz using HF2LI lock-in amplifier (from Zürich Instruments, Zürich, Switzerland). When single microorganisms pass through the detection zone, they change the impedance, which serves as a measurable signal corresponding to their electrical behavior (**Fig. IIa**).

Analysis at 1 MHz revealed different behavior between *S. oneidensis* and *E. coli*. Both bacteria contain a membrane that acts as a capacitor in the corresponding electrical circuit (**Fig. IIb**). An increase in the current value for *S. oneidensis* indicates a lower impedance of the cytoplasm compared to the surrounding physiological medium which, suggesting a short-circuited membrane (**Fig. IIc**). *E. coli*, on the other hand, showed a decrease in current at the same frequency (**Fig. IId**) which means that the total impedance is still higher than that of the surrounding medium. This comparison suggests that the membrane of the electroactive microorganism is short-circuited at lower frequency than that of *E. coli* due to extracellular electron transfer (EET).

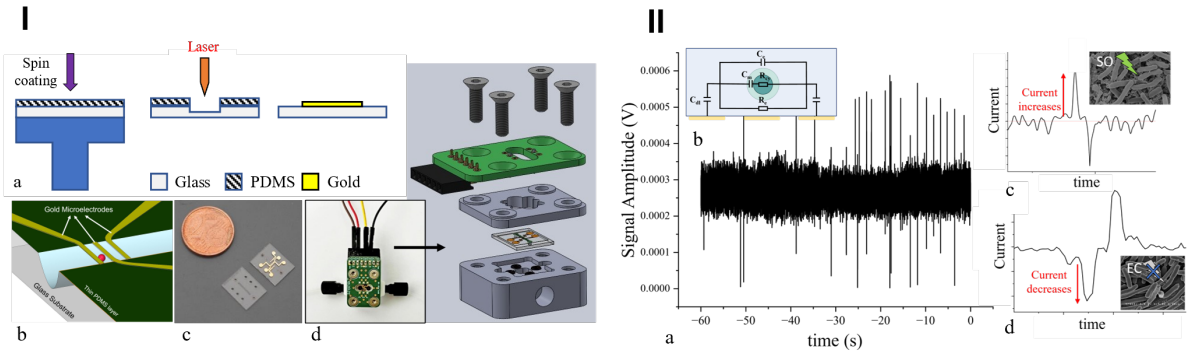

Figure: Ia) Fabrication of the microchannel and microelectrodes using femtosecond laser ablation and photolithography. **Ib)** Concept of impedance flow cytometer with the created sensing areas. **Ic)** Two separated parts of the microfluidic system and microelectrodes. **Id)** Assembled system with electric and fluidic connections. **IIa)** Signal variation showing the detection of microorganisms in an Impedance Flow Cytometer. **IIb)** Equivalent electrical circuit modelling the bacteria with membrane as a capacitor. **IIc)** Differential signal of single cell indicating the increase in the current in electrogenic *S. oneidensis* (SO) detection. **IId)** Differential signal of single cell indicating a decrease in the current in *E. coli* (EC).

References:

[1] Naradasu D, Miran W, Sakamoto M (2018). Frontiers in Microbiology 9, 3267.

Biomechanics of single cells using a microfluidic device to correlate transients of flow impedance and electrical impedance

O. Alalul[1]; J. Liu[2]; M. Böl[2]; A. Al-Halhouli [3] and A. Dietzel[1]

[1]Technische Universität Braunschweig, Institute of Microtechnology; Braunschweig (Germany)
[2]Technische Universität Braunschweig, Institute of Mechanics and Adaptronics, Braunschweig (Germany)
[3]German Jordanian University, Department of Mechatronics Engineering, Amman (Jordan)
osama.alalul@tu-braunschweig.de

Understanding cellular mechanics is fundamental for advancing developmental biology and reproductive medicine. However, conventional techniques such as atomic force microscopy and micropipette aspiration, while informative, are constrained by limited throughput [1]. To address this, we present a novel microfluidic device that enables real-time, impedance-based biomechanical characterization of single oocytes under flow. The system integrates three coplanar microelectrodes (E1, E2, E3) (Figure 1) within a constriction microchannel, allowing simultaneous mechanical deformation and electrical impedance measurement as cells transit through the chip. Impedance signals were acquired using a lock-in amplifier and current amplifier across a range of frequencies at 0.700 Vrms. Differential impedance readings between electrode pairs (E1–E2 and E2–E3) reflected variations in cell deformation and depth of penetration into the constriction channel. System calibration was performed using deformable hydrogel spheres, with impedance responses validated relative to distilled water. The use of SU-8-based microfluidic chips provided smooth channel surfaces and stable electrode performance, ensuring reproducibility and signal integrity under varying pressure conditions. This platform enables dynamic, label-free, and non-invasive assessment of oocyte biomechanics, establishing correlations between mechanical deformation and impedance responses. Unlike previous studies that focused on somatic cells, our system is specifically designed to accommodate the sensitivity of reproductive cells, broadening the applicability of impedance cytometry in reproductive biology. Our findings highlight the potential of this technique as a high-throughput screening tool for evaluating oocyte mechanical properties, with implications for diagnostics and assisted reproductive technologies.

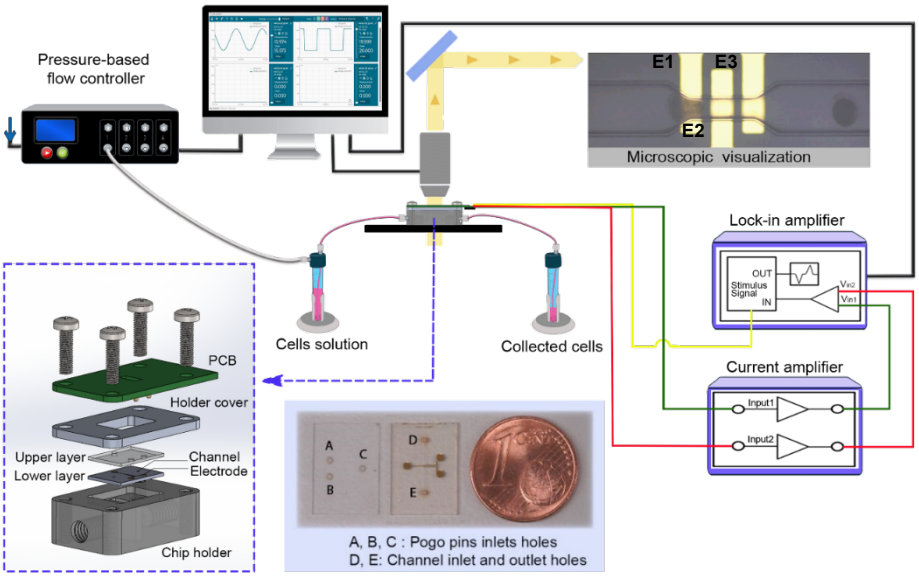

Figure 1: Schematic of the experimental setup.

References:

[1] Y. Chen, K. Guo, L. Jiang, S. Zhu, Z. Ni, and N. Xiang, "Microfluidic deformability cytometry: A review," Talanta, vol. 251, p. 123815, 2023, doi: 10.1016/j.talanta.2022.123815.

Electrical impedance spectroscopy at the service of complex tissue models

R. M. Owens

Department of Chemical Engineering and Biotechnology, University of Cambridge, Philippa Fawcett Drive, Cambridge CB3 0AS, UK.
rmo37@cam.ac.uk

The increasing demand for complexity in in vitro models of tissues to enhance their relevance in modelling human physiology, demands that monitoring techniques adapt at pace. Electrical impedance spectroscopy offers label-free, continuous, high content information on real time changes in cell morphology, behaviour and differentiation. In this talk I'll discuss a new generation of electrodes, based on conducting polymers. Unlike traditional electrodes, conducting polymer electrodes bring advantages in terms of improved interfacing with biology, mixed electronic and ionic conduction, increased versatility in terms of fabrication due to liquid formulation (e.g. conformability, transparency, 3-dimensionality etc) and enhanced signal to noise ratio. Bringing together principles of materials science, tissue engineering, 3D cell biology and bioelectronics, I will showcase how we are building advanced models of the gastrointestinal tract, with integrated 3D conducting polymer scaffolds to host and monitor the tissues, aiming to elucidate the role of microbiota in the gut-brain axis communication. Second, I'll discuss conformable electrodes we've developed for both monitoring of complex in vitro gut models, and validation with rodent tissues. These devices allow highly sensitive monitoring of impedance of the tissue (as an indicator of gut health).

Porous membrane electrical cell-substrate impedance sensing for barrier-on-chip modeling

C.A. Simmons

University of Toronto, Toronto (Canada)
c.simmons@utoronto.ca

Microfluidic organ-on-chip (OOC) systems that recapitulate specific human organ structures and functions hold great promise as advanced culture models for biological research, disease modeling, and drug development. OOCs are particularly well-suited for modeling biological barriers (e.g., vascular, epithelial) as they can mimic key aspects of the barrier microenvironment, including multiple interacting cell types, extracellular matrix, and fluid shear stresses. However, broad adoption of barrier-on-chip models has been hindered by their operational complexity, low throughput, and limited incorporation of biosensors for on-chip assays.

To facilitate adoption and translation of barrier-on-chip models, we have developed VitroFlo, a microfluidic system that enables co-culture and incorporation of 3D biomaterials in a simple-to-use membrane-based, 12-well configuration [1]. Of particular relevance to barrier modeling, unidirectional physiological shear stresses can be applied without the complexity of pumps, enabling long-term dynamic culture. In this talk, I will briefly discuss how we recently used VitroFlo to reveal insights into the role of perfusion on blood-brain barrier function in stem cell-derived models of Alzheimer's disease.

A persistent challenge with barrier-on-chip models is measuring barrier integrity within the complex culture set ups, where geometry, biomaterials, and fluid shear can confound measurements. To this end, I will discuss our work developing methods to adapt electrical cell-substrate impedance sensing (ECIS) to our membrane-based OOCs [2-4]. Using a simple, cost-effective prototyping method, gold electrodes can be embossed on to polyethylene terephthalate porous membranes with high fidelity. Porous membrane ECIS (PM-ECIS) performs similarly to solid-substrate ECIS, enabling sensitive, real-time measurement of endothelial cell barrier impedance with cell growth, barrier disruption, and fluid shear responses, with expected sensitivities to electrode size. Importantly for barrier modeling, PM-ECIS measurements are not confounded by 3D biomaterials typical of OOC models. In on-going work, we are incorporating PM-ECIS into VitroFlo as an integrated user-friendly, scalable, and cost-effective system that we expect will enable new insights into barrier function across a range of fields.

References:

[1] M. Lino; H. Persson; M. Paknahad; A. Ugodnikov; MF Ghahremani; L.E. Takeuchi; O. Chebotarev; C. Horst; C.A. Simmons, *Lab on a Chip* 25 (2025) 1489-1501.
[2] O. Chebotarev; A. Ugodnikov; C.A. Simmons, *ACS Applied Bio Materials*, 7 (2024) 2000-2011.
[3] A. Ugodnikov; O. Chebotarev; H. Persson; C.A. Simmons, *ACS Biomaterials Science & Engineering*, 10 (2024) 5327-5335.
[4] A. Ugodnikov; J. Lu; B. Yechuri; O. Chebotarev; C.A. Simmons. *ACS Applied Materials & Interfaces*, in press.

Combining TEER and high-resolution spatial impedance mapping on porous MEA for improved *in vitro* barrier measurements

I. Carmans[1,2]; S. E. Takalloo[2]; C. Campanella[2]; D. V. Ibanez[2]; C. Diacci[2]; C R. Domingo[2] and D. Braeken[2]

[1]KU Leuven, Leuven, Belgium
[2]imec, Leuven, Belgium
ina.carmans@imec.be

Accurate assessment of barrier integrity is vital for evaluating tissue barriers *in vitro*. While transepithelial and transendothelial electrical resistance (TEER) enable real-time, non-destructive quantification of barrier tightness on porous supports (Figure 1a), it only provides a single value of barrier tightness per time point. These single-value measurements mask cellular heterogeneity and may miss localized disruptions. To address this shortcoming, microelectrode arrays (MEAs) offer high spatial resolution impedance measurements [1] (Figure 1b). However, their conventional fabrication on solid, non-porous substrates restricts their integration in multi-compartment organ-on-chip models.

To overcome this issue, we developed a novel silicon-based porous microelectrode array (pMEA) comprising an 11 x 11 grid of titanium nitride (40µm diameter) electrodes. The pMEA is integrated into a Transwell-like setup and includes an additional large electrode in the top and bottom compartments, enabling simultaneous TEER measurements (Figure 1c).

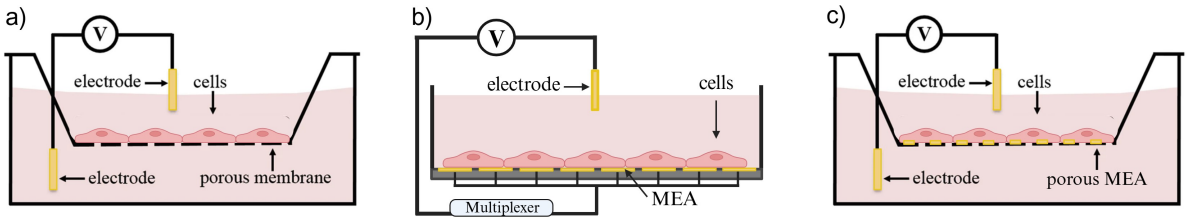

Figure 1: Conventional Transwell setup for measuring TEER (a). MEA for measuring cellular impedance (b). In-house developed Transwell setup with integrated porous MEA (pMEA) for simultaneous measurements of TEER and cellular impedance (c).

Endothelial cells (HUVECs) were cultured directly on the pMEA to monitor barrier formation. TEER gradually increased to 8.5 ± 1.8 Ω·cm^2, while the average pMEA impedance at 1 kHz increased from (1.5 ± 0.02) × 10^4 Ω to (9.1 ± 1.2) × 10^4 Ω. The spatial variability, defined as the coefficient of variation for the pMEA impedance across electrodes, decreased from 34 ± 11 % to 22 ± 2 % after 6 days, indicating that HUVECs remain heterogeneous even after maturation. Upon barrier disruption with biological agents such as tumor necrosis factor alpha (TNF-α), both TEER and pMEA impedance decreased. More interestingly, the pMEA spatial variability increased from 17 % to 33 %, revealing uneven barrier disruption, a feature not captured by TEER measurements alone.

Our results underscore the ability of the pMEA to capture barrier spatial heterogeneity in multicompartment setups, a critical feature for understanding disease mechanisms and one that is beyond the capabilities of traditional Transwell and TEER-based technology. In conclusion, the novel pMEA offers a powerful platform for investigating vascular and gut barrier function, enabling detailed study of dynamic processes such as pathogen translocation, immune cell migration and cancer cell metastasis.

References:

[1] Venz A., Duckert B., Lagae L., Takalloo S.E., Braeken D. *Sci Rep* 15, 1592 (2025). https://doi.org/10.1038/s41598-025-85783-9

A Versatile, Biomimetic, 3D Electrochemical Device for Monitoring Cell Growth and Epithelial Barrier Integrity

R. Acharya; D.v. Niekerk; M. Lopez Cavestany and R.M. Owens

University of Cambridge, Cambridge (United Kingdom)
ra646@cam.ac.uk

Three-dimensional (3D) cell culture and in-vitro bioelectronic systems have advanced significantly in recent years, offering new capabilities for monitoring and predicting biological activity in a variety of applications. While bioelectronic devices such as impedance sensors and electrochemical transistors have traditionally been based on two-dimensional (2D) organic semiconductor films, tissue engineering has developed 3D culture platforms—such as porous scaffolds, hydrogels, and fibre meshes—that better replicate native tissue architecture and physiology.

In this work, we present a novel bioelectronic device that integrates these two domains. The device is built around a 3D microporous scaffold based on the conducting polymer PEDOT:PSS, serving both as a biologically relevant substrate and as an active electronic interface. The scaffold functions as a transmembrane structure that hosts multiple cell types, enabling the formation of stratified tissue models, while simultaneously transducing biological (ionic) signals into readable electrical outputs.

We demonstrate the design, fabrication, and electrical characterization of this transmembrane bioelectronic platform, which combines dual sensing modalities: electrochemical impedance spectroscopy (EIS) for monitoring epithelial barrier formation and integrity, and organic electrochemical transistor (OECT) operation for real-time tracking of cell growth and extracellular matrix (ECM) deposition in 3D.

Using fibroblast cultures as a model, we monitored tissue development over a 10-day period. Changes in drain current provided a quantitative readout of cell proliferation and ECM accumulation. We evaluated the influence of initial seeding densities (125k, 250k, and 500k cells), observing distinct patterns of cell migration, proliferation, and matrix remodeling, which were corroborated with biological assays including immunofluorescence imaging and DNA quantification.

Additionally, we used EIS to monitor epithelial layer formation and barrier integrity over time and correlated this with the underlying fibroblast dynamics, demonstrating the device's ability to support and assess multi-layered tissue constructs.

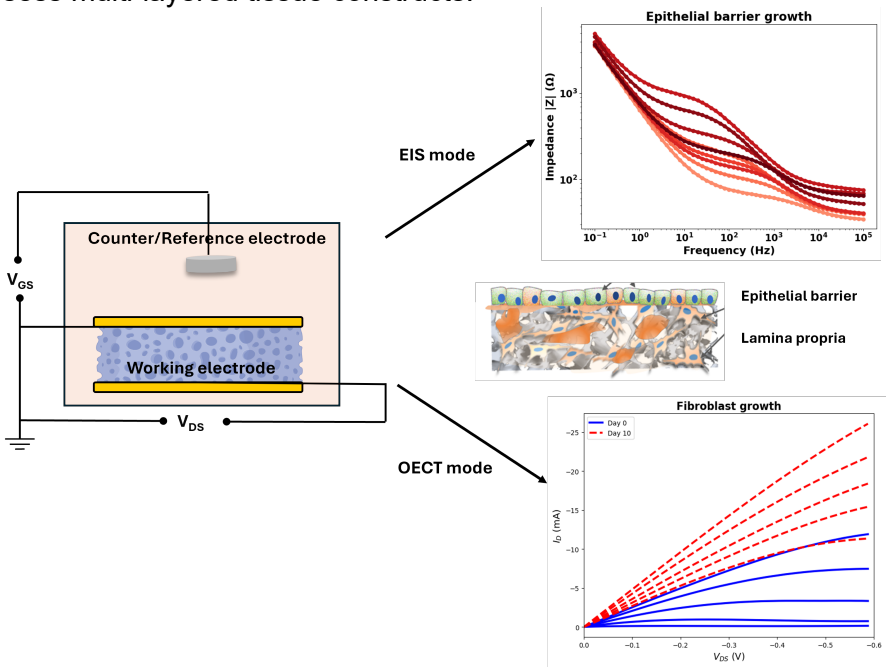

Vienna Calling - Innovations in Impedance-based analytical microsystems as advanced organs-on-a-chips

P. Ertl

Institute of Applied Synthetic Chemistry & Institute of Cemical Technologies and Analytics, Technical University Vienna, Austria
peter.ertl@tuwien.ac.at

Organ-on-a-chip technology has progressed from simplified “chip-in-a-lab” prototypes toward sophisticated, sensor-integrated microphysiological systems that recapitulate key aspects of human biology. Over the past decade, advances in automated microfluidics, tissue engineering, and embedded sensing have transformed these platforms into powerful tools for disease modeling and translational research. A central component of this evolution is the integration of impedance-based sensors, which enable non-invasive, label-free monitoring of cellular dynamics with high temporal resolution. By capturing changes in barrier integrity, cell adhesion, proliferation, and immune activation, impedance sensing provides a unique window into processes that are otherwise difficult to resolve in real time. At TU Wien, the *cellchip group* has contributed to this paradigm by developing novel electrode architectures, miniaturized sensor platforms, and integrative chip designs that enhance reproducibility and scalability across applications. Our research spans mucosal and gut-on-chip systems for host–environment interactions, vascularized platforms for infection and immunology, and sensor-embedded devices for studying inflammation, senescence, and transplant rejection. This presentation will provide an overview of our group’s work in impedance-enabled organ-on-a-chip systems, highlight lessons learned from integrating real-time sensing with complex biology, and outline the remaining challenges on the path toward multi-organ interoperability and a true “human-on-a-chip.” By bridging engineering, biology, and translational medicine, these technologies hold the potential to accelerate drug discovery, reduce reliance on animal models, and establish precision medicine platforms for the future.

Integrated sensing in microphysiological systems: the key role of microelectrode arrays

M. Mastrangeli

Delft University of Technology, Delft (The Netherlands)
m.mastrangeli@tudelft.nl

The technology of microphysiological systems (MPS) is establishing a plausible alternative to animal-based models for the study of human physiology under *in vitro* conditions [1]. MPS aim to recapitulate synthetically the main traits of cellular microenvironments for the growth and maturation of tissues under controlled conditions. Compared to established cell culture methods, MPS afford higher physiological relevance through the inclusion of mechanical, electrical and chemical cues that closely mimic *in vivo* conditions.
Continuous monitoring of the MPS microenvironment and of the status of cells and tissues across the duration of the assays is crucial for assessing health and metabolism of the biological constructs [2]. Among several available types, electrical sensing is particularly suitable for integration within the confined geometries of MPS and to complement optical inspection. Microelectrodes, which represent the interfacing elements between the tissues and the external readout, play thereby a crucial role. Geometry and material composition are particularly important parameters for the functionality of microelectrodes, and both are constrained by the fabrication methods.
In this contribution, I will showcase the opportunities offered by wafer-level microfabrication of MPS through the design, fabrication and characterization of a microfluidic tissue barrier sensor module (Fig. 1, left) [3-4] and of three-dimensional arrays of microelectrodes (Fig. 1, right) [7-8]. I will emphasize the reproducible fabrication of pre-defined geometries for microelectrodes as a step toward standardization of tissue impedance measurements in MPS, and conclude with the concept of modular platforms embedding multiple standardized modules as viable perspective for MPS advancement.

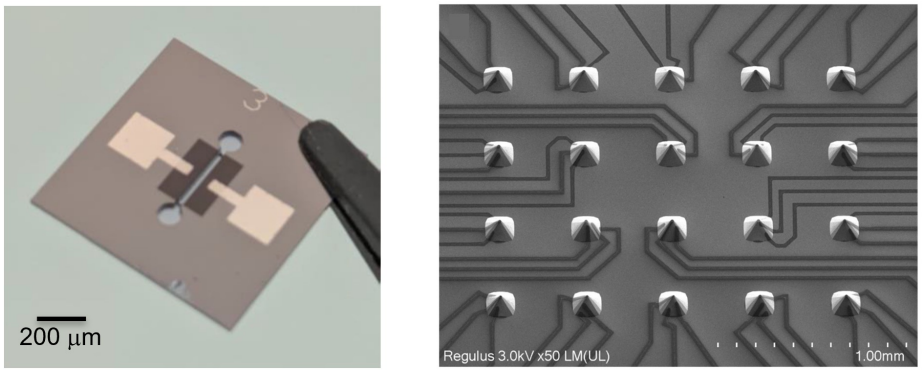

Figure 1. Tissue barrier sensor chip [3] (left), and 3D silicon-based microelectrode array [5] (right).

References:

[1] D. M. Nahon *et al.*, *Nature Biomedical Engineering* 8, 941-962 (2024)
[2] P. Tawade, M. Mastrangeli, *ChemBioChem* 25 (3), e202300560 (2024)
[3] P. Tawade *et al.*, *Proc. IEEE MEMS 2025*, 426-429
[4] J.-J. Yeh *et al.*, *Proc. TRANSDUCERS 2025*, forthcoming
[5] N. Revyn *et al., Proc IEEE MEMS 2022*, 102-105
[6] D. Sengupta *et al., Proc. TRANSDUCERS 2025*, forthcoming

Impedance-based Monitoring of two cell monolayers co-cultured without physical contact (cis-TER)

T. Naber[1,2]; L. Rottbauer[1]; J. Wegener[1,2]

[1]Universität Regensburg, Regensburg (Germany),
[2]Fraunhofer Institut für Elektronische Mikrosysteme und Festkörper-Technologien EMFT, Regensburg (Germany)
tobias.naber@emft.fraunhofer.de

The delivery of active ingredients over epithelial and endothelial barriers is a key parameter of drug efficacy. In addition, the effect of the drug not only on the target but on the passed barriers is of great interest. So far, the detection of these crucial parameters has to be performed by using several different assay types. In the presented work we describe the development of an assay platform monitoring the morphology of two indirectly co-cultured monolayers, offering the possibility to determine afore mentioned parameters in a single experiment. The assay platform is based on impedance spectroscopic monitoring and combines two different approaches of impedance readings. A first cell layer, the *sensing layer*, is cultured on a set of thin-film gold electrodes. Monitoring of this cell layer is based on the ECIS approach [1]. Simultaneously, a second cell layer, the *barrier forming layer*, is cultured on a permeable culture insert mounted above the first cell layer. By applying a stainless-steel dipping electrode on the apical side and the combination of the thin film gold electrodes as basolateral electrode, the TER and the TEC of the cell layer cultured on the permeable substrate can be monitored [2]. At the current status of development, the device offers a throughput of 24 individual co-cultures. We developed two different basolateral electrode set-ups convenient for different assay scenarios. Furthermore, we demonstrated the functionality of the monitoring system with a proof-of-principle experiment. We believe that an assay platform based on the *CIS-TER* approach can strongly assist future drug development processes.

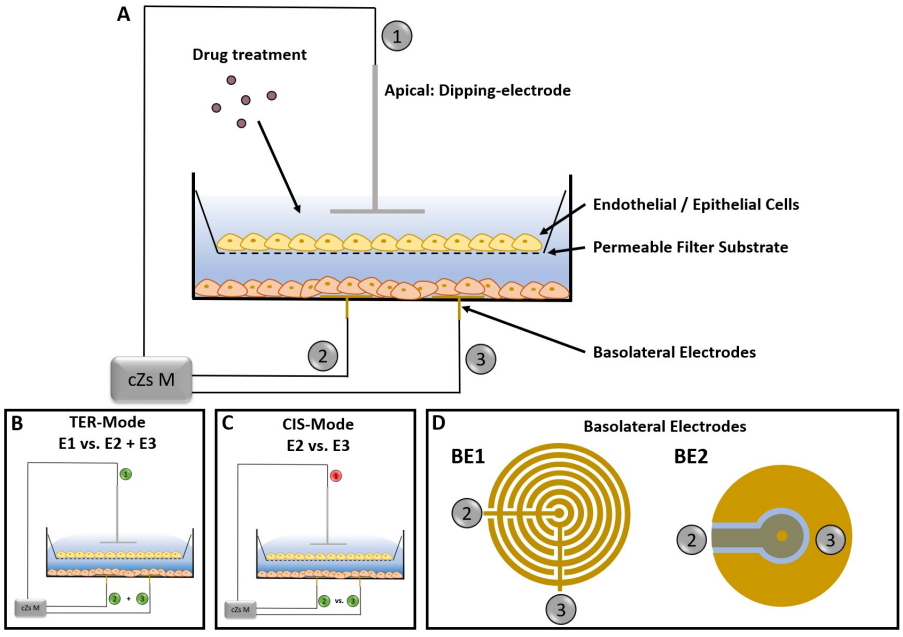

Figure 1 : (A) Schematic set-up of the CIS-TER assay. Possible measurement modes, determining the TER of the upper cell layer **(B)** and the impedance of the lower cell layer **(C)**. **(D)** Developed layouts for the basolateral set of electrodes.

References:

[1] J.A. Stolwijk and J. Wegener, *Bioanalytical Reviews*, vol 2. (2019) pp 1 - 75.
[2] J. Wegener, et al., *Biotechniques*, 37(4) (2004), pp 590 – 597.

Towards 3D Cell Behavior Monitoring with Advanced Electrical Impedance Tomography Reconstruction

P. Bagnaninchi

University of Edinburgh (United Kingdom)
pierre.bagnaninchi@ed.ac.uk

Two-dimensional impedance-based cellular assays [1], such as ECIS, have been widely adopted to monitor key aspects of cell behaviour, including viability, adhesion, and differentiation, in a label-free and real-time manner. As cell biology increasingly shifts towards three-dimensional (3D) models that better capture the complexity of in vivo tissues, there is a need for impedance-based methods that can profile the biophysical behaviour of 3D constructs such as tissue engineering scaffolds, organoids, and spheroids.

Electrical impedance tomography (EIT) offers this possibility by reconstructing conductivity maps within living tissues. Our recent studies have shown that miniature EIT sensors [4] can capture viability changes deep inside tumour spheroids [2] and tissue-engineered scaffolds [3], while integration with optical imaging has improved the fidelity of these reconstructions [5, 6, 7]. Together, these advances demonstrate that EIT can sensitively report on cell survival, differentiation, and drug responses in environments where traditional optical or biochemical assays fail.

In this talk, we will describe our progress towards building a new generation of 3D impedance assays, combining compact sensors with advanced reconstruction [8] and dual-mode approaches. Step by step, these developments are extending the power of impedance assays beyond the 2D monolayer, towards comprehensive monitoring of 3D cell behaviour. This paradigm shift will enable richer phenotyping of organoids, engineered tissues, and regenerative therapies, offering real-time, non-destructive insights into cell state across all dimensions.

References:

[1] Gamal, W., Wu, H., Underwood, I., Jia, J., Smith, S., & Bagnaninchi, P. O. (2018). Impedance-based cellular assays for regenerative medicine. *Philosophical Transactions of the Royal Society B: Biological Sciences*, 373, 20170226. https://doi.org/10.1098/rstb.2017.0226

[2] Wu, H., Yang, Y., Bagnaninchi, P. O., & Jia, J. (2018). Electrical impedance tomography for real-time and label-free cellular viability assays of 3D tumour spheroids. *Analyst*, 143, 4189–4198. https://doi.org/10.1039/c8an00729b

[3] Ogawa, R., Hallas-Potts, A., Wu, H., Jia, J., & Bagnaninchi, P. O. (2021). Measuring 3D cell culture viability in multiple 3D printed scaffolds within a single miniature electrical impedance tomography sensor. *Advanced Engineering Materials*, 23(10), 2100338. https://doi.org/10.1002/adem.202100338

[4] Yang, Y., Jia, J., Smith, S., Jamil, N., Gamal, W., & Bagnaninchi, P.-O. (2017). A miniature electrical impedance tomography sensor and 3D image reconstruction for cell imaging. *IEEE Sensors Journal*, 17(2), 514–523. https://doi.org/10.1109/JSEN.2016.2631263

[5] Liu, Z., Kang, X., Bagnaninchi, P. O., & Yang, Y. (2020). Impedance-optical dual-modal sensor and image reconstruction for cell spheroids imaging. *IEEE Sensors Journal*, 20(22), 13364–13375. https://doi.org/10.1109/JSEN.2020.3014936

[6] Liu, Z., Bagnaninchi, P., & Yang, Y. (2022). Impedance-optical dual-modal cell culture imaging with learning-based information fusion. *IEEE Transactions on Medical Imaging*, 41(4), 983–994. https://doi.org/10.1109/TMI.2021.3129739

[7] Fang, H., Liu, R. B., Sun, J., Bagnaninchi, P. O., Liu, Z., & Yang, Y. (2024). Multi-modal EIT imaging using lensfree and flexible impedance sensor. *IEEE Sensors Journal*, 24, 979–989. https://doi.org/10.1109/SENSORS.2024.10784633

[8] Chen, Z., Xiang, J., Bagnaninchi, P.-O., & Yang, Y. (2023). MMV-Net: A multiple measurement vector network for multifrequency electrical impedance tomography. *IEEE Transactions on Neural Networks and Learning Systems*, 34(11), 8938–8949. https://doi.org/10.1109/TNNLS.2022.3154108

Advancing 3D Impedance Tomography for *In-Vitro* models

B. Linkoon. P. Meenaketan[1]; J. Deng[2]; Y. Chin Chai[1]; T. Torfs[1]; J. D. Beenhouwer[2]; J. Sijbers[2]; D. Braeken[1]

[1]imec, Leuven, (Belgium) [2]University of Antwerp (Belgium)
BabuLinkoon.Meenaketan@imec.be

Three-dimensional in vitro models, such as organoids and spheroids, have redefined biomedical research and drug development by more accurately replicating tissue complexity than conventional two-dimensional cultures. They enable tissue differentiation, disease progression, and drug response, but analysis remains difficult when seeking high-quality information across their full depth without damage. Micro-Electrical Impedance Tomography (µEIT), a label-free and non-destructive imaging modality, addresses this challenge by enabling non-invasive imaging while preserving tissue integrity [1].

In this study, we present the design of a µEIT platform for analyzing 3D *in-vitro* models. The system comprises three main modules: a 3D measurement interface, a signal acquisition unit, and an imaging unit. The measurement interface is a cubic biocompatible chamber with micro-electrodes integrated on each sidewall. During operation, the chamber is filled with culture medium, and the *in-vitro* model is placed inside for imaging. The signal acquisition unit features a reconfigurable switching matrix that controls current injection and voltage sensing, with the acquired data transmitted to the imaging unit for 3D impedance reconstruction. The platform operates over a frequency range of 1–100 kHz with current amplitudes of 10–100 µA.

To reconstruct 3D images, the platform employs time-differential EIT (TD-EIT), which reduces modeling and electrode-related errors by subtracting measurements at two time points. Conventional Gauss–Newton (GN) methods provide accurate reconstructions but are computationally expensive due to large Jacobian and Hessian matrices, especially in 3D EIT applications. To address this, we propose a matrix-free GN (MF-GN) method, which avoids explicit matrix storage and reduces computation complexity. Computation efficiency is further improved through adaptive meshing, applying a dense grid to the region of interest and a coarser grid to the background, ensuring high spatial resolution while minimizing cost.

An in-house prototype of the µEIT Cube was validated across a range of targets, demonstrating its capability to resolve both structural detail and dielectric contrast. In experiments with hydrogels and cerebral organoids, the system successfully distinguished the samples from the surrounding culture medium, confirming its applicability to biological models. Tests with multilayer targets, such as pomegranate seeds, further demonstrated accurate reconstruction of internal layers with distinct dielectric properties, closely matching the ground truth. Collectively, these results highlight the µEIT Cube's potential for 3D imaging of complex biological systems.

In conclusion, we present a non-invasive, label-free MEA-based platform for real-time, in-depth imaging of 3D *in-vitro* models, achieved through the integration of rapid measurement techniques and advanced reconstruction algorithms.

References:

[1] Deng, J., Renders, J., Meenaketan, B. L. P., Ebrahimi Takalloo, S., Braeken, D., De Beenhouwer, J., and Sijbers, J. (2024). IEEE Sensors Journal 24, 24452-24465.

A virus-free impedance platform to emulate virus-induced cell fusion

A.-K. Grimm[1]; V. Borggraefe[1]; S. Einhauser[1]; R. Wagner[1] and J. Wegener[1,2]

[1]Universität Regensburg, Regensburg (Germany)
[2]Fraunhofer-Institut für Elektronische Mikrosysteme und Festkörper-Technologien EMFT, Regensburg (Germany)
Anne-Kathrin.Grimm@uni-regensburg.de

Monitoring cell fusion is essential for understanding viral infections and the development of antiviral therapies [1]. While fusion is typically observed by detecting morphological changes or exchange of intracellular materials microscopically [2], this study used impedance spectroscopy to assess cell fusion between two types of HEK293 cells: (i) HEK cells expressing the ACE2 receptor and (ii) HEK expressing the SARS-CoV-2 spike protein upon doxycycline induction. The latter serves as model for SARS-CoV-2 virus. In this project, impedance was monitored focusing on changes associated with cell-cell fusion. We found out that a time-dependent impedance increase at 4 kHz correlates with the extent of cell fusion between HEK-ACE2 and HEK-Spike, therefore, impedance magnitude can be used as a reliable measurand for evaluating cell fusion. In a second approach, we seeded HEK-ACE2 and HEK-Spike cells as co-cultures on electrodes and were able to induce cell-cell fusion at any selected time points by the addition of doxycycline, which served as inducer molecule for the expression of the spike protein in HEK spike cells in our system. Moreover, the intro-duction of anti-SARS-CoV-2 antibodies to the cell mixtures reduced the impedance increase, indicating inhibition of fusion through neutralization of the spike protein. A three-parameter fit model was applied to predict the number of fused cells without the need for staining or microscopy. Our results indicate that cell fusion is completed within 10 hours and involves almost all cells on the electrode. This approach provides a new impedance-based assay for detecting cell fusion in general, fusion as a consequence of viral infection and also to screen and to evaluate neutralizing antibodies with the capacity for high-throughput campaigns.

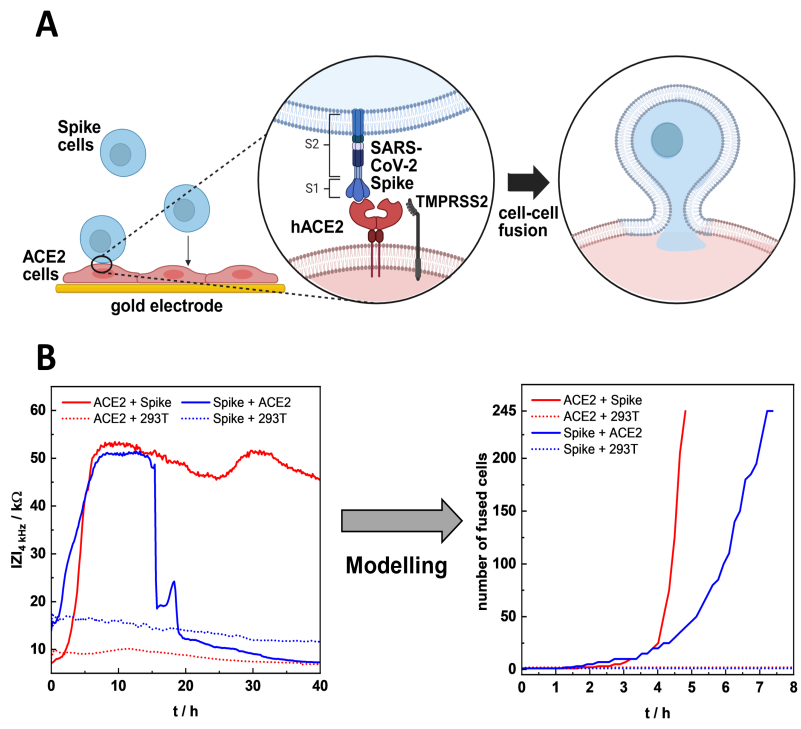

Impedance-based monitoring of receptor-mediated cell-cell fu-sion. **(A)** Schematic of experi-mental setup: cells expressing ACE2 cells are cultured on gold-film ECIS electrodes. Impedance is continuously measured during the addition of HEK cells ex-pressing the SARS-CoV-2 spike protein (or vice versa). Upon contact between the two cell types, membrane fusion – mi-micking the natural viral entry mechanism – is initiated. **(B)** Left: impedance time courses of cell-cell fusion (solid curves) and con-trol conditions (dashed curves). Right: prediction of number of fused cells after 3-parameter modelling. The model only allows for syncytia of ≤245 cells, bigger cell clusters are not predictable yet.

References:

[1] J.M. White and G.R. Whittaker, *Traffic* 17 (2016) 593-614.
[2] S. Martens and H.T. McMahon, *Nat Rev Mol Cell Biol* 9 (2008) 543-556.

Real-Time Monitoring of Pore-Forming Toxin Activity in Live Cells Using High-Throughput Impedance Assays

A.-S. Kittel[1,2]; T. Ensslen[3]; M. Ziller[4]; S. Stölzle-Feix[4]; N. Fertig[4]; J. C. Behrends[3,5] and W. Römer[1,2]

[1] Signalling Research Centres BIOSS and CIBSS, University of Freiburg, Freiburg, Germany
[2] Faculty of Biology, University of Freiburg, Freiburg, Germany
[3] Hahn-Schickard Institute for Microanalysis Systems e.V. Freiburg, Germany
[4] Nanion Technologies GmbH, Munich, Germany
[5] Department of Physiology II, Faculty of Medicine, University of Freiburg, Freiburg, Germany
anna-sophia.kittel@bioss.uni-freiburg.de

Pore-forming toxins (PFTs) are major virulence factors in many pathogens, disrupting cell membrane integrity and causing cell death. Beyond their pathogenic role, they can be harnessed for single-molecule sensing, where they are known as biological nanopores. Their capacity to kill cells by pore formation - sometimes involving specific receptors - also offers promising therapeutic potential, particularly in cancer treatment [1, 2]. However, for many PFTs, the detailed dynamics of action are often not completely understood.
In this study, we applied a high-throughput, label-free impedance assay to investigate the kinetics and cellular effects of two PFTs: SaroL-1 from *Salpingoeca rosetta* [3] and Aerolysin from *Aeromonas hydrophila* [4, 5]. Using cancer cell monolayers, we monitored real-time changes in electrical impedance to assess membrane disruption, cell adhesion, barrier function, and overall cellular health in both H1299 and HT-29 carcinoma cells. The method enabled us to differentiate between fast and delayed toxin activities, providing kinetic profiles of toxin action. Additionally, we examined the receptor specificity of SaroL-1 and Aerolysin towards the glycosphingolipid Gb3 by using Gb3-depleted cells and a specific inhibitor. The AtlaZ impedance platform enabled automated, scalable experiments, demonstrating its utility for screening neutralizing agents and elucidating dose-dependent PFT mechanisms. Our findings highlight impedance sensing as a powerful tool for real-time analysis of PFT-induced cytotoxicity and receptor dependency.

References:

[1] Y. Zhang and C. Cao, “Aerolysin Nanopores for Single-Molecule Analysis,” *Chimia (Aarau)*, vol. 79, no. 1–2, pp. 18–24, Feb. 2025, doi: 10.2533/chimia.2025.18.
[2] F. Piguet *et al.*, “Pore-forming toxins as tools for polymer analytics: From sizing to sequencing,” *Methods Enzymol*, vol. 649, pp. 587–634, 2021, doi: 10.1016/bs.mie.2021.01.017.
[3] S. Notova *et al.*, “The choanoflagellate pore-forming lectin SaroL-1 punches holes in cancer cells by targeting the tumor-related glycosphingolipid Gb3,” *Commun Biol*, vol. 5, no. 1, p. 954, Sep. 2022, doi: 10.1038/s42003-022-03869-w.
[4] I. Iacovache, S. De Carlo, N. Cirauqui, M. Dal Peraro, F. G. van der Goot, and B. Zuber, “Cryo-EM structure of aerolysin variants reveals a novel protein fold and the pore-formation process,” *Nat Commun*, vol. 7, p. 12062, Jul. 2016, doi: 10.1038/ncomms12062.
[5] T. Ensslen *et al.*, “BPS2025 - Quantitative and mechanistic analysis of protein membrane pore formation on a high-throughput electrophysiology platform,” *Biophysical Journal*, vol. 124, no. 3, p. 400a, Feb. 2025, doi: 10.1016/j.bpj.2024.11.2155.

Cell-substrate-fluctuations enable fast and coherent collective migration

A. Janshoff

University of Goettingen, Göttingen (Germany)
ajansho@gwdg.de

Collective cell migration emerges from long-range cell-cell communication governed by factors such as force transmission, the viscoelastic properties of individual cells, substrate interactions, and mechanotransduction. Here, we examine how changes in cell-substrate dynamics, adhesion, and traction forces affect the average velocity and spatiotemporal correlations in confluent monolayers of either wild-type MDCK II cells or highly contractile MDCK II cells depleted of zonula occludens 1/2 (dKD). Our data show that confluent dKD monolayers migrate more slowly than WT cells, which is accompanied by increased substrate adhesion, reduced traction forces, a more compact monolayer morphology, weakened cell-cell interactions, and diminished fluctuations in cell-substrate distance. Furthermore, depleting basal actin and myosin reinforces the idea that short-range cell-substrate interactions—specifically, fluctuations driven by the basal actomyosin cytoskeleton—play a key role in determining collective migration speed at larger scales.

Monitoring of Cellular Spatiotemporal Dynamics via Machine Learning-Enhanced Electrical Impedance Spectroscopy

M. Carrasco-Yague[1,2]; G. Lebedev[2] and A.I. Barakat[1]

[1]LadHyX, CNRS, Ecole Polytechnique, Palaiseau (France); [2]Sensome SAS, Massy (France)
abdul.barakat@polytechnique.edu

Monitoring cellular spatiotemporal dynamics is essential for understanding a broad array of complex biological processes such as organ development during embryogenesis, cellular migration during wound healing, and cellular invasion during cancer progression. Using live-cell fluorescence microscopy to track cellular dynamics is often limited by dye-induced cytotoxicity and cellular photodamage. The goal of the present study is to demonstrate that a platform combining a microelectrode array (MEA), electrical impedance spectroscopy (EIS), and machine learning (ML), as schematically depicted in the figure below, enables real-time monitoring of cellular spatiotemporal dynamics in a noninvasive and label-free manner.

The platform is applied to normal and cancerous breast epithelial cells in either mono- or co-culture, correlating EIS measurements with cell growth parameters obtained from automated microscopy image analysis. An ML model is implemented to accurately predict the spatiotemporal evolution of cell density and size and to classify the different cell types based solely on EIS recordings. The technology is also shown to be capable of tracking pertinent biological processes including spatial heterogeneities in cell proliferation patterns and cell competition in co-culture.

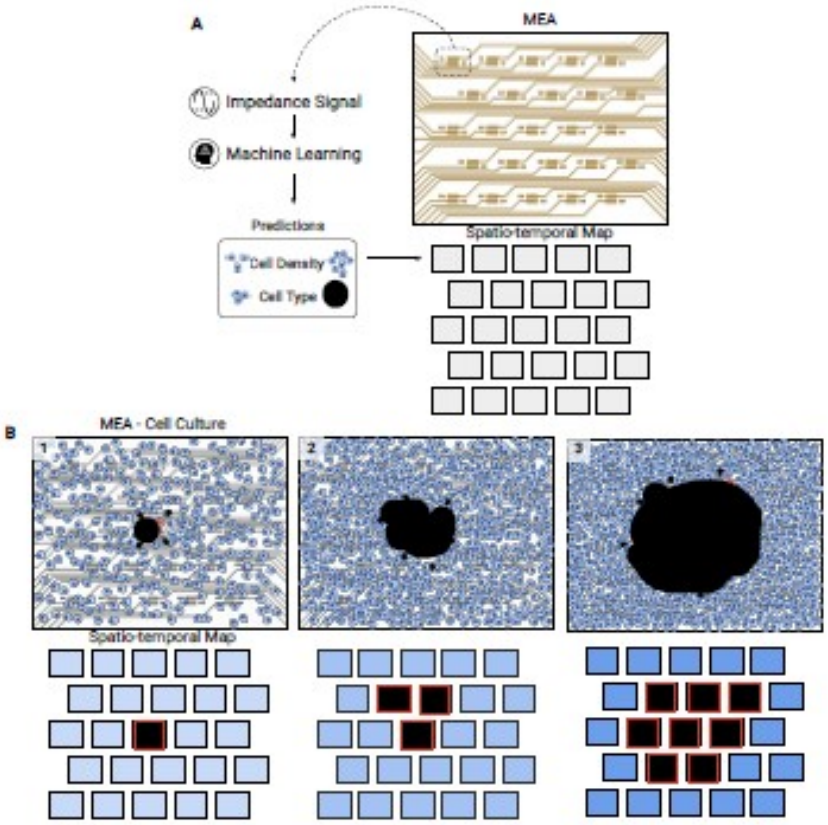

Schematic of the methodology to non-invasively monitor cell spatiotemporal dynamics. (A) An impedance signal is measured at each electrode pair position on the MEA. The signal is processed by a ML model to predict key parameters such as cell density, cell size, and cell type. The information is then used to construct a spatiotemporal map. (B) The system can monitor spatiotemporal patterns of cellular proliferation as well as competition between different cell types. Panels (1-3) correspond to different time points.

Smart Membrane: An On-Chip Cell Sensor for Monitoring Barrier Tissue Supported by an Artificial Neural Network

Bo Tang[1,2]; V. Krajka[1,2]; M. Liu[3]; W. Zhao[1]; S. Reichl[2,4]; A. Dietzel[1,2]

[1]Institute of Microtechnology, Technische Universität Brauschweig, Brauschweig (Germany)
[2]Center of Pharmaceutical Engineering (PVZ), Technische Universität Braunschweig, Braunschweig (Germany)
[3]Institute of Pharmaceutical Technology and Biopharmaceutics, Technische Universität Braunschweig, Braunschweig (Germany)
[4]German Research Center for Artificial Intelligence (DFKI), Kaiserslautern (Germany)
b.tang@tu-braunschweig.de, v.krajka@tu-braunschweig.de

The conventional transepithelial electrical resistance (TEER) technique only yields a single value for assessing cell layers and often requires off-incubator microscopy to reveal further details. Here, we present an electrical cell sensor platform that uses a smart nanoporous membrane for continuous electrical cell-substrate impedance sensing (ECIS). The device features an ultrathin, ultra-low-stress 700 nm Si_xN_y membrane that is monolithically integrated at the wafer-level into an organ on chip system which is sealed with a glass lid (Fig. 1) [1]. Coplanar electrodes interface with custom electronics for impedance measurement under sinusoidal excitation.
Human umbilical vein endothelial cells (HUVECs) were seeded and monitored via impedance spectra, which were corroborated by bright-field and fluorescence microscopy. Nyquist plots captured distinct stages of cell development. We trained a 1D convolutional neural network (Conv1d) to classify the phases of adhesion, spreading, monolayer formation, and barrier maturation. Model validation was achieved through pharmacological perturbation using PN159 and BAC, with >95% confidence in detecting reversible and irreversible barrier disruption. We benchmarked our sensor against conventional immunostaining for tight junction markers and demonstrated substantially higher sensitivity, enabling real-time and non-invasive detection of barrier dynamics.
To contextualize the impedance data, the ECIS spectra and phase descriptions were vectorized using OpenAI's semantic embeddings. A secondary Conv1d then projected both sets of data into a shared latent space, enabling a large language model (LLM) to generate descriptive interpretations of cell states directly from the ECIS data.
This approach allows for the non-invasive and automated monitoring of barrier dynamics in barrier-on-chip systems, eliminating the need for microscopy and endpoint assays. Integrating LLMs also supports intelligent, automated experimental reporting. We envisage its wide applicability in organ-on-chip platforms for real-time physiological and pathological studies.

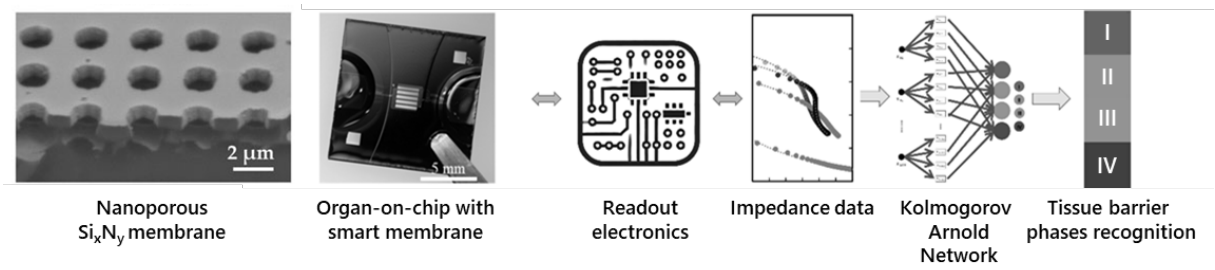

Acknowledgment: This work was funded by the Niedersächsische Landesregierung through the coordinated project "Micro Replace Systems (R2N)".

References:

[1] B.Tang., S. Bendas, V. Krajka, et al., *Frontiers in Sensors* 3 (2022)

A device to measure Electrical Impedance Sensing (EIS): an objective device tool to discriminate Dry Eye, Penfigoid and Sjogren Diseases

Bonetto, F.J.; Acerbo, E.; Bellotti, M.I.; Chehade, P.; Forghes F.; Gongora, N.; Meiling, A.; Saravia, M.

Laboratorio de Cavitación y Biotecnología. Instituto Balseiro, San C. de Bariloche (Argentina)
fabian.bonetto@gmail.com

The objective of this work was to design, build and test a detector that discriminates between normal human eyes and those suffering from dry eye disease (it is estimated that 20% of the world's population suffers from this pathology) using electrical impedance spectral techniques (EIS). For this purpose, we have designed, built and tested a sensor that is applied on the cornea surface accompanied by its corresponding electronics.

The sensor is constructed of biocompatible materials, gold (live) of 0.42 mm diameter, surrounded by a surgical stainless-steel cylinder of 1.3 mm internal diameter and 2.5 mm external diameter (neutral) embedded in a biocompatible resin. The impedance measured is between the live, the neutral, through the tear layer and the cornea.

The electronics excite the sensor with a chirp on voltage and the current is approximately 1 micro-ampere with a series load resistor. The electronics also senses the voltage on the sensor. Finally, it calculates the current flowing through the series circuit, which results in the resistance and capacitance of the sensor as a function of frequency.

This information is used to discriminate on average between normal eyes and eyes with pathologies as seen in the Figure for dry eye, Pemphigoid and Sjogren's pathologies. A clear discrimination is seen between these conditions.

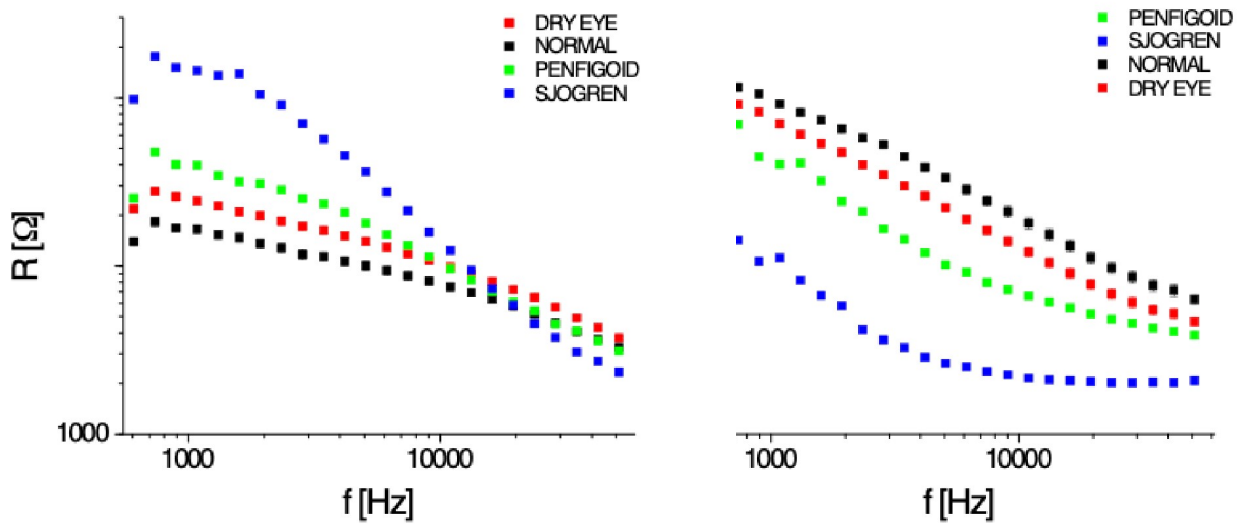

Cell–Electrode Models for Impedance Analysis of Epithelial and Endothelial Monolayers Cultured on Microelectrodes

C.-M. Lo[1]; W.-C Chiu[1]; W.-L. Chen[1]; Y.-T. Lai[2]; Y.-H. Hung[3]

[1]National Yang Ming Chiao Tung University, Taipei, 11221, Taiwan
[2]Research Center for Applied Sciences, Academia Sinica, Taipei 11529, Taiwan
[3]Department of Neurology, University of California, Irvine, CA 92697, USA
chunmin.lo@nycu.edu.tw

Electric cell–substrate impedance sensing (ECIS) provides a powerful, noninvasive method for monitoring the electrical characteristics of epithelial and endothelial cell monolayers cultured on microelectrodes, offering key parameters such as junctional resistance, cell–substrate separation, and membrane capacitance [1,2]. Historically, a three-path model (LGK model), which incorporates two transcellular pathways (apical and basal membranes) and a paracellular pathway through lateral intercellular spaces (LIS), has enabled detailed impedance analysis of epithelial cell layers, such as MDCK [3]. Yet, fitting this model can become challenging due to the six adjustable parameters, particularly the lateral resistance (R_l). To simplify the model fitting, we introduce a **simplified LGK model**, which omits the contribution of LIS resistance (assuming $R_l \ll$ junctional resistance, R_b) and treats the lateral membrane as a lumped impedance. This assumption yields a more tractable model with only five fitting parameters: R_b, α (related to cleft resistance α^2), apical capacitance (C_a), basal capacitance (C_b), and lateral capacitance (C_l) [4].

We demonstrate that this simplified model closely matches experimental impedance spectra measured across a frequency range of 31.25 Hz to 100 kHz for both MDCK and OVCA429 epithelial cell monolayers. Moreover, the model provides insight into how variations in each parameter, particularly C_a and C_b, affect the impedance response. When applied to cell types with substantially lower junctional resistance (e.g., HUVEC endothelial cells and HaCaT keratinocytes), the lateral current pathway becomes negligible. Under this condition, the simplified LGK model further reduces to a **modified two-path GK model**, involving only four parameters: R_b, α, C_a, and C_b. The impedance measurements for these cells closely align with predictions from the two-path model [4].

In summary, this study presents a hierarchy of cell–electrode models, moving from the full LGK model to a simplified five-parameter version and finally to a streamlined four-parameter model, tailored for different cell types depending on their junctional resistance. These models conserve accuracy while easing parameter fitting and interpretation, enhancing ECIS's utility in assessing cell–cell and cell–substrate interactions across diverse monolayer types.

References:

[1] I. Giaever; C.R. Keese, *Nature* 366 (1993) 591–592.
[2] I. Giaever; C.R. Keese, *Proc. Natl. Acad. Sci. USA* 88 (1991) 7896–7900.
[3] C.-M. Lo; C.R. Keese; I. Giaever, *Biophysical Journal* 69 (1995) 2800–2807.
[4] W.-C Chiu; W.-L. Chen; Y.-T. Lai; Y.-H. Hung; C.-M. Lo, *Sensors* 24 (2024) 4214.

Finite Difference Model Representing Cell Distribution in Monolayer

E. Acerbo; M. I. Bellotti and F. J. Bonetto

Universidad Nacional de Cuyo – Instituto Balseiro (Argentina)
Universidad Nacional de Rio Negro – Sede Andina (Argentina)
Consejo Nacional de Investigaciones Ciencia y Técnica – CONICET (Argentina)
esteban.acerbo@ib.edu.ar

In this work we developed a finite difference algorithm to calculate the spectral impedance of any distribution of square cells over an electrode. Allowing to simulate assays evolution, cell death dynamics, different cell morphologies and any electrode shape.

The spectral impedance is calculated as a function of alpha, Rb and Cm. The same parameters proposed by Giaever and Keese to analytically model a confluent culture over an infinite electrode [1]. Using the same parameters allows us to compare the simulation results of a non-confluent culture to its confluent equivalent.

As seen in the Figure, a simulation resume of a culture with 75% alive – 25% dead cells emplaced randomly. The results show the system spectral impedance between the bare electrode (100% dead cells) and GK model (100% alive cells) as expected.

This model is aimed to estimate the cell population above the electrode by contras-ting simulations with experimental measurements. For this it is necessary to simulate different cell distributions or assay evolutions, using a range of parameter to compare before the measurement as each simulation is computationally expensive.

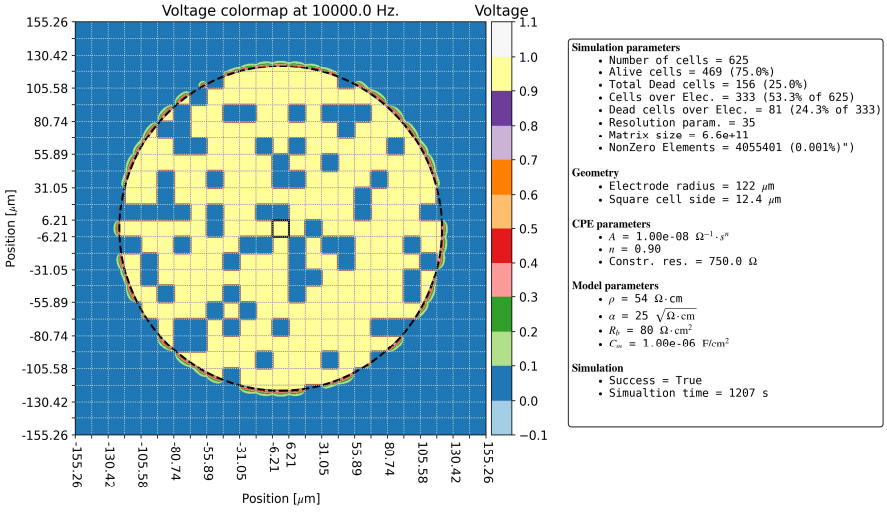

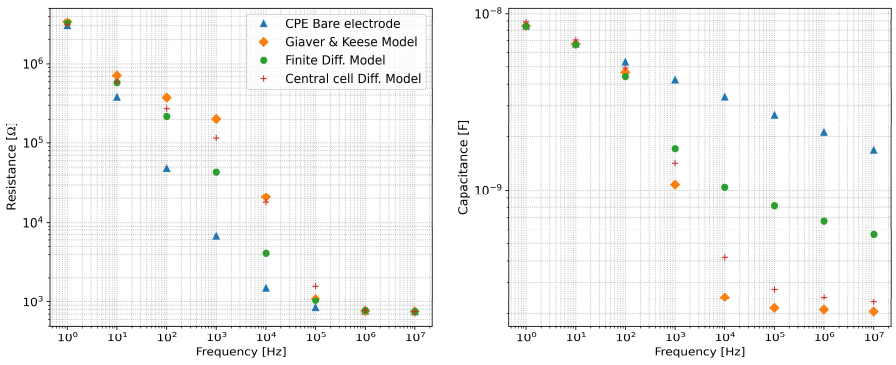

References:

[1] Lo, Chun-Min, Charles R. Keese, and Ivar Giaever. "Impedance analysis of MDCK cells measured by electric cell-substrate impedance sensing." *Biophysical journal* 69.6 (1995): 2800-2807.

Concept for high channel systems for cell sensing

U. Pliquett; C. Gansauge; D.Echtermeyer

Institut für Bioprozess- und Analysenmesstechnik, Heilbad Heiligenstadt (Germany)
uwe.pliquett@iba-heiligenstadt.de

In high-channel electrode systems for parallel impedance measurements on cells and biological tissues, a multiplexer is typically used to sequentially connect all electrodes to the impedance measuring device. This has the disadvantage that, especially with high-channel systems, the complete measurement across all electrodes takes a relatively long time, especially if an entire spectrum is to be recorded. As a result, cell dynamics in the subsecond range can only be achieved selectively over just a few electrodes.
In an alternative concept, the impedance is not directly measured in the frequency domain, but calculated from the relaxation behavior after a voltage step (time domain). The voltage step is applied centrally via a distant electrode, and the current through each electrode of a multi-electrode array is measured.
A special feature of relaxation in biological objects is the exponential decay of the current, which is primarily caused by the charging of membrane structures. Due to the rapid change at the beginning and the increasingly smaller change in the current after the step, it is sufficient to scan quickly at the beginning and then successively increase the intervals between the scanning points. A simple sampling regime of this type would violate the sampling theorem and inevitably lead to nonsensical results. This is counteracted by integration between the sampling points. For this purpose, an integrator is placed behind each electrode. This arrangement has the advantage that all integrators can be started simultaneously, whereby the integrated currents are present at all outputs simultaneously for one integration period. After these voltages have been read, the integrators are reset and integrated over the next period. In practice, four time instances are sufficient for one decade, meaning that only twenty-four sampling points are required to record a spectrum over six decades.
In this way, for example, a multi-electrode array with 10,000 electrodes could be realized [1], in which the impedance spectrum between 5 kHz and 1 MHz can be recorded across all electrodes within one second (8 seconds in the cited paper). Alternatively, individual electrodes can be recorded at a rate of 1,000 measurements per second.

References:

[1] Gansauge, C., K. Schieke, and U. Pliquett. "ECIS with 10,000 Channels–a Feasibility Study on Biofilm Growth." *International Journal of Bioelectromagnetism* 23.2 (2021).

Impedance in real-time monitoring of trophoblast spheroid invasion dynamics and future applications

D. Tang[1], L. Izmaylova[2,3], S. Ingebrandt[1,3], R. Leube[2,3], Z. Gao[1,3],*

[1] Institute of Materials in Electrical Engineering 1 (IWE1), RWTH Aachen University, 52074 Aachen, Germany.
[2] Institute of Molecular and Cellular Anatomy (MOCA), RWTH Aachen University, D-52074 Aachen, Germany.
[3] Mechanobiology in Epithelial 3D Tissue Constructs Graduate School (ME3T), RWTH Aachen, 52074 Aachen, Germany.
ziyu.gao@iwe1.rwth-aachen.de

Electric Cell-substrate Impedance Sensing (ECIS) technology was developed for a primary goal on label-free and non-invasive *in vitro* cell migration detection. However, most existing technologies are limited to single biological component system analyses with constrained resolution, posing challenges for studying more complex biological processes - from adhesion and migration to invasion and differentiation.
In our recent study, invasion of trophoblast derived spheroids through the monolayer of endometrial epithelial Ishikawa cells was investigated. In addition to classic cell proliferation and monolayer formation, a three-component *in vitro* measuring model that composed of electrode-electrolyte, monolayer and spheroid was developed to study spheroid invasion dynamics.
The interface between the spheroid and the Ishikawa monolayer was successfully detected through impedance characteristics. The measuring sensitivity to invasion dynamics was evaluated and visualized by comparing the resistance, capacitance and phase at defined low and high frequency with various spheroid-electrode coverage areas, which also aligns the assumption of biological change. Frequency-dependent semi-quantitative analysis of resistance, capacitance and phase were established to understand the cell-chip behavior over time.
Moreover, we extend *in vitro* equivalent electrical fitting (EEC) model from the conventional electrode-electrolyte double-layer interface theory to a three-component model using impedance-phase spectra. According to EEC fitting, a three-step invasion process was proposed: 1) preinvasion – non-contact condition with an intact cell monolayer, 2) early-stage invasion – spheroid attachment within 6 hours after transfer, and 3) late-stage invasion – 6 to 48 hours after spheroid transfer.
Further development of this technique could expand its scope to more complex biological mechanics sensing involving multiple factors, paving the way for more accurate and intelligent sensing systems for biomedical diagnostic such as cancer invasion and endometrial receptivity.

References:

[1] Wegener, J., Sieber, M. & Galla, H.-J. Impedance analysis of epithelial and endothelial cell monolayers cultured on gold surfaces. Journal of Biochemical and Biophysical Methods 32, 151-170 (1996).
[2] Wegener, J., Keese, C. R. & Giaever, I. Electric cell-substrate impedance sensing (ECIS) as a noninvasive means to monitor the kinetics of cell spreading to artificial surfaces. Exp Cell Res 259, 158-166 (2000).
[3] Jiang, H. et al. Metal-organic frameworks as an active substrate for cell-interaction studies and cell-on-a-chip platforms. Biosensors and Bioelectronics: X 19 (2024).

Impedance spectroscopy as a tool for real-time assessment of stem cell differentiation – a case study using neural stem cells

A. Heiskanen; F. Shah and J. Emnéus

Technical University of Denmark, Kgs. Lyngby (Denmark)
arhe@dtu.dk

Application of stem cells in different research areas, including biomedical engineering, has received an extensive focus during the past years. However, considering the diverse origin of stem cells, the protocols and biochemical processes involved, leading to the desired phenotype, vary from application to application. This presentation will focus on differentiation of neural stem cell models that have been designed to generate dopaminergic neurons applicable for cell replacement therapy of Parkinson's disease. To characterize the dopaminergic properties of differentiated neural stem cells, we have designed interdigitated electrode arrays that allow real-time monitoring of the cells' ability to release dopamine upon cell membrane depolarization. The designed electrode arrays have been used in both batch-based and microfluidic devices that facilitate initial cell culturing followed by cell differentiation. The goal to monitor the progress of stem cell differentiation on the electrode arrays without a need for continuous microscopic observations led to the interest in developing an impedance-based assay that would allow to assess the time point when the cell differentiation had been completed as well as to determine what electrodes in an electrode array had a fully developed cell population ready for monitoring dopamine release. Differentiation of neural stem cells starts from a population of adherent fusiform cells at a low cell density. Exposure to epigenetic factors leads to extensive formation of a dense neurite network that is not adherent to the culture substrate. The obtained results indicated that unlike our other applications of impedance-based monitoring of cellular behavior related to confluent monolayers of cancer cells (cytotoxicity of chemotherapeutic substances [1], effect of xenoestrogens [2], and cell invasion [3]), differentiation of neural stem cells required acquisition of complete impedance spectra combined with equivalent circuit analysis. Figure 1 shows the characteristic equivalent circuit model that describes the behavior of differentiating neural stems cells [4]. Our previous studies on the differentiation process of neural stem cells have shown the diverse aspects related to changes in gene expression, leading to synthesis of proteins that are characteristic of the differentiation outcome, i.e., dopaminergic neurons. However, from the point of view of impedance-based monitoring of cell differentiation, the obtained results indicated that the primary aspect that led to the characteristic impedance behavior was related to the distinct morphological changes when the neural cytoskeleton, composed of β-tubulin, was being formed. Overall, we can conclude that impedance-based monitoring can reveal details of stem cell differentiation and serve as a tool to assess the progress of differentiation. However, each type of stem cell application and type of stem cell requires thorough characterization of impedance behavior during differentiation. No generic impedance assay protocol automatically fits all stem cell applications.

References:

[1] C. Caviglia; K. Zór; L. Montini; V. Tilli; S.Canepa; F. Melander; H.B. Muhammad; M. Carminati; G. Ferrari; R. Raiteri; A. Heiskanen; T. Andresen; and J. Emnéus, *Anal. Chem* 87 (2015) 2204-2212.

[2] N. Pupinyo; C. D'Costa; A. Heiskanen; W. Laiwattanapaisal and J. Emnéus, *ACS EST Water* 2 (2022) 446-456.

[3] N. Pupinyo; A. Heiskanen; C. Orawon; L. Gorton; J. Emnéus and W. Laiwattanapaisal, Sens. Biosensing Res. 29 (2020) 100354.

[4] F. Shah; C. Caviglia; K. Zór; M. Carminati; G. Ferrari; M. Sampietro; A. Martínez-Serrano; J. Emnéus and A.R. Heiskanen, *J. Electr. Bioimp.* 12 (2021) 34-49.

Impedance-guided Evaluation of Cancer Therapy: A new route for personalized medicine?

S. Knafl[1]; N. Karami[1]; S. Kigilli[1]; L. Ermoneit[1]; N. Pruggmayer[1]; F. Delic[1]; M. Kerbler[1]; F. Azizian[1]; A. Katthab[2]; G. Zeck[2]; S. Prado Lopez[1]; H. D. Wanzenboeck[1]

[1]TU Wien, Institute for Solid State Electronics, 1040 Vienna, Austria
[2]TU Wien, Institute for Bioelectronics, 1040 Vienna, Austria
Heinz.Wanzenboeck@tuwien.ac.at

The rise of personalized medicine promises individualized therapies with higher treatment success rates. Patient-derived microtissues and cell spheroids are central to this approach, enabling custom-tailored cancer treatments specific to a patient's tumor phenotypes. Even patient-specific tumor heterogeneity can be addressed. This creates a need for non-destructive, label-free technologies to assess tumor growth and test therapies before clinical use.
We present an impedance-based cellular assay (IBCA) for evaluating anti-tumor therapy on 3D tumor spheroids, and finally patient-derived microtumors. A custom chip with four independent microwells, each containing six sensors, allows simultaneous study of up to 24 spheroids and four treatment conditions. Each sensor units consist of planar interdigitated electrodes optimized to measure impedance of spheroids. Positioning the 3D cell constructs on top of the electrodes is challenging, but essential for high sensitivity. We have tested additional placement structures and will summarize the results and further improvements.

In an initial validation using Triton X-100, a membrane-permeabilizing reagent, the cellular response to drug exposure was studied. Ongoing studies are investigating the effect of established chemotherapeutics, such as 5-fluorouracil, on tumor spheroids, and recent results will be discussed. Finally, we will give an outlook on our ultimate goal of analyzing patient-derived microtumors by electrochemical impedance spectroscopy (EIS) to monitor the effects of CAR-T cell therapies and present some of the first promising results.

Concluding, the developed chip has been successfully for real-time, label-free monitoring of the multi-cellular tumor spheroids. We propose that in future such *in vitro* tumor models provide patient-specific insights as label-free tool for personalized therapy of tumor patients.

Figure 1: Left: Microscope image of a single well with six IDES sensors (E1-E6), 24 hours after seeding three HT-29 spheroids onto electrodes E1, E4, and E6. Right: Normalized impedance amplitude spectra of the spheroid-free (E2, E3, E6) and spheroid-covered (E1, E4, E5) sensors, The presence of spheroids causes an impedance increase.

References:

[1] Gamal W., Wu H., Underwood I., Jia J., Smith S. and Bagnaninchi P. O. Impedance-based cellular assays for regenerative medicine, Phil. Trans. R. Soc. B37320170226 http://doi.org/10.1098/rstb.2017.0226

Ready-to-use Insect cell-based Sensor for Pesticide Testing

S. Friedrich[1,2]; N. Malagimani[1]; S. Michaelis[2]; J. Wegener[1,2]

[1]Universität Regensburg, Regensburg (Germany)
[2]Fraunhofer Institute for Electronic Microsystems and Solid State Technologies EMFT; Cell-Based Sensor Technology, Regensburg (Germany)
Sandra.friedrich@uni-regensburg.de

In-vitro systems enable faster, simpler and more cost-effective testing of pharmaceuticals, chemicals, or pesticides, while also helping to reduce ethical concerns associated with animal testing.[1] To truly benefit from these advantages, ready-to-use, stockpiled cell systems are essential since conventional cell culture work is time-consuming, requires trained personnel and demands special equipment. [2]
Here, we present a ready-to-use sensor platform for the detection of harmful effects of pesticides on insects that is based on insect cells frozen inside the wells of multi-electrode arrays. Pesticides contribute largely to the decline of insect populations which poses a significant threat to human life due to reliance on insect pollination for food production.

Model insect cells (here Sf21 cells derived from *Spodoptera frugiperda* and Kc167 cells from *drosophila melanogaster*) are cryopreserved directly on thin gold-film electrodes of 8W10E electrode arrays. Cells can be stored assay-ready in suspension in frozen state at –80 °C and thawed on demand for pesticide testing. [3] Harmful impacts of pesticides have been detected in less than 1 hour assay time. Results are in good agreement with those recorded in experiments using living insects. Studies using the model pesticide Banvel M demonstrated that sensitivity of the ready-to-use assay and cell viability are maintained for at least one year. Further assay simplification by automation of pesticide testing has been accomplished through the development of the benchtop device KERMIT (Kinetics of Ecotoxicological Responses Measured with Insect Tests), developed in collaboration with Fraunhofer EMFT, Munich. Using KERMIT, thawing, sample addition and connection to the ECIS device are fully automated, enabling the cell-based assay to be performed easily by anyone, anywhere.

References:

[1] M. C. J. Chang; F. B. Grieder, *Lab animal*, 53 (2024) 295–297.
[2] O. Wehmeier; A. Loa, *Methods Mol Biol.,* 2095 (2019) 17–25.
[3] S. Friedrich; N. Malagimani, S. Michaelis, and J. Wegener, *Appl Res.* 3 (2024).

Poster Presentations

Finite Difference Model Representing Cell Distribution in Monolayer

E. Acerbo; M. I. Bellotti and F. J. Bonetto

Universidad Nacional de Cuyo – Instituto Balseiro (Argentina)
Universidad Nacional de Rio Negro – Sede Andina (Argentina)
Consejo Nacional de Investigaciones Ciencia y Técnica – CONICET (Argentina)
esteban.acerbo@ib.edu.ar

In this work we developed a finite difference algorithm to calculate the spectral impedance of any distribution of square cells over an electrode. Allowing to simulate assays evolution, cell death dynamics, different cell morphologies and any electrode shape.

The spectral impedance is calculated as a function of alpha, Rb and Cm. The same parameters proposed by Giaever and Keese to analytically model a confluent culture over an infinite electrode [1]. Using the same parameters allows us to compare the simulation results of a non-confluent culture to its confluent equivalent.

As seen in the Figure, a simulation resume of a culture with 75% alive – 25% dead cells emplaced randomly. The results show the system spectral impedance between the bare electrode (100% dead cells) and GK model (100% alive cells) as expected.

This model is aimed to estimate the cell population above the electrode by contras-ting simulations with experimental measurements. For this it is necessary to simulate different cell distributions or assay evolutions, using a range of parameter to compare before the measurement as each simulation is computationally expensive.

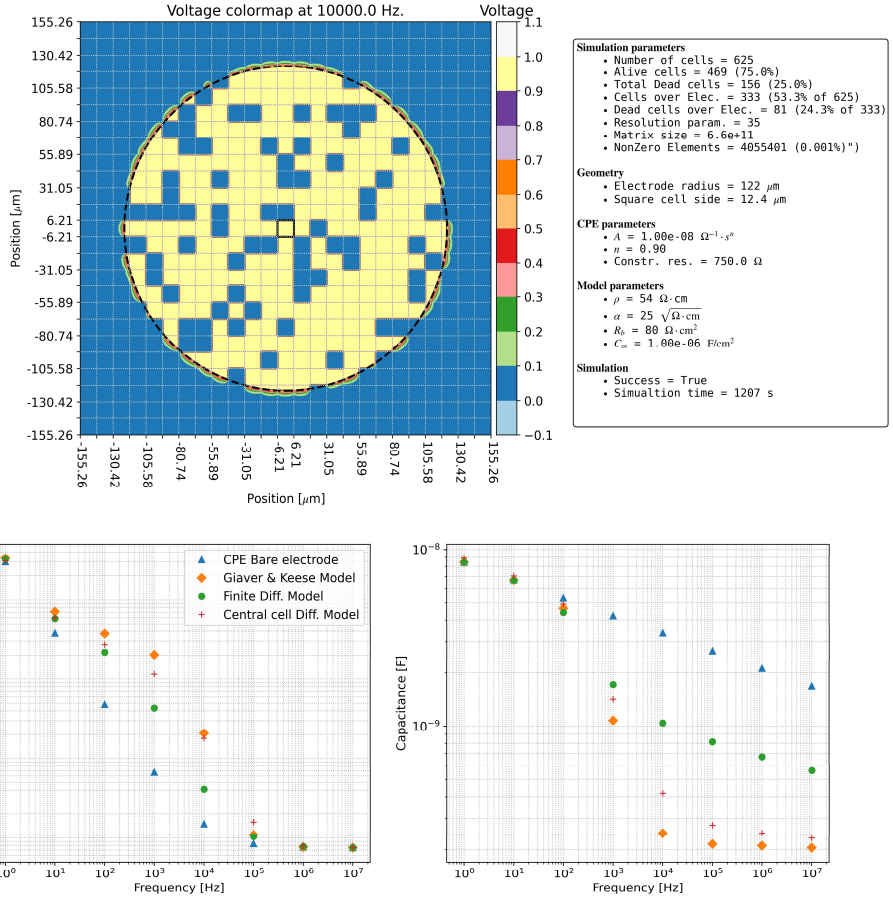

References:

[1] Lo, Chun-Min, Charles R. Keese, and Ivar Giaever. "Impedance analysis of MDCK cells measured by electric cell-substrate impedance sensing." *Biophysical journal* 69.6 (1995): 2800-2807.

A Versatile, Biomimetic, 3D Electrochemical Device for Monitoring Cell Growth and Epithelial Barrier Integrity

R. Acharya; D.v. Niekerk; M. Lopez Cavestany and R.M. Owens

University of Cambridge, Cambridge (United Kingdom)
ra646@cam.ac.uk

Three-dimensional (3D) cell culture and in-vitro bioelectronic systems have advanced significantly in recent years, offering new capabilities for monitoring and predicting biological activity in a variety of applications. While bioelectronic devices such as impedance sensors and electrochemical transistors have traditionally been based on two-dimensional (2D) organic semiconductor films, tissue engineering has developed 3D culture platforms—such as porous scaffolds, hydrogels, and fibre meshes—that better replicate native tissue architecture and physiology.

In this work, we present a novel bioelectronic device that integrates these two domains. The device is built around a 3D microporous scaffold based on the conducting polymer PEDOT:PSS, serving both as a biologically relevant substrate and as an active electronic interface. The scaffold functions as a transmembrane structure that hosts multiple cell types, enabling the formation of stratified tissue models, while simultaneously transducing biological (ionic) signals into readable electrical outputs.

We demonstrate the design, fabrication, and electrical characterization of this transmembrane bioelectronic platform, which combines dual sensing modalities: electrochemical impedance spectroscopy (EIS) for monitoring epithelial barrier formation and integrity, and organic electrochemical transistor (OECT) operation for real-time tracking of cell growth and extracellular matrix (ECM) deposition in 3D.

Using fibroblast cultures as a model, we monitored tissue development over a 10-day period. Changes in drain current provided a quantitative readout of cell proliferation and ECM accumulation. We evaluated the influence of initial seeding densities (125k, 250k, and 500k cells), observing distinct patterns of cell migration, proliferation, and matrix remodeling, which were corroborated with biological assays including immunofluorescence imaging and DNA quantification.

Additionally, we used EIS to monitor epithelial layer formation and barrier integrity over time and correlated this with the underlying fibroblast dynamics, demonstrating the device's ability to support and assess multi-layered tissue constructs.

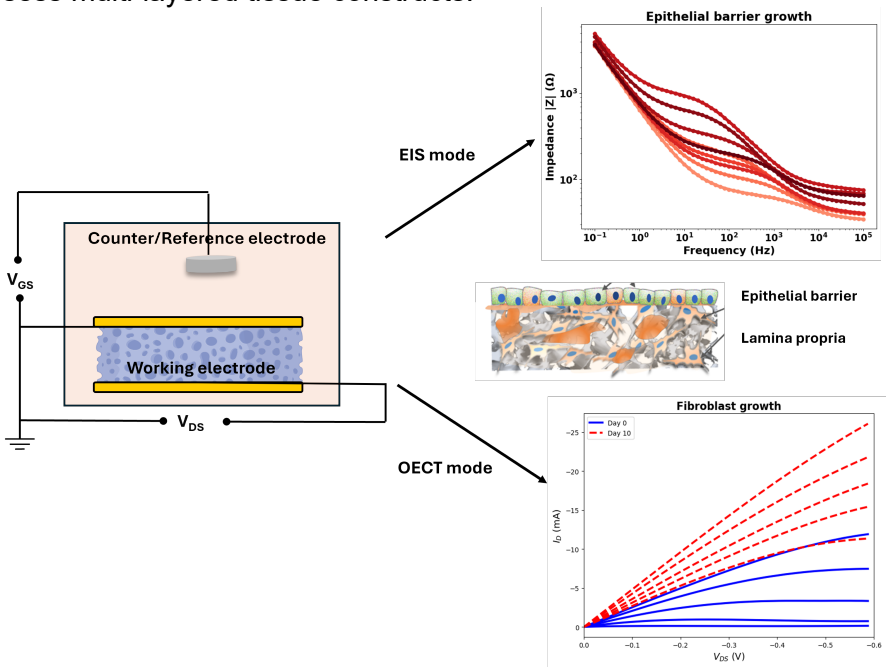

Biomechanics of single cells using a microfluidic device to correlate transients of flow impedance and electrical impedance

O. Alalul[1]; J. Liu[2]; M. Böl[2]; A. Al-Halhouli[3] and A. Dietzel[1]

[1]Technische Universität Braunschweig, Institute of Microtechnology; Braunschweig (Germany)
[2]Technische Universität Braunschweig, Institute of Mechanics and Adaptronics, Braunschweig (Germany)
[3]German Jordanian University, Department of Mechatronics Engineering, Amman (Jordan)
osama.alalul@tu-braunschweig.de

Understanding cellular mechanics is fundamental for advancing developmental biology and reproductive medicine. However, conventional techniques such as atomic force microscopy and micropipette aspiration, while informative, are constrained by limited throughput [1]. To address this, we present a novel microfluidic device that enables real-time, impedance-based biomechanical characterization of single oocytes under flow. The system integrates three coplanar microelectrodes (E1, E2, E3) (Figure 1) within a constriction microchannel, allowing simultaneous mechanical deformation and electrical impedance measurement as cells transit through the chip. Impedance signals were acquired using a lock-in amplifier and current amplifier across a range of frequencies at 0.700 Vrms. Differential impedance readings between electrode pairs (E1–E2 and E2–E3) reflected variations in cell deformation and depth of penetration into the constriction channel. System calibration was performed using deformable hydrogel spheres, with impedance responses validated relative to distilled water. The use of SU-8-based microfluidic chips provided smooth channel surfaces and stable electrode performance, ensuring reproducibility and signal integrity under varying pressure conditions. This platform enables dynamic, label-free, and non-invasive assessment of oocyte biomechanics, establishing correlations between mechanical deformation and impedance responses. Unlike previous studies that focused on somatic cells, our system is specifically designed to accommodate the sensitivity of reproductive cells, broadening the applicability of impedance cytometry in reproductive biology. Our findings highlight the potential of this technique as a high-throughput screening tool for evaluating oocyte mechanical properties, with implications for diagnostics and assisted reproductive technologies.

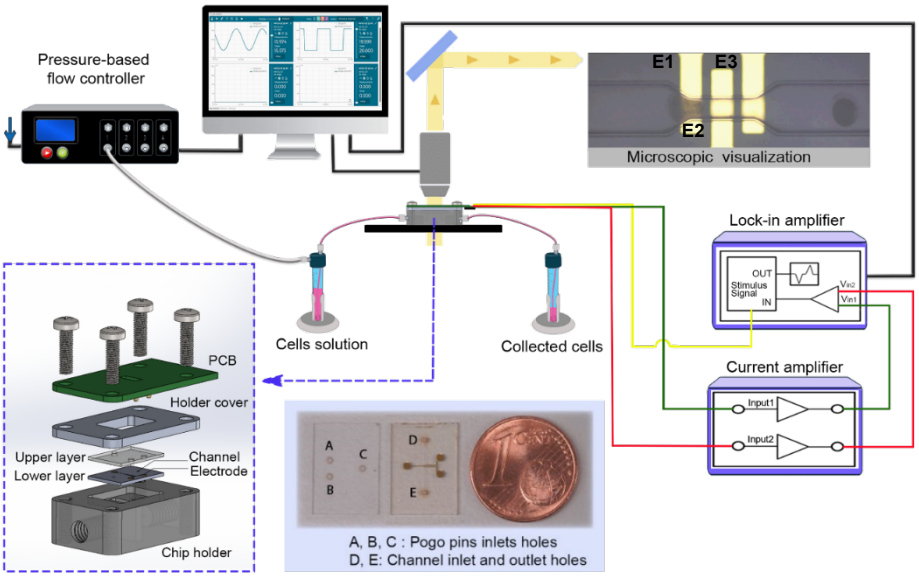

Figure 1: Schematic of the experimental setup.

References:

[1] Y. Chen, K. Guo, L. Jiang, S. Zhu, Z. Ni, and N. Xiang, "Microfluidic deformability cytometry: A review," Talanta, vol. 251, p. 123815, 2023, doi: 10.1016/j.talanta.2022.123815.

Detection of cell occupation on Cochlear Implants (CI) for long-term monitoring of stimulation efficiency

M.B. Bhavsar[1]; M. Sehlmeyer[2]; Y. Roger[3]; A. Hoffmann[3]; N. Prenzler[1]; A. Kral[1]; S. Zimmermann[2]; H. Maier[1]

[1]Department of Otolaryngology (NIFE), Hannover Medical School, Hannover, Germany
[2]Institute of Electrical Engineering and Measurement Technology, Leibniz University Hannover, Germany
[3]Clinic of Orthopaedic Surgery (NIFE), Hannover Medical School, Hannover, Germany
bhavsar.mit@mh-hannover.de

Cochlear implants (CIs) have proven to be highly effective neural prostheses, widely used to restore hearing in individuals with sensorineural hearing loss. However, following implantation, CIs can trigger an immune response that leads to cell layer formation (fibrosis) in the cochlea causing low stimulation efficiency and suboptimal clinical outcomes. Electrochemical Impedance Spectroscopy (EIS) offers a powerful method for assessing the functionality of CI both during and after surgery. However, its full potential, particularly in analyzing the electrical properties of CIs, detecting the cell layer and distinguishing between different cell types, remains unutilized. This study aims to develop and validate an equivalent electrical circuit (EEC) model that accurately represents the electrical properties of CI electrodes and can reliably detect formation of cell layer on a CI electrode array.

The study involves four CI electrode arrays from different manufacturers (MED-EL, Advanced Bionics, Oticon, and Cochlear). Impedance measurements were conducted using an HP4192A impedance analyzer in a frequency range from 5 Hz to 13 MHz. The electrical equivalent circuit (EEC) of the CI electrodes was modelled, involving linear elements, as well as the electrode-electrolyte interface, using two non-linear bilayer models (Cole-Cole and Schwan-Faraday). A layer of human mesenchymal stromal cells (MSCs) was developed on the CI electrodes and impedance measurements were conducted to analyze changes in the impedance.

A general nonlinear electric element circuit model applicable to all types of CIs was derived that allows the determination of local impedances between neighboring CI array electrodes with an accuracy of < 10%. Our cell layer experiments demonstrated a clear increase in impedance across the frequency range when a layer of cells was present on the CI electrode. This increase was reversed after enzymatic cleaning, confirming that the observed impedance changes were due to the cell layer. These findings validate the use of impedance spectroscopy for detecting biological layers on cochlear implant electrodes.

In conclusion, our study developed and validated an EEC model to describe the electrical properties of CI electrode arrays along with its ability to detect presence of cell layer on CI electrodes using precision impedance spectroscopy. Our findings underscore the potential of modelling and identifying the coverage of electrodes with biological material using impedance spectroscopy.

This work has been funded by the Deutsche Forschungsgemeinschaft (German Research Foundation) SFB/TRR 298 SIIRI Project ID 426335750 as well as under Germany's Excellence Strategy "Hearing4all" EXC 2177/1 Project ID 390895286.

Fish cell-based detection of ecotoxicological effects and development of a ready-to-use cell-based sensor

L. Bruckbauer[1]; S. Friedrich[1,2]; S. Michaelis[2]; J. Wegener[1,2]

[1]Universität Regensburg, Regensburg (Germany)
[2]Fraunhofer EMFT, Cell-Based Sensor Technology, Regensburg (Germany)
Laureen.bruckbauer@chemie.uni-regensburg.de

Due to the widespread use of plastics and their extended environmental persistence, plastic residues are now found everywhere in the environment. When polymer additives such as Bisphenol A (BPA), that has been frequently used as a plasticizer, enter aquatic ecosystems, they end up leaching in water and accumulating in aquatic organisms [1]. Cell-based assays have become a widely used, versatile, and effective tool for assessing the potential ecotoxicological effects of plastics, polymer additives, pesticides, and other harmful substances on aquatic organisms. Such cell-based sensors typically provide fast readouts. When the sensor cells are stored in frozen state in multi-well plates used to conduct the assay, compound testing is separated from producing the sensor cells by routine cell culture work and independent thereof [2]. The latter offers many practical advantages.
Here, we present an assay based on *rainbow trout gill cells* (RTgill-W1) that were grown in ECIS (electric cell-substrate impedance sensing) electrode arrays to detect concentration- and time-dependent toxicity [3] of two model compounds: *BPA* and the well-known pesticide *RoundUp*. These substances cause reproductive disruption, feminization of males, developmental toxicity, and, in severe cases, mortality in aquatic ecosystems. Initially, the assay has been conducted with fresh cells, i.e. no cryopreservation was involved.
RTgill-W1 cells were seeded on ECIS gold-film electrodes. Substances under test were added in different concentrations 48 h after inoculation and acute toxicity is measured by time-resolved impedance readings. For BPA, EC_{50} values of 89 µM were determined in presence of 10 % (v/v) fetal bovine serum (FBS) and 40 µM in its absence. Accordingly, in absence of FBS the cells are more sensitive to chemical insults. It is noteworthy, that the bioactive concentrations of BPA were significantly higher in these assays than reported in assays addressing endocrine disruption. Environmental BPA concentrations in polluted surface waters are between 0.1 and 10 nM [4]. High levels – exceeding 0.1 µM – are only observed near industrial sites or wastewater treatment plant discharges. In most aquatic environments, BPA concentrations remain well below these thresholds [5]. For RoundUp, EC_{50} values ranged from (12 ± 1) mM in presence of FBS compared to (4 ± 1) mM without FBS. In agriculturally contaminated freshwater, RoundUp concentrations are generally below 0.03 mM, typically even under 0.001 mM. [6] Thus, the real-world concentrations do not have any direct impact on RTgill-W1 cell physiology. Current research aims to freeze the cells on the electrode arrays for long term storage combined with immediate availability after thawing.

References:

[1] W. Schwarz et al. (2023): Chemical and toxicological assessment of leachates from UV-degraded plastic materials using in-vitro bioassays. In: *PeerJ*, p. 1-26.
[2] K. A. Finlayson; F. D. L. Leusch; J. P. van de Merwe (2022): Review of ecologically relevant *in vitro* bioassays to supplement current *in vivo* tests for whole effluent toxicity testing - Part 1: Apical endpoints. In: *Science of the total environment* (851).
[3] J. Wegener; C. R. Keese; I. Giaever (2000): Electric Cell–Substrate Impedance Sensing (ECIS) as a Noninvasive Means to Monitor the Kinetics of Cell Spreading to Artificial Surfaces. In: *Experimental Cell Research*, p. 158-166.
[4] https://www.umweltbundesamt.de/themen/neue-grenzwerte-für-massenchemikalie-bisphenol-a. Accessed 8.08.2025.
[5] B. Petrie et al. (2019): Assessment of bisphenol-A in the urban water cycle. In: *Science of the total environment*, p. 900-907.
[6] B. Bastos Gonçalves et al. (2019): Ecotoxicology of Glyphosate-Based Herbicides on Aquatic Environment. In: *IntechOpen*, p. 10-108.

Combining TEER and high-resolution spatial impedance mapping on porous MEA for improved *in vitro* barrier measurements

I. Carmans[1,2]; S. E. Takalloo[2]; C. Campanella[2]; D. V. Ibanez[2]; C. Diacci[2]; C. R. Domingo[2] and D. Braeken[2]

[1]KU Leuven, Leuven, Belgium
[2]imec, Leuven, Belgium
ina.carmans@imec.be

Accurate assessment of barrier integrity is vital for evaluating tissue barriers *in vitro*. While transepithelial and transendothelial electrical resistance (TEER) enable real-time, non-destructive quantification of barrier tightness on porous supports (Figure 1a), it only provides a single value of barrier tightness per time point. These single-value measurements mask cellular heterogeneity and may miss localized disruptions. To address this shortcoming, microelectrode arrays (MEAs) offer high spatial resolution impedance measurements [1] (Figure 1b). However, their conventional fabrication on solid, non-porous substrates restricts their integration in multi-compartment organ-on-chip models.

To overcome this issue, we developed a novel silicon-based porous microelectrode array (pMEA) comprising an 11 x 11 grid of titanium nitride (40µm diameter) electrodes. The pMEA is integrated into a Transwell-like setup and includes an additional large electrode in the top and bottom compartments, enabling simultaneous TEER measurements (Figure 1c).

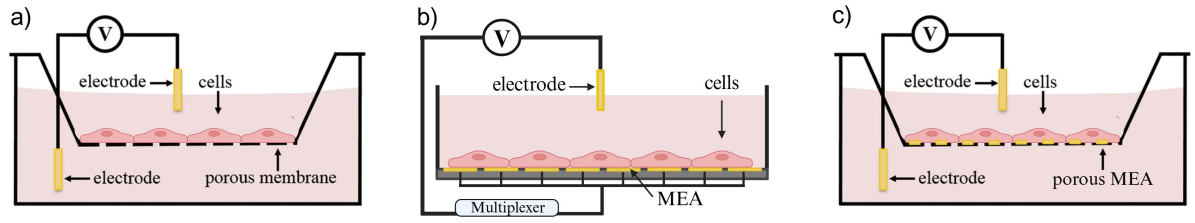

Figure 1: Conventional Transwell setup for measuring TEER (a). MEA for measuring cellular impedance (b). In-house developed Transwell setup with integrated porous MEA (pMEA) for simultaneous measurements of TEER and cellular impedance (c).

Endothelial cells (HUVECs) were cultured directly on the pMEA to monitor barrier formation. TEER gradually increased to 8.5 ± 1.8 Ω·cm^2, while the average pMEA impedance at 1 kHz increased from (1.5 ± 0.02) × 10^4 Ω to (9.1 ± 1.2) × 10^4 Ω. The spatial variability, defined as the coefficient of variation for the pMEA impedance across electrodes, decreased from 34 ± 11 % to 22 ± 2 % after 6 days, indicating that HUVECs remain heterogeneous even after maturation. Upon barrier disruption with biological agents such as tumor necrosis factor alpha (TNF-α), both TEER and pMEA impedance decreased. More interestingly, the pMEA spatial variability increased from 17 % to 33 %, revealing uneven barrier disruption, a feature not captured by TEER measurements alone.

Our results underscore the ability of the pMEA to capture barrier spatial heterogeneity in multicompartment setups, a critical feature for understanding disease mechanisms and one that is beyond the capabilities of traditional Transwell and TEER-based technology. In conclusion, the novel pMEA offers a powerful platform for investigating vascular and gut barrier function, enabling detailed study of dynamic processes such as pathogen translocation, immune cell migration and cancer cell metastasis.

References:

[1] Venz A., Duckert B., Lagae L., Takalloo S.E., Braeken D. *Sci Rep* 15, 1592 (2025). https://doi.org/10.1038/s41598-025-85783-9

Alleviation of LPS-induced Endothelial Dysfunction with Bone Morphogenetic Protein 10

Y.-L. Chen[1]; W.-K. Yu[2]; W.-L. Chen[1]; C.-M, Lo[1]

[1]National Yang Ming Chiao Tung University, Taipei, Taiwan
[2]Department of Chest Medicine, Taipei Veterans General Hospital, Taipei, Taiwan
410170327@gms.tku.edu.tw

Endothelial dysfunction and injury are critical factors in the development of acute lung injury/acute respiratory distress syndrome (ALI/ARDS). Bone morphogenetic protein 10 (BMP10), which is primarily produced in the right atrium and released into the bloodstream, has been shown to promote vascular endothelial development and proliferation, maintain quiescence, and prevent apoptosis. BMP10 is also a valuable biomarker for predicting the onset of various conditions, such as pulmonary arterial hypertension, recurrent atrial fibrillation, decompensated liver cirrhosis, and ischemic stroke. However, it remains unknown whether BMP10 plays a role in regulating inflammation-induced ALI.

To validate BMP10 as a protective factor contributing to the maintenance of endothelial barrier function, human pulmonary microvascular endothelial cells (HPMECs) were cultured on 8W1E and 8W10E array wells and measured using electrical cell-substrate impedance sensing (ECIS) [1]. Once reaching confluence, HPMECs were subjected to culture with or without BMP10 at a concentration of 10 ng/mL for 24 hours. Subsequently, they were stimulated with LPS at a concentration of 10 μg/ml, and endothelial permeability was monitored continuously for 48 hours by measuring impedance spectra via ECIS. The application of LPS resulted in a reduction in the resistance of the HPMEC monolayer, as detected by ECIS, indicating the disruption of the endothelial barrier. In contrast, BMP10 treatment exhibited a mitigating effect on the increased endothelial permeability induced by LPS. Our data, combined with other biochemical results, suggest that BMP10 is an effective protective factor in ameliorating LPS-induced endothelial dysfunction and injury [2].

References:

[1] D. Opp; B. Wafula; J. Lim; E. Huang; J.-C. Lo, C.-M. Lo, *Biosensors and Bioelectronics* 24 (2009) 2625–2629.

[2] W.−K. Yu; W.−C. Chen; H.−C. Shen; C.−Y. Sun; H.−J. Yu; V. Y.−F. Su; K.−Y. Yang, *Journal of Translational Medicine* 23 (2025) 755.

Application of ECIS to Assess WI38 Cell Migration under BMP10 Treatment and Bleomycin Stimulation

T.-Y. Chiu; W.-L. Chen; C.-M, Lo

National Yang Ming Chiao Tung University, Taipei, Taiwan
tiffany150160@gmail.com

Electric cell-substrate impedance sensing (ECIS) is a quantitative and label-free method that enables the sensitive monitoring of morphological changes in adherent cells in vitro. In this study, human pulmonary fibroblasts (WI38) were cultured on 8W1E array wells to evaluate fibroblastic migration following BMP10 treatment, BLM stimulation, and their combination. After the cells reached confluence, they were treated with or without BMP10 (10 ng/mL) for 24 hours. Subsequently, they were stimulated with bleomycin at various concentrations, from 1 μg/ml to 100 μg/ml, for an additional 24 hours, and fibroblastic migration was monitored using the ECIS wound-healing assay [1,2]. To induce controlled wounds on the cell monolayer, a high-current pulse (1.4 mA at 40 kHz) was applied for 10 seconds, causing localized cell death and detachment from the sensing electrode. This electrical wound resulted in a quick drop in resistance, indicating a cell-free electrode state. After wounding, viable fibroblasts at the periphery migrated inward to repair the damaged area, and the measured resistance gradually increased. The rate of wound recovery migration is inversely proportional to T50, defined as the halfway recovery time from baseline to plateau. Our results demonstrated concentration-dependent cytotoxic effects of bleomycin on the proliferation and migration rate of WI38 cells. Additionally, the pretreatment of BMP10 mitigated the cytotoxic effect of bleomycin on WI38 cells.

References:

[1] C.R. Keese; J. Wegener; S.R. Walker; I. Giaever, *Proc. Natl. Acad. Sci. USA* 101 (2004) 1554-1559.
[2] S.-P. Chiu; Y.-W. Lee; L.-Y. Wu; T.-H. Tung; S. Gomez; C.-M. Lo; J.-Y. Wang, *Sensors* 19 (2019) 3210.

Revealing Cellular Signaling Dynamics with Light-Activated Molecules: From Receptor Ligands to Second Messenger

J. Erl[1]; C. Haag[1]; B. König[1]; J. Wegener[1,2]

Faculty of Chemistry and Pharmacy, University of Regensburg, 93053 Regensburg (Germany)
Frauenhofer Research Institution for Microsystems and Solid State Technology EMFT, Division Cell-Based Sensor Systems, 93053 Regensburg (Germany)
julia.erl@chemie.uni-regensburg.de

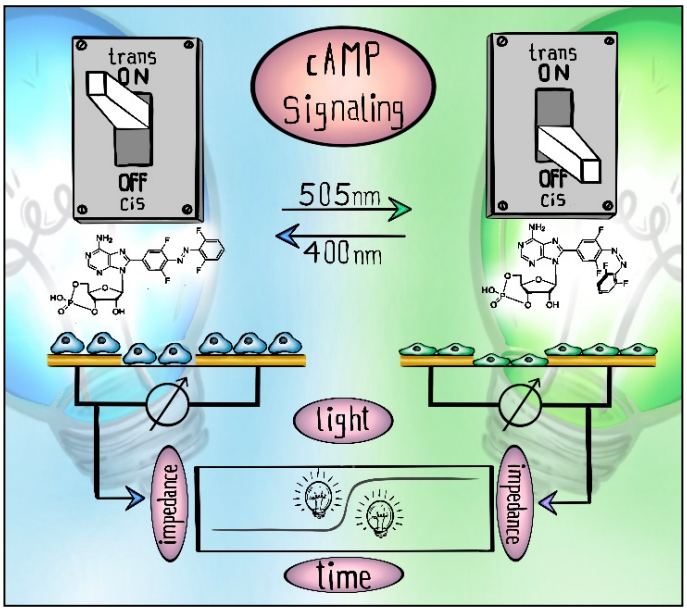

Figure 1 : Schematic illustration of the measurement principle. Cells cultured on gold-film electrodes are stimulated with photochromic molecules, such as cAMP derivatives. Light-induced conformational changes in these molecules modulate cellular signaling, leading to alterations in cell shape that are detected as changes in the impedance signal.

Decoding the spatiotemporal dynamics of G protein–coupled receptor (GPCR) signaling remains a major challenge in cell biology. Classical pharmacological approaches often fail to capture the reversible and dynamic nature of these pathways. To overcome this, we employed photoresponsive molecules as optical triggers in combination with impedance-based readouts. At the receptor level, photoswitchable ligands for the neuropeptide Y4 receptor enabled precise, light-controlled GPCR activation. [1]

A novel two-electrode ECIS configuration further allowed localized stimulation within a single well and simultaneous monitoring of cellular responses. Downstream in the same pathway, photochromic derivatives of cyclic adenosine monophosphate (cAMP) were synthesized to directly modulate a key second messenger and assess its role in shaping signaling output. [2].

These optically controllable molecules, combined with real-time impedance measurements, provide unprecedented temporal and spatial resolution for dissecting GPCR-mediated signal transduction.

References:

[1] J. Erl, U. Wirth, S. Azzam, C. Höring, M. Skiba, R. Singh, K. Hochmuth, M. Keller, J. Wegener, B. König, *Angew. Chem. Int. Ed.* 62 (2023) e202215547.

[2] C. Haag, J. Erl, K. Helbig, J. Wegener, B. Koenig, *ChemRxiv*, (2024); 10.26434/chemrxiv-2024-cq5rz

Ready-to-use Insect cell-based Sensor for Pesticide Testing

S. Friedrich[1,2]; N. Malagimani[1]; S. Michaelis[2]; J. Wegener[1,2]

[1]Universität Regensburg, Regensburg (Germany)
[2]Fraunhofer Institute for Electronic Microsystems and Solid State Technologies; Cell-Based Sensor Technology
Sandra.friedrich@uni-regensburg.de

In-vitro systems enable faster, simpler and more cost-effective testing of pharmaceuticals, chemicals, or pesticides, while also helping to reduce ethical concerns associated with animal testing.[1] To truly benefit from these advantages, ready-to-use, stockpiled cell systems are essential since conventional cell culture work is time-consuming, requires trained personnel and demands special equipment. [2]
Here, we present a ready-to-use sensor platform for the detection of harmful effects of pesticides on insects that is based on insect cells frozen inside the wells of multi-electrode arrays. Pesticides contribute largely to the decline of insect populations which poses a significant threat to human life due to reliance on insect pollination for food production.

Model insect cells (here Sf21 cells derived from *Spodoptera frugiperda* and Kc167 cells from *drosophila melanogaster*) are cryopreserved directly on thin gold-film electrodes of 8W10E electrode arrays. Cells can be stored assay-ready in suspension in frozen state at –80 °C and thawed on demand for pesticide testing. [3] Harmful impacts of pesticides have been detected in less than 1 hour assay time. Results are in good agreement with those recorded in experiments using living insects. Studies using the model pesticide Banvel M demonstrated that sensitivity of the ready-to-use assay and cell viability are maintained for at least one year. Further assay simplification by automation of pesticide testing has been accomplished through the development of the benchtop device KERMIT (Kinetics of Ecotoxicological Responses Measured with Insect Tests), developed in collaboration with Fraunhofer EMFT, Munich. Using KERMIT, thawing, sample addition and connection to the ECIS device are fully automated, enabling the cell-based assay to be performed easily by anyone, anywhere.

References:

[1] M. C. J. Chang; F. B. Grieder, *Lab animal*, 53 (2024) 295–297.
[2] O. Wehmeier; A. Loa, *Methods Mol Biol.,* 2095 (2019) 17–25.
[3] S. Friedrich; N. Malagimani, S. Michaelis, and J.Wegener, *Appl Res.* 3 (2024).

Soft Graphene Electrodes and Screen-Printed Carbon Electrodes for Monitoring Cell Adhesion Using Non-Faradaic Electrochemical Impedance Spectroscopy

E. Fuhry[1]; V. Guglielmotti[1,2]; T.J. Neubert[1]; M. Kuhl[1]; I. Wachta[1]; D. Pallarol[2]; J. Höök[1]; K. Balasubramanian[1]

[1]Dept. Of Chemistry, Humboldt-Universität zu Berlin, Germany; [2]Instituto de Nanosistemas, Universidad Nacional de General San Martin, San Martin, Argentina.
* nano.anchem@hu-berlin.de

Impedance sensors for detecting cell adhesion or cellular interactions are typically realized on hard substrates. Cells are known to interact with their microenvironment. Hence, the stiffness of the substrate where cells grow plays a crucial role in cell behavior, adhesion, growth and proliferation. [1]. Providing a substrate with a stiffness similar to the cellular microenvironment will help minimize deviations in the natural behavior of cells during the electrochemical measurements. Hence, impedance sensors on soft substrates are needed. Here, we present a soft biomaterial platform, wherein a soft elastic substrate made up of poly(dimethylsiloxane) (PDMS) is coated with a single graphene sheet as electrode material for the real-time detection of cell adhesion using impedance sensing. [2] While metal electrodes can also be realized on PDMS, we demonstrate using nanomechanical measurements, that the softness of PDMS is lost with deposited metal layers, due to the requirement of several nanometers of the metal. By contrast, the transfer of graphene as a single atomic layer on to PDMS brings a negligible increase in stiffness. Using such sensors, we have followed the adhesion of MCF-7 cancer cells to a soft graphene electrode in real-time using electrochemical impedance spectroscopy (EIS) in the absence of added redox probes (non-Faradaic). The EIS response can be correlated with different phases of cell adhesion on to the soft substrate.

One important challenge in monitoring cell adhesion using EIS is the understanding of the mechanism of the impedance response and its correlation with specific interfacial or cellular events. With this goal, we have used the sedimentation of silica beads on to a screen-printed carbon electrode as a model system for cell adsorption on to an electrode. Silica beads as models for cells is advantageous since they sediment rapidly on the electrode surface and their interaction is reversible and non-specific. Typically, in EIS the DC potential is left at open circuit or maintained at a constant value to measure the impedance response. We have introduced the DC potential as an additional variable and monitor non-Faradaic impedance as a function of the applied DC potential. Using this technique, referred to as Non-Faradaic Potentiodynamic EIS (NF-PDEIS) we demonstrate that the sensitivity towards interfacial processes in the impedance signal can be improved by choosing an appropriate potential. [3] Moreover, by elaborate modeling, we show that the non-Faradaic impedance is also able to detect changes in the point-of-zero-charge (pzc) and interfacial charge density. Using this model, the impedance response due to the adhesion of MCF-7 cells can be well-understood.

References:

[1] D.E. Discher, P. Janmey, Y-L. Wang, Tissue Cells Feel and Respond to the Stiffness of Their Substrate. *Science* 4 (2005) 310. 10.1126/science.1116995

[2] V. Guglielmotti, E. Fuhry, T.J. Neubert, M. Kuhl, D. Pallarola, and K. Balasubramanian, Real-Time Monitoring of Cell Adhesion onto a Soft Substrate by a Graphene Impedance Biosensor. *ACS Sensors* 4 (2024) e202400037. 10.1021/acssensors.3c01705

[3] E. Fuhry, V. Guglielmotti, I. Wachta, D. Pallarola, and K. Balasubramanian, Real-Time Non-Faradaic Potentiodynamic Impedance Sensing Using Screen-Printed Carbon Electrodes. *Analysis & Sensing* 9 (2024) 101-109. 10.1002/anse.202400037

A virus-free impedance platform to emulate virus-induced cell fusion

A.-K. Grimm[1]; V. Borggraefe[1]; S. Einhauser[1]; R. Wagner[1] and J. Wegener[1,2]

[1]Universität Regensburg, Regensburg (Germany)
[2]Fraunhofer-Institut für Elektronische Mikrosysteme und Festkörper-Technologien EMFT, Regensburg (Germany)
Anne-Kathrin.Grimm@uni-regensburg.de

Monitoring cell fusion is essential for understanding viral infections and the development of antiviral therapies [1]. While fusion is typically observed by detecting morphological changes or exchange of intracellular materials microscopically [2], this study used impedance spectroscopy to assess cell fusion between two types of HEK293 cells: (i) HEK cells expressing the ACE2 receptor and (ii) HEK expressing the SARS-CoV-2 spike protein upon doxycycline induction. The latter serves as model for SARS-CoV-2 virus. In this project, impedance was monitored focusing on changes associated with cell-cell fusion. We found out that a time-dependent impedance increase at 4 kHz correlates with the extent of cell fusion between HEK-ACE2 and HEK-Spike, therefore, impedance magnitude can be used as a reliable measurand for evaluating cell fusion. In a second approach, we seeded HEK-ACE2 and HEK-Spike cells as co-cultures on electrodes and were able to induce cell-cell fusion at any selected time points by the addition of doxycycline, which served as inducer molecule for the expression of the spike protein in HEK spike cells in our system. Moreover, the intro-duction of anti-SARS-CoV-2 antibodies to the cell mixtures reduced the impedance increase, indicating inhibition of fusion through neutralization of the spike protein. A three-parameter fit model was applied to predict the number of fused cells without the need for staining or microscopy. Our results indicate that cell fusion is completed within 10 hours and involves almost all cells on the electrode. This approach provides a new impedance-based assay for detecting cell fusion in general, fusion as a consequence of viral infection and also to screen and to evaluate neutralizing antibodies with the capacity for high-throughput campaigns.

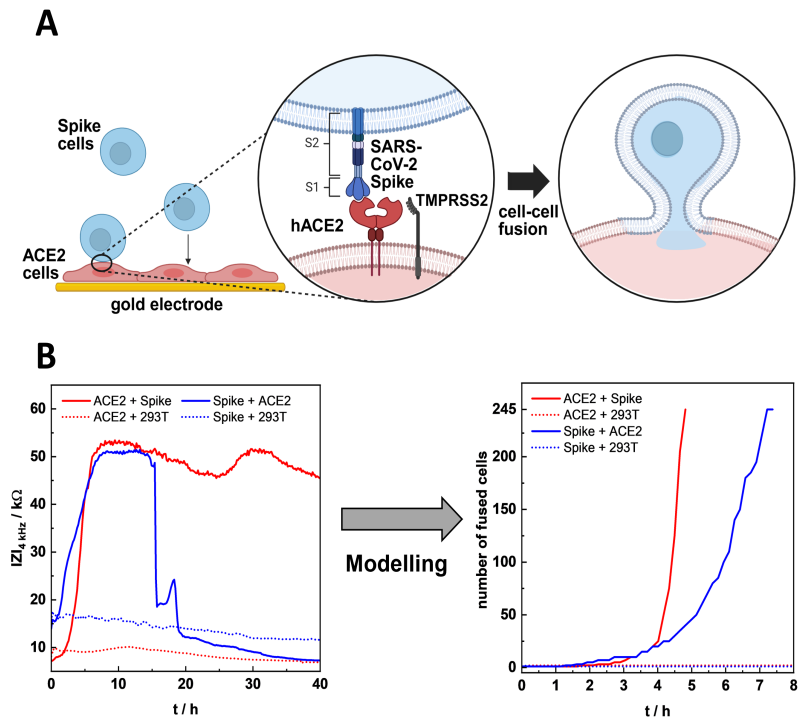

Impedance-based monitoring of receptor-mediated cell-cell fu-sion. **(A)** Schematic of experi-mental setup: cells expressing ACE2 cells are cultured on gold-film ECIS electrodes. Impedance is continuously measured during the addition of HEK cells ex-pressing the SARS-CoV-2 spike protein (or vice versa). Upon contact between the two cell types, membrane fusion – mi-micking the natural viral entry mechanism – is initiated. **(B)** Left: impedance time courses of cell-cell fusion (solid curves) and con-trol conditions (dashed curves). Right: prediction of number of fused cells after 3-parameter modelling. The model only allows for syncytia of ≤245 cells, bigger cell clusters are not predictable yet.

References:

[1] J.M. White and G.R. Whittaker, *Traffic* 17 (2016) 593-614.
[2] S. Martens and H.T. McMahon, *Nat Rev Mol Cell Biol* 9 (2008) 543-556.

Hydrogel-Coated Graphene Impedance Sensor for Real-Time Monitoring of Cell Adhesion

J. Höök[1]; E. Fuhry[1]; M. Geidel[1]; G. Graeber[1]; Diego Pallarola[2] and K. Balasubramanian[1]

[1]Dept. Of Chemistry, Humboldt-Universität zu Berlin, Germany. [2]Instituto de Nanosistemas, Universidad Nacional de General San Martín, San Martín, 1650 Provincia de Buenos Aires, Argentina
julia.hoeoek@hu-berlin.de

We present the development and characterization of compact and transparent graphene-based impedance sensors [1] with a soft, tissue-like hydrogel interface. The sensors are designed to monitor cell adhesion while minimally disrupting the natural cellular behavior during electrochemical measurements. As cells interact with their microenvironment, a soft, tissue-like interface such as a hydrogel is favorable for adhesion, growth and proliferation. [2] In our sensors, a monolayer graphene electrode on a quartz substrate is coated with a thin hydrogel layer on top. The porosity of the hydrogel provides a high ionic conductivity for impedance measurements. [3] The transparency of the sensor components also allowed for simultaneous optical monitoring under a microscope.

We successfully characterized the electrochemical impedance spectroscopy (EIS) response of our sensors without adding redox-active species (non-Faradaic) and proposed an equivalent circuit model. First, we used the adsorption of silica beads (silica particles with 7 µm diameter) as a model system for cell adhesion. Bead sedimentation is reversible and their interactions with the sensor surface are non-specific. This allowed us to study the fundamental EIS response and corroborate these to specific interfacial events.

In EIS, an AC modulation superimposed on a DC potential is used to probe the system, where the DC potential is typically the open circuit potential (OCP). In our experiments, we additionally varied the DC potential to force a polarization of the system, a method referred to as potentiodynamic EIS (PDEIS). [4] In this manner, we identified the DC potential that delivered the most sensitive impedance response for bead sedimentation. Finally, using non-Faradaic PDEIS we demonstrated that adhesion of MCF-7 cancer cells could be sensitively detected in real time, despite the presence of a hydrogel layer on top of the graphene electrode.

References:

[1] V. Guglielmotti, E. Fuhry, T.J. Neubert, M. Kuhl, D. Pallarola, and K. Balasubramanian, Real-Time Monitoring of Cell Adhesion onto a Soft Substrate by a Graphene Impedance Biosensor. *ACS Sensors* 4 (2024) e202400037. 10.1021/acssensors.3c01705

[2] D.E. Discher, P. Janmey, Y-L. Wang, Tissue Cells Feel and Respond to the Stiffness of Their Substrate. *Science* 4 (2005) 310. 10.1126/science.1116995

[3] X. Yao, J. Liu, C. Yang, X. Yang, J. Wei, Y. Xia, X. Gong, Z. Suo, Hydrogel paint. *Adv. Mater.* 31 (2019) 1903062.

[4] E. Fuhry, V. Guglielmotti, I. Wachta, D. Pallarola, and K. Balasubramanian, Real-Time Non-Faradaic Potentiodynamic Impedance Sensing Using Screen-Printed Carbon Electrodes. *Analysis & Sensing* 9 (2024) 101-109. 10.1002/anse.202400037

Probing the EGTA-Mediated Barrier Impairment of MDCK Cells by Electric Cell-Substrate Impedance Sensing

C.-T Huang; T.-Y. Wu; W.-L. Chen; C.-M, Lo

National Yang Ming Chiao Tung University, Taipei, Taiwan
chuting127@gmail.com

Monitoring cell barrier formation and integrity is crucial in biological research and drug development, as these barriers play vital roles in many physiological and pathological processes. In this study, electric cell-substrate impedance sensing (ECIS) was applied to assess EGTA-mediated barrier properties of MDCK-II cells. EGTA (ethylene glycol-bis(beta-aminoethyl ether)-N,N,N′,N′-tetraacetic acid) is a chelating agent that binds to calcium ions and can disrupt the integrity of cell-cell junctions by reducing calcium levels. This disruption results in a loss of barrier function and a reduction in transepithelial electrical resistance (TEER). With ECIS 8-well transfilter arrays (8wTFA), TEER data of MDCK monolayers were collected before, during, and after the treatment of 5 mM EGTA for 1.5 hours. As expected, the measured resistance at 125 Hz decreased from 700 ohms to 200 ohms during the EGTA treatment. By subtracting the resistance of the cell-free membrane insert, ~200 ohms, and multiplying the area of membrane insert, 0.3 cm^2, the measured TEER approximately decreased from 150 ohms·cm^2 to 0 ohms·cm^2. Following the 1.5-hour EGTA treatment, the medium was changed to complete culture medium without EGTA, and TEER recovery was observed.

We also used 8W1E arrays to monitor EGTA-mediated barrier disruption and recovery of MDCK-II cells. Comparing the measured impedance spectrum of confluent MDCK monolayers with the calculated values obtained from the cell-electrode model and the impedance spectrum from the blank electrode, both junctional resistance (R_b) and cleft resistance (α^2) can be determined [1]. After MDCK cells were treated with 5 mM EGTA, both junctional resistance and cleft resistance dropped quickly, from 20 ohms·cm^2 to 0 ohms·cm^2 and from 100 ohms·cm^2 to 15 ohms·cm^2 respectively. Interestingly, the summation of junctional resistance and cleft resistance is close to the TEER value measured with transfilter arrays. The findings suggest that the cleft resistance resulting from cell-substrate contact should be considered when interpreting TEER values [2].

References:

[1] C.-M. Lo; C. R. Keese; I. Giaever, *Biophysical Journal* 69 (1995) 2800-2807.
[2] C.-M. Lo; C. R. Keese; I. Giaever, *Experimental Cell Research* 250 (1999) 576-580.

Impedance-guided Evaluation of Cancer Therapy: A new route for personalized medicine?

S. Knafl[1]; N. Karami[1]; S. Kigilli[1]; L. Ermoneit[1]; N. Pruggmayer[1]; F. Delic[1]; M. Kerbler[1]; F. Azizian[1]; A. Katthab[2]; G. Zeck[2]; S. Prado Lopez[1]; H. D. Wanzenboeck[1]

[1]TU Wien, Institute for Solid State Electronics, 1040 Vienna, Austria
[2]TU Wien, Institute for Bioelectronics, 1040 Vienna, Austria
Heinz.Wanzenboeck@tuwien.ac.at

The rise of personalized medicine promises individualized therapies with higher treatment success rates. Patient-derived microtissues and cell spheroids are central to this approach, enabling custom-tailored cancer treatments specific to a patient's tumor phenotypes. Even patient-specific tumor heterogeneity can be addressed. This creates a need for non-destructive, label-free technologies to assess tumor growth and test therapies before clinical use.
We present an impedance-based cellular assay (IBCA) for evaluating anti-tumor therapy on 3D tumor spheroids, and finally patient-derived microtumors. A custom chip with four independent microwells, each containing six sensors, allows simultaneous study of up to 24 spheroids and four treatment conditions. Each sensor units consist of planar interdigitated electrodes optimized to measure impedance of spheroids. Positioning the 3D cell constructs on top of the electrodes is challenging, but essential for high sensitivity. We have tested additional placement structures and will summarize the results and further improvements.

In an initial validation using Triton X-100, a membrane-permeabilizing reagent, the cellular response to drug exposure was studied. Ongoing studies are investigating the effect of established chemotherapeutics, such as 5-fluorouracil, on tumor spheroids, and recent results will be discussed. Finally, we will give an outlook on our ultimate goal of analyzing patient-derived microtumors by electrochemical impedance spectroscopy (EIS) to monitor the effects of CAR-T cell therapies and present some of the first promising results.

Concluding, the developed chip has been successfully for real-time, label-free monitoring of the multi-cellular tumor spheroids. We propose that in future such *in vitro* tumor models provide patient-specific insights as label-free tool for personalized therapy of tumor patients.

Figure 1: Left: Microscope image of a single well with six IDES sensors (E1-E6), 24 hours after seeding three HT-29 spheroids onto electrodes E1, E4, and E6. Right: Normalized impedance amplitude spectra of the spheroid-free (E2, E3, E6) and spheroid-covered (E1, E4, E5) sensors, The presence of spheroids causes an impedance increase.

References:

[1] Gamal W., Wu H., Underwood I., Jia J., Smith S. and Bagnaninchi P. O. Impedance-based cellular assays for regenerative medicine, Phil. Trans. R. Soc. B37320170226 http://doi.org/10.1098/rstb.2017.0226

Effects of the Conditioned Media Obtained from Biodegradable Mg-Zn-Sn Alloys on Human Dental Pulp Stem Cells

S.-Y. Lai; W.-L. Chen and C.-M. Lo

National Yang Ming Chiao Tung University, Taipei, Taiwan
jenny1209578@gmail.com

Magnesium (Mg) alloys are promising candidates for orthopedic implants due to their excellent biocompatibility, biodegradability, and favorable mechanical properties [1, 2]. However, their rapid degradation may lead to excessive hydrogen gas evolution and high Mg ion concentrations, resulting in tissue swelling and cytotoxic effects [3, 4]. In this study, electric cell-substrate impedance sensing (ECIS) was employed to evaluate the effects of Mg-Zn-Sn alloys containing three different calcium (Ca) contents on the attachment, morphology, and migration behavior of human dental pulp stem cells (hDPSCs).

The Mg alloy was immersed in culture medium, with the medium being collected and replaced every three days over 30 days. The collected media were labeled sequentially from Group a to Group j based on the collection time point. Subsequently, hDPSCs were seeded onto 8W1E array chips. After initial cell attachment, the original culture medium was replaced with the respective Mg alloy-conditioned media from each group. Using MFT and frequency scan, cell attachment and morphological changes were continuously monitored for 24 hours. The results showed that the use of 2-fold diluted MSZN-0.3Ca medium, whether from group c or group j, effectively promoted hDPSC attachment and proliferation. In contrast, 2-fold diluted MSZN-0.1Ca (group c) and MSZN (group j) media were associated with poor cell adhesion and even partial cell detachment. Furthermore, under all dilution conditions, the Rb values of MSZN-0.3Ca from group c were consistently higher than those of the control group, indicating stronger intercellular connections and enhanced cell adhesion and barrier formation.

Additionally, wound healing assays were applied after 24 hours of culture in conditioned medium to assess cell migration. Consistent with earlier observations, hDPSCs exposed to conditioned medium from MSZN-0.1Ca (group c) and MSZN (group j) at two-fold dilution exhibited a complete loss of migratory capacity. In contrast, the resistance of MSZN-0.3 Ca in group j increased significantly under all dilution conditions compared to the control group, which fully demonstrated that the conditioned medium could improve the cell migration ability. Cell viability, assessed by the CCK-8 assay, also showed that MSZN-0.3Ca conditioned medium from groups g to j could potentially promote hDPSC proliferation.

Overall, these findings suggest that MSZN-0.3Ca exhibits superior biocompatibility among the tested compositions, without compromising cell viability or migration, and may represent an optimal formulation for biodegradable orthopedic implants.

References:

[1] M.N. Azadani; A. Zahedi; O.K. Bowoto and B.I. Oladapo, *Prog Biomater* 11(1) (2022) 1-26.
[2] Y. Yang; C. He; D. E; W. Yang; F. Qi; D. Xie; L. Shen; S. Peng and C. Shuai, *Materials & Design* 185 (2020) 108259.
[3] D. Maradze; D. Musson; Y. Zheng; J. Cornish; M. Lewis and Y. Liu, *Sci. Rep*. 8(1) (2018) 10003.
[4] X. Li; X. Liu; S. Wu; K.W.K. Yeung; Y. Zheng and P.K. Chu, *Acta biomaterialia*, 45 (2016) 2-30.

Development of a Fully DLP-Printed Sensor-Integrated Cell Culture Well for Electrochemical Evaluation

C. Leuschner; J. Krauß; M. Schimpf; A. Lorenz; P. Ertl; S. Schobesberger and M. Frauenlob

TU Wien, Faculty of Technical Chemistry, Vienna (Austria)
chiara.leuschner@tuwien.ac.at

Digital light processing (DLP) 3D printing has emerged as a powerful route to rapidly prototype and customise bioanalytical devices by providing high resolution and dimensional accuracy [1]. However, sensor integration in cell culture platforms still relies on multi-step assembly. In addition, standard DLP resins are electrically insulating, which limits on-device electrochemical measurements [2]. This study aims to fabricate fully DLP-printed, sensor-integrated cell culture wells by modifying a commercially available photocurable resin with electrically conductive additives. The development and validation process comprised three stages. First, thin-film samples of cured resin with different additives were fabricated and screened using the two-point probe method to identify the most conductive formulation. Second, the printing parameters for the conductive resin were identified and optimised through comparisons of printed vs. designed geometries. Finally, sensor-integrated wells were fabricated via the Print-Pause-Print approach and validated using electrochemical impedance spectroscopy (EIS) and cyclic voltammetry (CV). We were able to demonstrate that silver-coated aluminium spheres at concentrations between 50 and 65 wt% of total resin, yielded in conductivity > 100 S/m. The evaluation of the printed geometries confirmed that, with the optimised DLP printing parameters for conductive resins, the average deviation between designed and produced geometry was 0.76%. Finally, EIS and CV verified the capability of the printed, sensor-integrated wells to support electrochemical readouts using saline solutions in the range of 1.25 to 100 mM. In conclusion, this work provides a general workflow for fully DLP-printed wells with integrated electrodes, with scope for further refinement towards more complex microphysiological devices.

References:

[1] A. Fritschen *et al.*, *Biomaterials Science* 10 (2022) 1981-1994.
[2] S. K. Mahato *et al.*, *Materials Today: Proceedings* 113 (2024) 25 -32.

Advancing 3D Impedance Tomography for *In-Vitro* models

B. Linkoon P. Meenaketan[1]; J. Deng[2]; Y.-C. Chai[1]; T. Torfs[1]; J. D. Beenhouwer[2]; J. Sijbers[2]; D. Braeken[1]

[1]imec, Leuven, (Belgium) [2]University of Antwerp (Belgium)
BabuLinkoon.Meenaketan@imec.be

Three-dimensional in vitro models, such as organoids and spheroids, have redefined biomedical research and drug development by more accurately replicating tissue complexity than conventional two-dimensional cultures. They enable tissue differentiation, disease progression, and drug response, but analysis remains difficult when seeking high-quality information across their full depth without damage. Micro-Electrical Impedance Tomography (µEIT), a label-free and non-destructive imaging modality, addresses this challenge by enabling non-invasive imaging while preserving tissue integrity [1].

In this study, we present the design of a µEIT platform for analyzing 3D *in-vitro* models. The system comprises three main modules: a 3D measurement interface, a signal acquisition unit, and an imaging unit. The measurement interface is a cubic biocompatible chamber with micro-electrodes integrated on each sidewall. During operation, the chamber is filled with culture medium, and the *in-vitro* model is placed inside for imaging. The signal acquisition unit features a reconfigurable switching matrix that controls current injection and voltage sensing, with the acquired data transmitted to the imaging unit for 3D impedance reconstruction. The platform operates over a frequency range of 1–100 kHz with current amplitudes of 10–100 µA.

To reconstruct 3D images, the platform employs time-differential EIT (TD-EIT), which reduces modeling and electrode-related errors by subtracting measurements at two time points. Conventional Gauss–Newton (GN) methods provide accurate reconstructions but are computationally expensive due to large Jacobian and Hessian matrices, especially in 3D EIT applications. To address this, we propose a matrix-free GN (MF-GN) method, which avoids explicit matrix storage and reduces computation complexity. Computation efficiency is further improved through adaptive meshing, applying a dense grid to the region of interest and a coarser grid to the background, ensuring high spatial resolution while minimizing cost.

An in-house prototype of the µEIT Cube was validated across a range of targets, demonstrating its capability to resolve both structural detail and dielectric contrast. In experiments with hydrogels and cerebral organoids, the system successfully distinguished the samples from the surrounding culture medium, confirming its applicability to biological models. Tests with multilayer targets, such as pomegranate seeds, further demonstrated accurate reconstruction of internal layers with distinct dielectric properties, closely matching the ground truth. Collectively, these results highlight the µEIT Cube's potential for 3D imaging of complex biological systems.

In conclusion, we present a non-invasive, label-free MEA-based platform for real-time, in-depth imaging of 3D *in-vitro* models, achieved through the integration of rapid measurement techniques and advanced reconstruction algorithms.

References:

[1] Deng, J., Renders, J., Meenaketan, B. L. P., Ebrahimi Takalloo, S., Braeken, D., De Beenhouwer, J., and Sijbers, J. (2024). IEEE Sensors Journal 24, 24452-24465.

PEDOT:PSS as transparent, low-cost electrode material for impedance-based cell analysis

S. Michaelis[1]; C. Götz[1,2] and J. Wegener[1,2]

[1]Fraunhofer EMFT, Division *Cell-Based Sensor Technology*, Regensburg (Germany)
[2]University of Regensburg, Regensburg (Germany)
stefanie.michaelis@emft.fraunhofer.de

Conducting polymers are increasingly integrated into everyday technologies and scientific equipment. Conventional electrode materials, such as gold or indium tin oxide, are progressively being substituted in certain applications, since conducting polymers combine low cost with advantageous material properties, such as mechanical flexibility, optical transparency, and favorable dielectric behavior. Among them, PEDOT:PSS exhibits the strongest potential for application in impedance-based cellular assays [1]. Its ability to disperse in aqueous media makes it compatible with scalable manufacturing approaches, including screen printing. When exposed to aqueous environments, PEDOT:PSS electrodes undergo swelling, which enhances the interfacial capacitance between electrode and electrolyte. This property renders PEDOT:PSS highly promising as a transparent transducing layer for impedance-based cell monitoring. The present work investigates PEDOT:PSS as an electrode material for impedance-based cell analysis as conducted in typical ECIS assays. Electrode arrays were fabricated through screen-printing, revealing considerable promise for commercial deployment. A performance comparison between screen printed PEDOT:PSS electrodes and conventional gold electrodes highlights both, advantages and limitations of this polymer material. Ongoing studies address diverse applications, with initial findings suggesting that the unique dielectric response of PEDOT:PSS provides enhanced sensitivity in probing cell-cell and cell-substrate junctions, thereby enabling impedance-based evaluation of cell types previously inaccessible by this technique. Furthermore, its low-cost production and facile processing may pave the way for mass scale industrial fabrication of electrodes, for instance, in reel-to-reel processes.

References:

[1] Michaelis, S., et al. *Applied Research* 4.1 (2025): e70004.

Impedance Flow Cytometry for Electrogenic Microorganisms

M. Mozafari[1]; P. Erfle[1]; J. Block[2,3]; R. Krull[2,3,4]; A. Dietzel[1,4]

[1]Institute of Microtechnology, TU Braunschweig
[2]Institute of Biochemical Engineering, TU Braunschweig
[3]Braunschweig Integrated Centre of Systems Biology, TU Braunschweig
[4]Center of Pharmaceutical Engineering, TU Braunschweig
m.mozafari@tu-braunschweig.de

This study expands upon recent discoveries highlighting the important role of electrogenic gut bacteria [1]. The main objective is to develop and demonstrate impedance-based flow cytometry that can detect electrogenic microorganisms based on their electrical properties in real time and without markers with high precision. For this purpose, a microfluidic system was designed and manufactured. The system consists of a microchannel with three microelectrodes allowing differential measurements. The microchannel was structured on a glass wafer together with a thin PDMS layer using femtosecond laser ablation techniques, while co-planar microelectrodes were fabricated separately using gold and titanium via sputtering and photolithography. Both parts of the system were then aligned and sealed with a previously spin-coated PDMS layer (**Fig. Ia,c,d**). The impedance measurements were conducted using two microorganisms: *Escherichia coli*, a non-electrogenic model organism, and *Shewanella oneidensis*, a well-known electrogenic microorganism at 1MHz using HF2LI lock-in amplifier (from Zürich Instruments, Zürich, Switzerland). When single microorganisms pass through the detection zone, they change the impedance, which serves as a measurable signal corresponding to their electrical behavior (**Fig. IIa**).

Analysis at 1 MHz revealed different behavior between *S. oneidensis* and *E. coli*. Both bacteria contain a membrane that acts as a capacitor in the corresponding electrical circuit (**Fig. IIb**). An increase in the current value for *S. oneidensis* indicates a lower impedance of the cytoplasm compared to the surrounding physiological medium which, suggesting a short-circuited membrane (**Fig. IIc**). *E. coli*, on the other hand, showed a decrease in current at the same frequency (**Fig. IId**) which means that the total impedance is still higher than that of the surrounding medium. This comparison suggests that the membrane of the electroactive microorganism is short-circuited at lower frequency than that of *E. coli* due to extracellular electron transfer (EET).

References:

[1] Naradasu D, Miran W, Sakamoto M (2018). Frontiers in Microbiology 9, 3267.

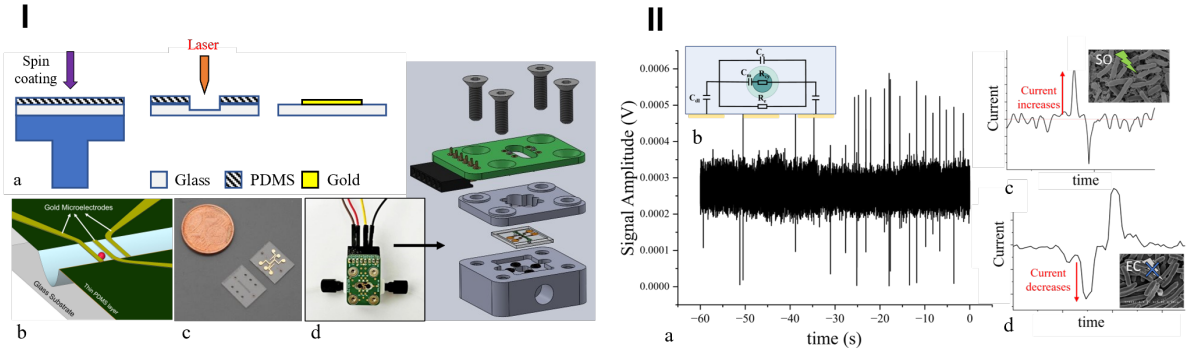

Figure: Ia) Fabrication of the microchannel and microelectrodes using femtosecond laser ablation and photolithography. **Ib)** Concept of impedance flow cytometer with the created sensing areas. **Ic)** Two separated parts of the microfluidic system and microelectrodes. **Id)** Assembled system with electric and fluidic connections. **IIa)** Signal variation showing the detection of microorganisms in an Impedance Flow Cytometer. **IIb)** Equivalent electrical circuit modelling the bacteria with membrane as a capacitor. **IIc)** Differential signal of single cell indicating the increase in the current in electrogenic *S. oneidensis* (SO) detection. **IId)** Differential signal of single cell indicating a decrease in the current in *E. coli* (EC).

Impedance-based monitoring of two cell monolayers co-cultured without physical contact (cis-TER).

T. Naber[1,2]; L. Rottbauer[1]; J. Wegener[1,2]

[1]Universität Regensburg, Regensburg (Germany),
[2]Fraunhofer Institut für Elektronische Mikrosysteme und Festkörper-Technologien EMFT, Regensburg (Germany)
tobias.naber@emft.fraunhofer.de

The delivery of active ingredients over epithelial and endothelial barriers is a key parameter of drug efficacy. In addition, the effect of the drug not only on the target but on the passed barriers is of great interest. So far, the detection of these crucial parameters has to be performed by using several different assay types. In the presented work we describe the development of an assay platform monitoring the morphology of two indirectly co-cultured monolayers, offering the possibility to determine afore mentioned parameters in a single experiment. The assay platform is based on impedance spectroscopic monitoring and combines two different approaches of impedance readings. A first cell layer, the *sensing layer*, is cultured on a set of thin-film gold electrodes. Monitoring of this cell layer is based on the ECIS approach [1]. Simultaneously, a second cell layer, the *barrier forming layer*, is cultured on a permeable culture insert mounted above the first cell layer. By applying a stainless-steel dipping electrode on the apical side and the combination of the thin film gold electrodes as basolateral electrode, the TER and the TEC of the cell layer cultured on the permeable substrate can be monitored [2]. At the current status of development, the device offers a throughput of 24 individual co-cultures. We developed two different basolateral electrode set-ups convenient for different assay scenarios. Furthermore, we demonstrated the functionality of the monitoring system with a proof-of-principle experiment. We believe that an assay platform based on the *CIS-TER* approach can strongly assist future drug development processes.

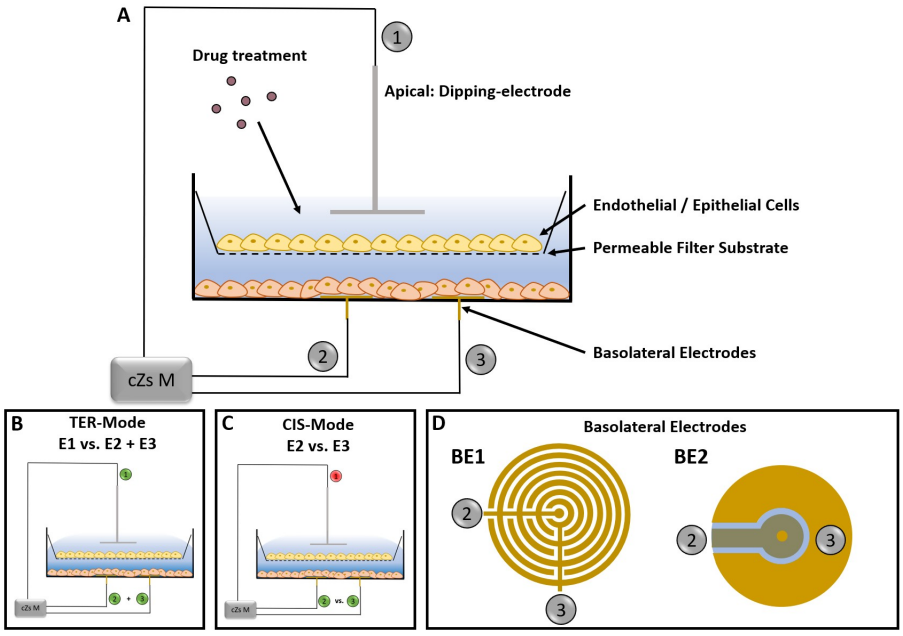

Figure 1: (A) Schematic set-up of the CIS-TER assay. Possible measurement modes, determining the TER of the upper cell layer **(B)** and the impedance of the lower cell layer **(C)**. **(D)** Developed layouts for the basolateral set of electrodes.

References:

[1] J.A. Stolwijk and J. Wegener, *Bioanalytical Reviews*, vol 2. (2019) pp 1 - 75.
[2] J. Wegener, et al., *Biotechniques*, 37(4) (2004), pp 590 – 597.

Application of Thermal Dielectrospectroscopy in Studying the Membrane of Human Erythrocytes

B. Paarvanova and I.T. Ivanov

Medical Faculty, Trakia University, 6000 Stara Zagora, Bulgaria
boyana.parvanova@trakia-uni.bg

Thermal Dielectrospectroscopy is a method based on the simultaneous uniform heating and applying of an alternating external electrical field to a suspension of erythrocytes, erythrocyte ghost membranes or isolated submembrane cytoskeletons. At 49.5°C (T_A), spectrin monomers from the cytoskeleton in erythrocyte membranes (EM) denature. This leads to the loss of dielectric activity of spectrin network and at the same time does not affect that of the cytosol and the suspension medium. Thus, the changes in the dielectric parameters of the suspension (ΔZ_{im}, ΔZ_{re}, ΔY_{im}, ΔY_{re}, ΔC_{im}, and ΔC_{re}) at T_A provide information about the dielectric activity and molecular dynamics of the submembrane cytoskeleton in its native state.
The dependence of ΔY_{im} on ΔY_{re}, in the complex plane plot for erythrocytes or isolated EM, shows a frequency dependence which is obtained in the form of two semicircles Fig. 1. Each of them corresponds to a dielectric relaxation in EM, associated with a distinct polarization mechanism. Two dielectric relaxations were identified: β_{sp} (1.4 MHz) and $\gamma1_{sp}$ (9 MHz), which were used to study the complex structure of EM.

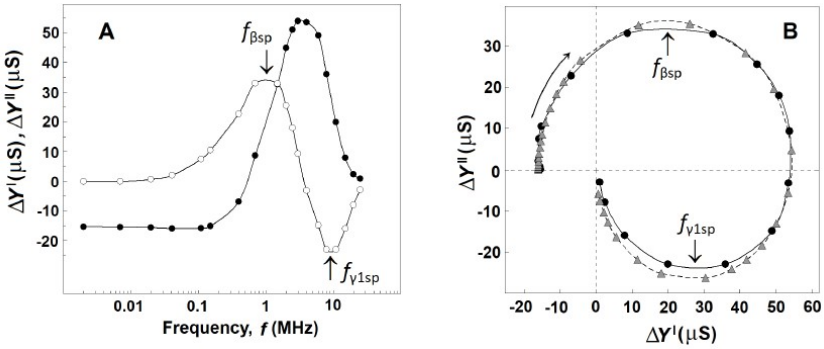

Fig. 1. (A) Frequency dependence of the change in complex admittance of a suspension with control RBCs at the spectrin denaturation temperature, T_A. The changes in the real part, ΔY'/μS (●), and imaginary part, ΔY"/μS (○), are presented as functions of the frequency, f (MHz). **(B)** Complex plain plot of the spectrin-linked portion of the complex admittance of control erythrocytes. Shown is the ΔY" vs. ΔY' dependence.

During stepwise extraction of up to 60% of membrane lipids, the $\gamma1_{sp}$ relaxation was preserved, while the β_{sp} relaxation was gradually eliminated. When the NaCl concentration on both sides of the EM was increased to 100 mM, the β_{sp} relaxation increased linearly, while the $\gamma1_{sp}$-relaxation remained unchanged. In a medium with NaCl concentration between 100 and 150 mM, β_{sp} relaxation became slightly inhibited, while $\gamma1_{sp}$ relaxation nearly disappeared probably due to reduced electrostatic repulsion, allowing erythrocytes to come closer to each other. In the presence of 10–30 mg/mL of dextran (MW 7 kDa), polyethylene glycol or polyvinylpyrrolidone (40 kDa), or albumin, the $\gamma1_{sp}$ relaxation was enhanced by approximately tenfold, while β_{sp} relaxation was either enhanced or preserved [1].
The results showed that dielectric spectroscopy can sensitively evaluate erythrocyte membrane properties. β_{sp}-relaxation is linked to deformability and spectrin integrity, while $\gamma1_{sp}$-relaxation is associated with intermembrane interactions and cell aggregation. These findings have potential diagnostic value for disorders affecting erythrocyte mechanics and aggregation.

References:

[1] I.T. Ivanov and B.K. Paarvanova, *Membranes* Volume 13 (2023) Article number 658.

Concept for high channel systems for cell sensing

U. Pliquett; C. Gansauge; D. Echtermeyer

Institut für Bioprozess- und Analysenmesstechnik, Heilbad Heiligenstadt (Germany)
uwe.pliquett@iba-heiligenstadt.de

In high-channel electrode systems for parallel impedance measurements on cells and biological tissues, a multiplexer is typically used to sequentially connect all electrodes to the impedance measuring device. This has the disadvantage that, especially with high-channel systems, the complete measurement across all electrodes takes a relatively long time, especially if an entire spectrum is to be recorded. As a result, cell dynamics in the subsecond range can only be achieved selectively over just a few electrodes.
In an alternative concept, the impedance is not directly measured in the frequency domain, but calculated from the relaxation behavior after a voltage step (time domain). The voltage step is applied centrally via a distant electrode, and the current through each electrode of a multi-electrode array is measured.
A special feature of relaxation in biological objects is the exponential decay of the current, which is primarily caused by the charging of membrane structures. Due to the rapid change at the beginning and the increasingly smaller change in the current after the step, it is sufficient to scan quickly at the beginning and then successively increase the intervals between the scanning points. A simple sampling regime of this type would violate the sampling theorem and inevitably lead to nonsensical results. This is counteracted by integration between the sampling points. For this purpose, an integrator is placed behind each electrode. This arrangement has the advantage that all integrators can be started simultaneously, whereby the integrated currents are present at all outputs simultaneously for one integration period. After these voltages have been read, the integrators are reset and integrated over the next period. In practice, four time instances are sufficient for one decade, meaning that only twenty-four sampling points are required to record a spectrum over six decades.
In this way, for example, a multi-electrode array with 10,000 electrodes could be realized [1], in which the impedance spectrum between 5 kHz and 1 MHz can be recorded across all electrodes within one second (8 seconds in the cited paper). Alternatively, individual electrodes can be recorded at a rate of 1,000 measurements per second.

References:

[1] Gansauge, C., K. Schieke, and U. Pliquett. "ECIS with 10,000 Channels–a Feasibility Study on Biofilm Growth." *International Journal of Bioelectromagnetism* 23.2 (2021).

Biophysical Profiling of MASLD-MASH Disease Transition

C. Rafferty[1]; D. Neill[1]; A. Martinez Lyons[1]; S. Mitchell[2]; J. Cholewa-Waclaw[3]; M. Vermeren[3]; L. Charlton[4]; A. Elfick[1]; L. Bandiera[1]; P. Bagnaninchi[3], and L. Nelson[1,3,5,6]

[1]Institute for Bioengineering, University of Edinburgh, Edinburgh, UK
[2]School of Biological Sciences, University of Edinburgh, Edinburgh, UK
[3]Institute for Regeneration and Repair, University of Edinburgh, Edinburgh, UK
[4]Centre for Science at Extreme Conditions, University of Edinburgh, Edinburgh, UK
[5]School of Applied Sciences, Edinburgh Napier University, Edinburgh, UK
Centre for Inflammation Research, University of Edinburgh, Edinburgh, UK
s2620368@ed.ac.uk

Metabolic dysfunction-associated steatotic liver disease (MASLD) affects ~30% of adults globally and is characterised by hepatocyte lipid droplet (LD) accumulation. Left untreated, it can progress to metabolic dysfunction-associated steatohepatitis (MASH), marked by chronic inflammation. Although both stages are reversible, limited diagnostics hinder early and targeted intervention [1,2]. Biophysical changes during MASL-to-MASH progression may both reflect and contribute to hepatocellular dysfunction, but remain poorly understood. This study aimed to characterise biophysical signatures of healthy, MASLD-, and MASH-like hepatic cells *in vitro* to uncover early diagnostic and therapeutic targets. We used HepaRG116 hepatocyte:cholangiocyte co-cultures or primary human hepatocytes treated with basal medium (healthy), oleate (MASLD), or lactate, pyruvate, octanoate, and ammonia (LPON; MASH). Live cell behaviour, including barrier integrity, was assessed using Electric Cell-substrate Impedance Sensing (ECIS). Confocal microscopy, transmission electron microscopy, atomic force microscopy, and protein assays evaluated LD accumulation, tight junction integrity, ultrastructure, stiffness, and endoplasmic reticulum (ER) stress. LPON treatment, indicative of MASH, disrupted cell-cell junctions (Fig. 1C), reduced levels of tight junction protein ZO-1, and increased LD accumulation (Fig. 1A). Additionally, cellular stiffness, mitochondrial fission, and ER stress were elevated, alongside a depletion of ATP. Our results suggest that enhanced LD-mitochondrial tethering (Fig. 1B) likely promotes β-oxidation and reactive oxygen species (ROS) generation, leading to compromised mitochondrial function and amplified cytoskeletal remodelling, increasing stiffness and barrier disruption. This work demonstrates biophysical profiling as a robust approach to correlate metabolic dysfunction with cellular mechanical properties, revealing potential novel avenues for early detection and targeted intervention in MASLD and MASH.

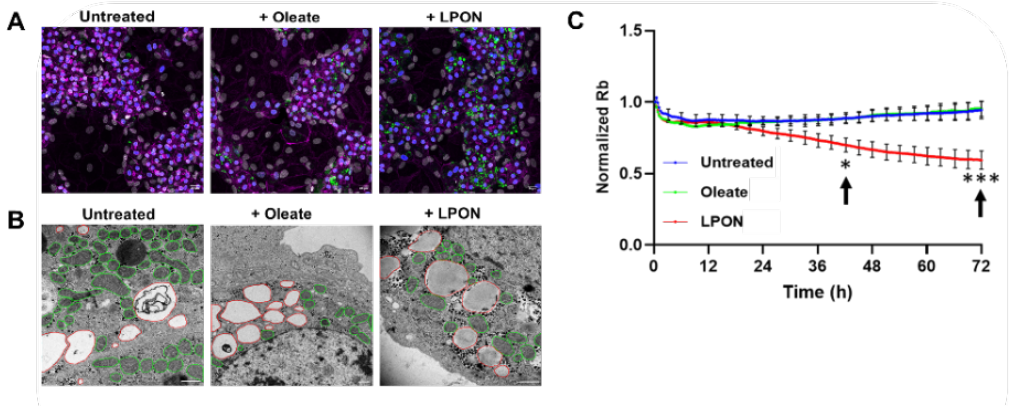

Figure 1. LPON-treated HepaRG cells displayed increased lipid droplet (LD; green) accumulation (A) and LD (red)- mitochondria (green) tethering (B), indicative of β-oxidation and ROS generation. These features were associated with significant cell-cell junction disruption (C), suggesting a link between lipid burden, organelle interaction, and barrier integrity in MASH-like conditions.

References:

[1] Z.M. Younossi; P. Golabi; J.M. Paik; A. Henry; C. Van Dongen and L. Henry. The global epidemiology of nonalcoholic fatty liver disease (NAFLD) and nonalcoholic steatohepatitis (NASH): a systematic review. *Hepatology.* 77 (2023) 1335-1347.

[2] E.Y. Tan; M.D. Muthiah and A.J. Sanyal. Metabolomics at the cutting edge of risk prediction of MASLD. *Cell Rep Med.* 5 (2024) 101853.

ECIS-O_2: Dual Sensor Approach to Monitor Metabolic Respiration and Cell Morphology

L.C. Rottbauer; T. Naber and J. Wegener

Universität Regensburg, Regensburg (Germany)
lisa-christin.rottbauer@uni-regensburg.de

Monitoring multiple cellular phenotypes simultaneously *in vitro* provides valuable insights into cellular processes, disease pathways, and the modes of action of compounds. In this context, cell morphology and metabolic respiration are two key parameters. Several dual-sensor platforms that enable the parallel recording of impedance and the electrochemical detection of oxygen consumption rates (OCR) have been developed in recent years and are now commercially available.
In this project, impedance-based cell analysis and optical readout of OCR were integrated side-by-side to independently record two phenotypic parameters upon exposure of the cells to different stimuli. An oxygen-permeable polymer foil doped with oxygen-sensitive luminophores was deposited beside a set of coplanar gold film electrodes on a transparent polycarbonate substrate. Oxygen content was determined ratiometrically using a commercial imaging system (VisiSens TD), while regular ECIS measurements were conducted simultaneously. We coined the term **'ECIS-O_2'** for this dual measurement principle.
This biocompatible, dual-sensor system enables the multiparametric assessment of cellular responses in real time. Its performance was validated using pharmacological tool compounds with well-characterized effects on cellular respiration and morphology.

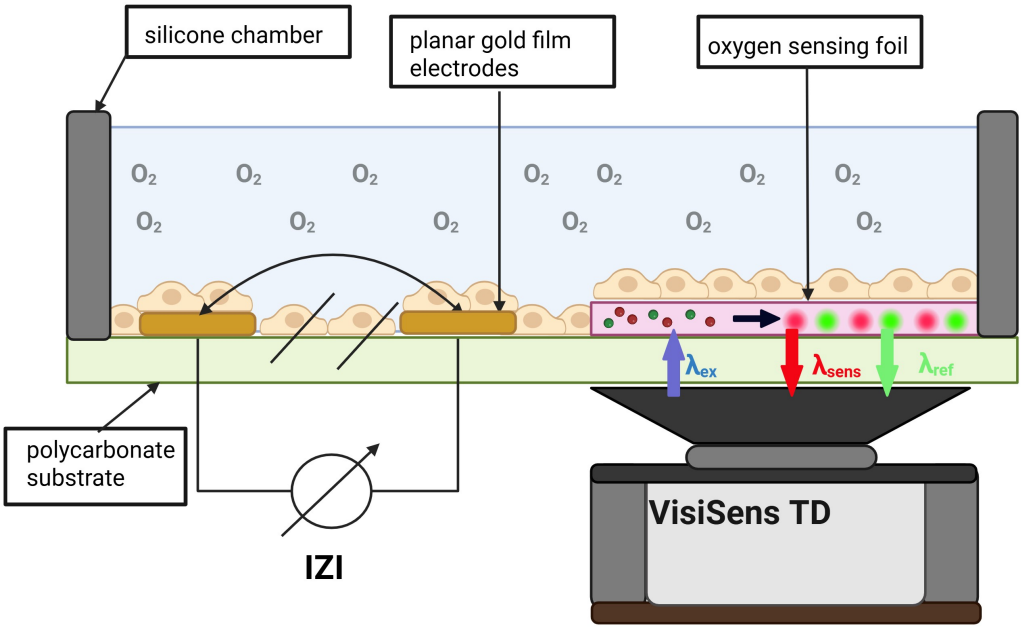

Figure 1: Schematic set-up of the ECIS-O_2 chip combining impedance spectroscopy and ratiometric oxygen imaging.

Electrochemical Impedance Analysis of Poly-phosphocholinated Liposomes Stability on Solid Electrode Surfaces

G. Savova[1]; M. Karabaliev[1]; B. Paarvanova[1]; B. Tacheva[1]; S. Jahn[2] and R. Georgieva[1,3]

[1]Medical Faculty, Trakia University, 6000 Stara Zagora, Bulgaria
[2]Liposphere Ltd., Aarava 1, 5400804 Givaat Shemuel, Israel
[3]Institute of Transfusion Medicine, Charité-Universitätsmedizin, 10117 Berlin, Germany
gergana.savova@trakia-uni.bg

Zwitterionic liposomes, especially poly[2--(methacryloyloxy)ethyl phosphorylcholine] (pMPC) liposomes are of particular interest in biomedicine, due to their potential to enhance lubrication in biological tissues. Their stability and resistance to fusion are critical for their performance as boundary lubricants in osteoarthritis. In the current study, we investigated the interaction between pMPC liposomes and two conductive substrates – gold and carbon with different hydrophilicity, using electrochemical impedance spectroscopy (EIS). The method was used to determine whether liposomes remain intact on the surface of electrode or spread around to form lipid films. Impedance spectra showed no significant increase in charge transfer resistance or decrease in apparent capacitance, indicating the absence of lipid film formation [1]. In contrary unmodified phosphatidylcholine liposomes, which were used for comparison, showed significant surface coverage and changes in impedance parameters, consistent with lipid film formation. These results confirmed that pMPC liposomes adsorb physically on electrode surfaces without disrupting interfacial electrochemical properties, supporting their use in applications requiring prolonged integrity and lubrications.

References:

[1] M. Karabaliev; B. Paarvanova, G. Savova et. al., *Molecules* Volume 29 (2024) Article number 3511.

Dual Monitoring of Impedance-Based Barrier Function and NF-κB Reporter Signaling in a Caco-2 Intestinal Inflammation Model

M. Schaffer and J. Heilmann

Department of Pharmaceutical Biology, University of Regensburg, Regensburg (Germany)
michael.schaffer@ur.de

Chronic inflammatory bowel disease (CIBD) is associated with factors such as the microbiome, genetics, and environmental influences. However, a dysregulated immune response, including cytokine signaling, and impaired intestinal barrier function are especially contributing to disease pathogenesis [1]. Besides interleukin-1β (IL-1β) and interferon-γ (IFN-γ), tumor necrosis factor-α (TNF-α) is particularly known for its critical role in regulating intestinal inflammation and is therefore a key target for biological therapies in CIBD [2]. However, TNF-α signaling in intestinal epithelial cells (IECs) is pleiotropic, contributing not only to pathological processes but also to the maintenance of intestinal homeostasis [3,4].
The transcription factor NF-κB is a key transducer of TNF-α and IL-1β signaling [5]. To monitor its activation over time, we developed a stable Caco-2 reporter cell line expressing a secreted luciferase. In combination with impedance spectroscopy, this system enables simultaneous monitoring of NF-κB activity and barrier function during cytokine-induced inflammation in a differentiated Caco-2 intestinal model (see Figure 1). Interestingly, IL-1β did not influence transepithelial electrical resistance (TEER), but increased NF-κB activation. While TNF-α alone had minimal impact on IEC barrier function, IFN-γ led to an initial TEER increase. Co-treatment revealed synergistic TEER breakdown after the initial increase. As NF-κB activity was not significantly altered by co-stimulation with IFN-γ, additional signaling pathways might be involved. Furthermore, IFN-γ stimulation was direction-independent, whereas TNF-α stimulation showed higher sensitivity of the basolateral membrane.
Our model provides valuable insights into cytokine-mediated responses of IECs, integrating intracellular signaling with functional readouts. A better understanding of these mechanisms may contribute to the development of more effective targeted therapies for CIBD.

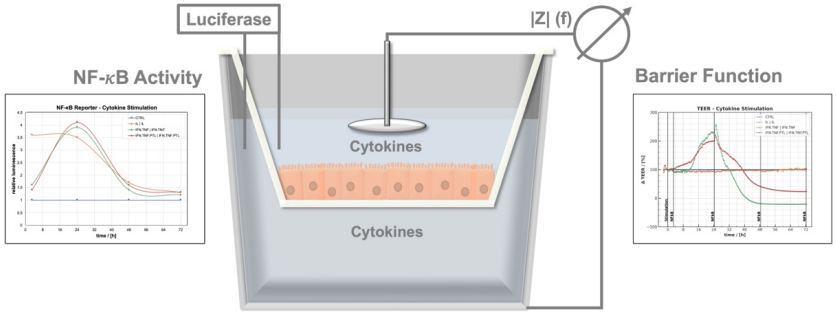

Figure 1: Dual monitoring of NF-kB activation by Caco-2 reporter cell line and impedance-based barrier function during cytokine-induced inflammation

References:

[1] J. Jang and S. Jeong, *BioChip Journal* 17 (2023) 403–430.
[2] M. Friedrich; M. Pohin and F. Powrie, *Immunity* 50 (2019) 992–1006.
[3] M. E. Delgado and T. Brunner, *Genes and Immunity* 20 (2019) 609–626.
[4] P. E. Dubé; S. Punit and D. B. Polk, *American Journal of Physiology-Gastrointestinal and Liver Physiology* 308 (2015) G161–G170.
[5] Q. Guo; Y. Jin; X. Chen; X. Ye; X. Shen; M. Lin; C. Zeng; T. Zhou and J. Zhang, *Signal Transduction and Targeted Therapy* 9 (2024) 53.

Correlation between label-free impedance analysis and Ca^{2+} fluorescence *in vitro* imaging

P. Schwenk; J. Erl; A-K. Grimm; J. Wegener; J. Schlossmann

Department of Pharmacology and Toxicology, University of Regensburg, Regensburg (Germany)
philipp.schwenk@ur.de

There are several approaches for investigating and unraveling GPCR-dependent signaling pathways using cell-based assays. You can choose between label-based and label-free measurement methods. One of the more modern label-based fluorescence indicators is the popular and frequently used genetically encoded calcium indicator GCaMP [1], which can be utilized to measure intracellular Ca^{2+} levels. Since Ca^{2+} is a crucial second messenger involved in various cellular mechanisms and signaling pathways, the GCaMP sensor can be applied to investigate GPCR-dependent signaling cascades. In addition to label-based methods, label-free, non-invasive measurement methods can also be used to detect possible GPCR activation, such as by measuring impedance, also known as ECIS (electric cell-substrate impedance sensing). In the ECIS assay, any change in cell shape results in a change in the measured impedance [2]. Since GPCR activation can lead to a remodeling of the actin cytoskeleton [3], this label-free measurement method is also well-suited for investigating GPCR pharmacology. Although these two different measurement methods (GCaMP and ECIS) are often used independently, there are no scientific studies yet that use both assay approaches and investigate how and to what extent the results of these two methods correlate. If a strong correlation exists, combining Ca^{2+} fluorescence imaging with label-free impedance analysis has great potential for analyzing and deciphering GPCR signaling pathways more holistically, considering multiple perspectives. To investigate a possible correlation between the different approaches and their results, HEK293T cells were first transiently transfected with a plasmid of the Ca^{2+} sensor pN1-GCaMP6m-XC [4] and an empty vector, then incubated for 40–48 hours. The cells were subsequently preincubated with various inhibitors or chelators (FR900359 [Gq inhibitor], thapsigargin [SERCA inhibitor], BAPTA-AM [Ca^{2+} chelator], and Y-27632 [Rho kinase inhibitor]) at different concentrations before being stimulated with ATP to activate the GPCR signaling pathway. The measurement data of fluorescence and impedance signals were finally compared. In both label-based Ca^{2+} fluorescence imaging and label-free impedance analysis, the various inhibition approaches of the GPCR signaling pathway and changes in intracellular Ca^{2+} concentration after ATP stimulation are similarly well recognizable, making the results obtained highly consistent and reproducible. The combined use of Ca^{2+} fluorescence imaging and label-free impedance analysis thus offers enormous potential for analyzing and deciphering various GPCR signaling pathways more holistically, considering multiple perspectives.

References:

[1] Nakai, J.; Ohkura, M. and Imoto, K. A high signal-to-noise Ca2+ probe composed of a single green fluorescent protein. *Nat Biotechnol* **19**, 137–141 (2001).

[2] Lieb, S.; Michaelis, S. and Wegener, J. Label-free versus conventional cellular assays: Functional investigations on the human histamine H1 receptor. *Pharmacological Research* **114**, 13–26 (2016).

[3] Cotton, M. and Claing, A. G protein-coupled receptors stimulation and the control of cell migration. *Cellular Signalling* **21**, 1045–1053 (2009).

[4] Yang, Y.; Liu, N. and Liu, X. Improved calcium sensor GCaMP-X overcomes the calcium channel perturbations induced by the calmodulin in GCaMP. *Nat Commun* **9**, 1504 (2018).

Impedance-Based Analysis of Human Erythrocytes in Hereditary Spherocytosis

B. B. Tacheva; B. K. Paarvanova; M. I. Karabaliev and I. T. Ivanov

Medical Faculty, Trakia University, 6000 Stara Zagora, Bulgaria
bilyana.tacheva@trakia-uni.bg

Thermal Dielectrospectroscopy was employed to study red blood cells (RBCs) from healthy individuals and patients with hereditary spherocytosis (HS) or other anemias. Using a controlled heating protocol, changes in complex electric admittance ($Y^* = Y' + jY''$) near the spectrin denaturation temperature ($T_A \approx 49.5\,°C$) were recorded. After temperature correction, the spectrin-linked contribution to admittance revealed two distinct dielectric relaxations: β_{sp} (1.4 MHz), associated with the glycophorin C–actin–spectrin bridge, and $\gamma1_{sp}$ (9 MHz), linked to the spectrin–ankyrin–band 3 complex.
In hereditary spherocytosis due to spectrin deficiency, both β_{sp} and $\gamma1_{sp}$ strengths were reduced by ~70%, and $\gamma1_{sp}$ frequency decreased by 33%. Milder HS cases showed intermediate changes, while hemoglobinopathy samples remained comparable to healthy controls (Fig. 1). A model using two parallel RC circuits quantitatively fitted the complex admittance data ($\Delta Y''$ vs. $\Delta Y'$), illustrating the semicircular arcs corresponding to the β_{sp} and $\gamma1_{sp}$ relaxations.

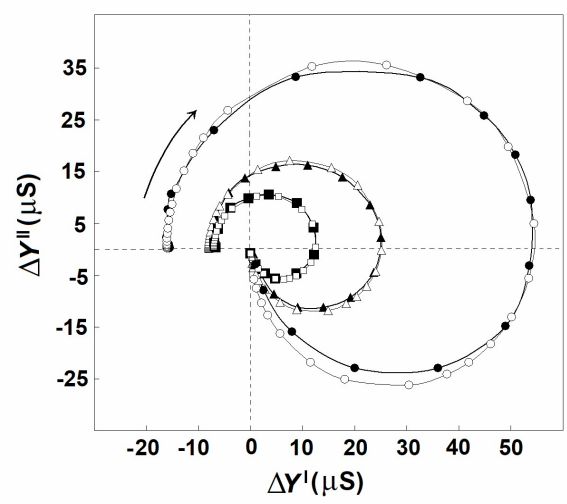

Fig. 1: Complex plain plot of spectrin-linked portion of the complex admittance of anemic RBCs. The tested suspensions contained control RBCs (●, ○), RBCs with hereditary spherocytosis due to severe spectrin deficiency (■, □) and RBCs with hereditary spherocytosis due to deficiency of band 3 (▲, Δ).

These findings show that β_{sp} and $\gamma1_{sp}$ relaxations, extracted from admittance data, serve as sensitive markers of membrane-cytoskeletal defects and can aid in differentiating membrano-pathies from other anemias.

References:

[1] B.K. Paarvanova; B.B. Tacheva; M.I. Karabaliev; I. Chakaarov; P. Chakaarova; and I.T. Ivanov, *Current Topics in Electrochemistry* 24 (2022) 69-75.

Effect of Hyperbranched Poly-L-lysine on Cell Adhesion to Surfaces

B.B. Tacheva; B.K. Paarvanova; G.D. Savova and M. I. Karabaliev

Trakia University, Stara Zagora (Bulgaria)
miroslav.karabaliev@trakia-uni.bg

Hyperbranched poly-L-lysine (HBPLL) is used to modify gold surfaces for the stable immobilisation of red blood cells (RBCs) [1]. Gold interdigitated electrodes (IDEs) were incubated in RBC suspension, and cell behavior was monitored in real time. A structured RBC layer formed on HBPLL-modified electrodes, while no such layer was observed on unmodified electrodes. The enhanced cell attachment is attributed to the cationic nature of HBPLL, promoting strong electrostatic interactions with the negatively charged RBC membranes and facilitating agglomerate formation and the further RBC adhesion as a relatively structured and intact monolayer [2].

Real-time impedance measurements were conducted using screen-printed gold electrodes modified with HBPLL. Both the real and imaginary components of the impedance increased over time and reached saturation approximately nine hours after the start of the RBC layer formation. This behavior suggests densification of the cell layer, potentially limiting access of electroactive species to the electrode surface. However, a residual electrolyte volume may remain between the electrode and the cells, which could explain the relatively moderate increase in resistance.

These findings highlight the potential of HBPLL for creating stable and reproducible RBC layers on gold electrodes, offering a promising approach for biosensor applications. Further studies are needed to elucidate the exact structure of the cell layer and its correlation with impedance behavior.

References:

[1] W. Ahmed; H. Zhang and C. Gao, Influence of enantiomeric polylysine grafted on gold nanorods on the uptake and inflammatory response of bone marrow-derived macrophages in vitro. *J. Biomed. Mater. Res. - Part A* **2022**, *110*, 143–155.

[2] W.T. Coakley; L.A. Hewison and D. Tilley, Interfacial instability and the agglutination of erythrocytes by polylysine. *Eur. Biophys. J.* **1985**, *13*, 123–130.

Smart Membrane: An On-Chip Cell Sensor for Monitoring Barrier Tissue Supported by an Artificial Neural Network

B. Tang[1,2]; V. Krajka[1,2]; M. Liu[3]; W. Zhao[1]; S. Reichl[2,4]; A. Dietzel[1,2]

[1]Institute of Microtechnology, Technische Universität Brauschweig, Brauschweig (Germany)
[2]Center of Pharmaceutical Engineering (PVZ), Technische Universität Braunschweig, Braunschweig (Germany)
[3]Institute of Pharmaceutical Technology and Biopharmaceutics, Technische Universität Braunschweig, Braunschweig (Germany)
[4]German Research Center for Artificial Intelligence (DFKI), Kaiserslautern (Germany)
b.tang@tu-braunschweig.de, v.krajka@tu-braunschweig.de

The conventional transepithelial electrical resistance (TEER) technique only yields a single value for assessing cell layers and often requires off-incubator microscopy to reveal further details. Here, we present an electrical cell sensor platform that uses a smart nanoporous membrane for continuous electrical cell-substrate impedance sensing (ECIS). The device features an ultrathin, ultra-low-stress 700 nm Si_xN_y membrane that is monolithically integrated at the wafer-level into an organ on chip system which is sealed with a glass lid (Fig. 1) [1]. Coplanar electrodes interface with custom electronics for impedance measurement under sinusoidal excitation.
Human umbilical vein endothelial cells (HUVECs) were seeded and monitored via impedance spectra, which were corroborated by bright-field and fluorescence microscopy. Nyquist plots captured distinct stages of cell development. We trained a 1D convolutional neural network (Conv1d) to classify the phases of adhesion, spreading, monolayer formation, and barrier maturation. Model validation was achieved through pharmacological perturbation using PN159 and BAC, with >95% confidence in detecting reversible and irreversible barrier disruption. We benchmarked our sensor against conventional immunostaining for tight junction markers and demonstrated substantially higher sensitivity, enabling real-time and non-invasive detection of barrier dynamics.
To contextualize the impedance data, the ECIS spectra and phase descriptions were vectorized using OpenAI's semantic embeddings. A secondary Conv1d then projected both sets of data into a shared latent space, enabling a large language model (LLM) to generate descriptive interpretations of cell states directly from the ECIS data.
This approach allows for the non-invasive and automated monitoring of barrier dynamics in barrier-on-chip systems, eliminating the need for microscopy and endpoint assays. Integrating LLMs also supports intelligent, automated experimental reporting. We envisage its wide applicability in organ-on-chip platforms for real-time physiological and pathological studies.

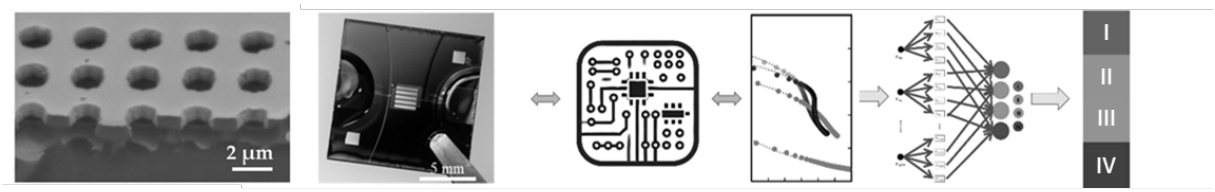

Acknowledgment: This work was funded by the Niedersächsische Landesregierung through the coordinated project "Micro Replace Systems (R2N)".

References:

[1] B.Tang., S. Bendas, V. Krajka, et al., *Frontiers in Sensors* 3 (2022)

Impedance in real-time monitoring of trophoblast spheroid invasion dynamics and future applications

D. Tang[1], L. Izmaylova[2,3], S. Ingebrandt[1,3], R. Leube[2,3], Z. Gao[1,3],*

[1] Institute of Materials in Electrical Engineering 1 (IWE1), RWTH Aachen University, 52074 Aachen, Germany.
[2] Institute of Molecular and Cellular Anatomy (MOCA), RWTH Aachen University, D-52074 Aachen, Germany.
[3] Mechanobiology in Epithelial 3D Tissue Constructs Graduate School (ME3T), RWTH Aachen, 52074 Aachen, Germany.
ziyu.gao@iwe1.rwth-aachen.de

Electric Cell-substrate Impedance Sensing (ECIS) technology was developed for a primary goal on label-free and non-invasive *in vitro* cell migration detection. However, most existing technologies are limited to single biological component system analyses with constrained resolution, posing challenges for studying more complex biological processes - from adhesion and migration to invasion and differentiation.
In our recent study, invasion of trophoblast derived spheroids through the monolayer of endometrial epithelial Ishikawa cells was investigated. In addition to classic cell proliferation and monolayer formation, a three-component *in vitro* measuring model that composed of electrode-electrolyte, monolayer and spheroid was developed to study spheroid invasion dynamics.
The interface between the spheroid and the Ishikawa monolayer was successfully detected through impedance characteristics. The measuring sensitivity to invasion dynamics was evaluated and visualized by comparing the resistance, capacitance and phase at defined low and high frequency with various spheroid-electrode coverage areas, which also aligns the assumption of biological change. Frequency-dependent semi-quantitative analysis of resistance, capacitance and phase were established to understand the cell-chip behavior over time.
Moreover, we extend *in vitro* equivalent electrical fitting (EEC) model from the conventional electrode-electrolyte double-layer interface theory to a three-component model using impedance-phase spectra. According to EEC fitting, a three-step invasion process was proposed: 1) preinvasion – non-contact condition with an intact cell monolayer, 2) early-stage invasion – spheroid attachment within 6 hours after transfer, and 3) late-stage invasion – 6 to 48 hours after spheroid transfer.
Further development of this technique could expand its scope to more complex biological mechanics sensing involving multiple factors, paving the way for more accurate and intelligent sensing systems for biomedical diagnostic such as cancer invasion and endometrial receptivity.

References:

[1] Wegener, J., Sieber, M. & Galla, H.-J. Impedance analysis of epithelial and endothelial cell monolayers cultured on gold surfaces. Journal of Biochemical and Biophysical Methods 32, 151-170 (1996).
[2] Wegener, J., Keese, C. R. & Giaever, I. Electric cell-substrate impedance sensing (ECIS) as a noninvasive means to monitor the kinetics of cell spreading to artificial surfaces. Exp Cell Res 259, 158-166 (2000).
[3] Jiang, H. et al. Metal-organic frameworks as an active substrate for cell-interaction studies and cell-on-a-chip platforms. Biosensors and Bioelectronics: X 19 (2024).

Age-related differences in renewal potential of equine ASCs

E.G. Vachkova[1]; M. Karabaliev[2]; V. Petrova[1]; S. Arnhold[3]; M. Heimann[3]

[1]Department of Pharmacology, Animal Physiology, Biochemistry and Chemistry, Faculty of Veterinary Medicine, Trakia University, 6000 Stara Zagora, Bulgaria
[2]Department of Medical physics, biophysics, radiology and radiology, Faculty of Medicine, Trakia University, 6000 Stara Zagora, Bulgaria
[3]Institute of Veterinary Anatomy, Histology and Embryology, Justus-Liebig-University of Giessen, 35392 Giessen, Germany
ekaterina.vachkova@trakia-uni.bg

Subcutaneous adipose tissue is a rich and accessible source of mesenchymal stem cells (MSCs), which hold significant promise for treating traumatic injuries in athletic horses. Many factors, such as the age of donors, passage number, culturing microenvironment, etc., could influence cellular vitality, proliferation rate, and senescence, compromising their regenerative potential. To our knowledge, this is the first report using the EICS system to characterize the equine ASCs' behavior in vitro.

Equine ASCs from two age groups (up to ten and over fifteen-year-old donors) at fifth passage were seeded at a density of $1x10^5$ cells per well and cultured in standard medium (low glucose DMEM, 10% FBS, antibiotic/antimycotic solution) in 5% CO2 humidified conditions. After electrical fence, the impedance differences were monitored for 36 hours by the ECIS Z-Theta system equipped with an 8-well chamber with 40 circular gold L-cystein-coated electrodes in each well. The mean cellular volume, total number, and cellular fraction 6-8 µm were also evaluated at the end of the experimental period.

During the growth phase, the cells from younger donors showed a faster exponential phase and higher impedance values at the beginning of the stationary phase. In contrast, the impedance value in the cells from older donors was higher during the stationary phase and lacked detectable impedance deviations caused by apoptotic cell death in both groups. The mean cellular volume did not differ markedly, but the 6-8 µm cellular fraction percentage in the up to 10 years old group was approximately 4-fold higher.

Based on the impedance pattern, the cells from younger donors showed a faster renewal rate and higher proliferative capacity than the older ones. The lower impedance values in the younger group during the stationary phase are probably due to the higher percentage of 6-8 µm cellular fraction with a smaller adhesive surface. Overall, the data indicate that ASCs from up to ten-year-old donors are preferred for regenerative purposes.

Microphysiometric Organ-on-Chip System

J. Wiest and S. Eggert

cellasys, Kronburg (Germany)
wiest@cellasys.tech

Microphysiometry is applied since the 1990s with various applications in toxicology, pharmacology, and personalized medicine [1,2]. Here the usage of label-free sensors allows time-series analysis of morphologic and metabolic changes of cellular models. To increase reproducibility and through-put of such Organ-on-Chip systems the Microphysiometric Organ-ON-chip System (MOONS) was developed. The computer-controlled platform consists of an incubator for temperature control, a pipetting robot for automated media dispensing, a HEPA filter unit to prevent contaminations and a 24well reader. The MOONS plate-I is a 24well plate for measurement of changes in impedance. It can be used for investigation of 2D cell layers (planar electrodes) as well as 3D tissue insert (transepithelial electrical impedance). Each of the 24wells is assisted with an inflow channel, a waste medium reservoir and an apical access to allow interconnection of the wells and the realization of an air-liquid interface. Figure 1 depicts the MOONS plate-I as well as results from a six-hour experiment with Caco-2 cells.

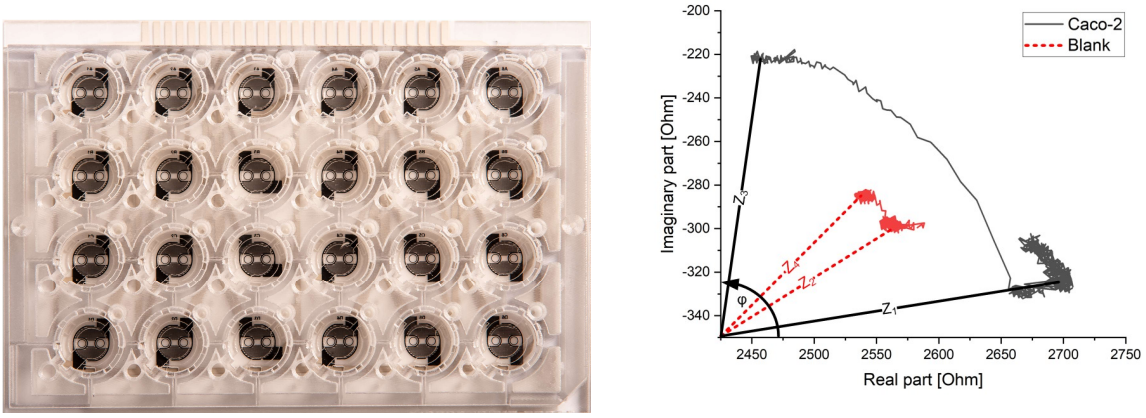

Figure 1 Left: Top view of a MOONS plate-I with 24 planar impedance sensors in wells equipped with fluidic channels [3]. Right: Imaginary part vs real part plot of Caco-2 cells treated with 0,2 % SDS. Z_1: Confluent Caco-2; Z_3: Caco-2 treated with SDS; Z_2: Blank medium; Z_4: Medium with SDS

It should be noted that there is only a relatively small change in the magnitude comparing confluent with treated cells. While the experiment shows that the MOONS is performant, the presented data stresses the importance to maintain real and imaginary part (or magnitude and phase) to fully exploit impedance measurements.

References:

[1] J. Wiest, *Organs-on-a-Chip* 4 (2022) 100016, doi:10.1016/j.ooc.2022.100016.
[2] M. Brischwein, J. Wiest, *In: Wegener J. (eds) Label-Free Monitoring of Cells in vitro. Bioanalytical Reviews*, 2 (2018) 163-188doi.org/10.1007/11663_2018_2
[3] https://cellasys.tech/wp-content/uploads/2024/04/IFU-490104_MOONS_plate-I_data_sheet_V2_2.pdf

Development of a label-free method for measuring Transwell Matrigel cell invasion

W.-L. Chen; C.-M. Lo
National Yang Ming Chiao Tung University, Taipei (Taiwan)
bet1233.be11@nycu.edu.tw

Invasive cancer cells can spread outward and penetrate neighboring normal tissues, leading to cancer progression and increased mortality [1]. Currently, the assessment of cancer cell invasiveness largely relies on endpoint methods such as immunostaining. However, these techniques are prone to deviations due to operator variability and subjective interpretation [2]. In this study, we applied electric cell-substrate impedance sensing (ECIS) technology, combined with commercially available Transwell inserts uniformly coated with Matrigel, to establish a real-time ECIS trans-filter invasion assay for monitoring the invasive behavior of MDA-MB-231. Through this approach, we evaluated the effects of different anticancer drugs on the invasiveness of MDA-MB-231 cells and dynamically recorded their penetration through Matrigel using continuous impedance measurements. The results showed that when MDA-MB-231 cells were treated with low concentrations of cisplatin or doxorubicin, they retained invasive abilities, as evidenced by a steady increase in capacitive reactance. When the drug concentrations were increased, the cells initially remained invasive; however, the capacitive reactance decreased from 8 ohms to 2 ohms after 10 hours, indicating that the drug began to exert an inhibitory effect. In contrast, treatment with high concentrations of paclitaxel maintained a capacitive reactance of 2 ohms from the beginning, with no significant changes, indicating that cell invasion behavior was almost completely inhibited.

In addition, we compared the ECIS trans-filter invasion assay developed in this study with the conventional and widely used Transwell Matrigel invasion assay by analyzing the proportion of cells that penetrated through each method. Under drug-free conditions, the Transwell Matrigel invasion assay detected only 6.7% of MDA-MB-231 cells as having penetrated the Transwell. In contrast, the ECIS trans-filter assay detected 57.2% of cells successfully invading through the Matrigel. Following treatment with 1 μM paclitaxel, the Transwell Matrigel assay detected only 2.1% cell penetration, while the ECIS trans-filter invasion assay revealed a penetration rate of 11.5%. Based on the above results, the ECIS trans-filter invasion assay is not only real-time and highly sensitive, but also can quickly and accurately measure the invasion behavior of cancer cells, providing a potential innovative tool for future evaluation of anticancer drug efficacy and research on cancer invasion.

References:

[1] C. Wittekind; M. Neid, *Oncology* 69 (2005) 14-16.
[2] N. Kramer; A. Walzl; C. Unger; M. Rosner; G. Krupitza; M. Hengstschläger and H. Dolznig, *Mutation Research* 752 (2013) 10-24.

Electrically Monitoring Osteogenic Differentiation of Human Dental Pulp Stem Cells Using Electric Cell-Substrate Impedance Sensing

J.-W. Chen[1], W.-L. Chen[1], Chun-Min Lo[1*]
Department of Biomedical Engineering, National Yang Ming Chiao Tung University, Taipei 112, Taiwan
conniegiwawa0302@gmail.com

This study investigates the biodegradability, ion release behavior, pH variation, and effects on the proliferation and differentiation of human dental pulp stem cells (hDPSCs) using MSZN-Ca alloy scaffolds. Both MSZN-0 Ca and MSZN-0.3 Ca scaffolds exhibited a slow and stable degradation rate over 30 days of immersion, indicating favorable stability in physiological environments. ICP-MS analysis confirmed sustained release of Mg^{2+} (~1000 ppm), Zn^{2+}, and Ca^{2+} ions, with Mg^{2+} being closely associated with stem cell differentiation [1-5].

pH analysis showed that the conditioned medium of MSZN-0.3 Ca stabilized by day 9, while MSZN-0 Ca required approximately 15 days. Based on ion release and pH stability, the 9-day conditioned medium (C group) was selected for subsequent experiments. ARS staining and morphological assessment revealed significant calcium deposition and increased cell spreading from day 14 in differentiated human dental pulp stem cells (hDPSCs). The MSZN-0.3 Ca C group demonstrated superior differentiation effects compared to the MSZN-0 Ca C group.

ECIS data further supported these findings, showing that the cell junctional resistance (R_b) in the differentiated groups was generally lower than that in the undifferentiated groups. Notably, the average junctional resistance of the MSZN-0.3 Ca C group fell below that of the standard differentiation medium after approximately 10 days of culture. In contrast, the MSZN-0 Ca C group showed no significant change. In addition, the Rb value in the MSZN-0.3 Ca C group demonstrated a continuous decline over time, further indicating its superior potential to enhance hDPSCs differentiation. Microscopic observations at day 30 showed mineralized precipitates on electrodes and distinct cell morphologies between differentiated and undifferentiated cells. These findings confirm the correlation between calcium deposition and differentiation.

In summary, the MSZN-0.3 Ca C group exhibited a higher potential to promote hDPSC differentiation, highlighting its promise for regenerative medicine applications.

References:

[1] H. Zhou, B. Liang, H. Jiang, Z. Deng and K. Yu, *Journal of Magnesium and Alloys* 9 (2021) 779-804.
[2] K. Dachasa, T.C. Aklilu B.G. Ewnete, B.M. Ejeta and F.F. Bakare, *Advances in Materials Science and Engineering* 2024 (2024) 1325004.
[3] A. Shanmugavadivu, S. Lekhavadhani, S. Babu, N. Suresh and N. Selvamurugan, *Journal of Magnesium and Alloys* 12 (2024) 2231-2248.
[4] V. Manescu, I. Antoniac, A. Antoniac, D. Laptoiu, G. Paltanea, R. Ciocoiu, I.V. Nemoianu, L.G. Gruionu and H. Dura, *Biomimetics* 8 (2023) 618.
[5] Y. Wang, X. Wu, W. Yang, P. Feng, W. Tan, Y. Deng and C. Shuai, *Journal of Nanomaterials*, 2022 (2022) 3273077.

List of Posters

P01	Acerbo, E.	Finite Difference Model Representing Cell Distribution in Monolayer
P02	Acharya, R.	A Versatile, Biomimetic, 3D Electrochemical Device for Monitoring Cell Growth and Epithelial Barrier Integrity
P03	Alalul, O.	Biomechanics of single cells using a microfluidic device to correlate transients of flow impedance and electrical impedance
P04	Bhavsar, M.B.	Detection of cell occupation on Cochlear Implants (CI) for long-term monitoring of stimulation efficiency
P05	Bruckbauer, L.	Fish cell-based detection of ecotoxicological effects and development of a ready-to-use cell-based sensor
P06	Carmans, I.	Combining TEER and high-resolution spatial impedance mapping on porous MEA for improved *in vitro* barrier measurements
P07	Chen, Y.-L.	Alleviation of LPS-induced Endothelial Dysfunction with Bone Morphogenetic Protein 10
P08	Chiu, T.-Y..	Application of ECIS to Assess WI38 Cell Migration under BMP10 Treatment and Bleomycin Stimulation
P09	Erl, J.	Revealing Cellular Signaling Dynamics with Light-Activated Molecules: From Receptor Ligands to Second Messenger
P10	Friedrich, S.	Ready–to–use Insect cell-based Sensor for Pesticide Testing
P11	Fuhry, E.	Soft Graphene Electrodes and Screen-Printed Carbon Electrodes for Monitoring Cell Adhesion Using Non-Faradaic Electrochemical Impedance Spectroscopy
P12	Grimm, A.-K.	A virus-free impedance platform to emulate virus-induced cell fusion
P13	Höök, J.	Hydrogel-Coated Graphene Impedance Sensor for Real-Time Monitoring of Cell Adhesion
P14	Huang, C.T.	Probing the EGTA-Mediated Barrier Impairment of MDCK Cells by Electric Cell-Substrate Impedance Sensing
P15	Knafl, S.	Impedance-guided Evaluation of Cancer Therapy: A new route for personalized medicine?
P16	Lai, S.Y.	Effects of the Conditioned Media Obtained from Biodegradable Mg-Zn-Sn Alloys on Human Dental Pulp Stem Cells
P17	Leuschner, C.	Development of a Fully DLP-Printed Sensor-Integrated Cell Culture Well for Electrochemical Evaluation
P18	Meenaketan, B. L.	Advancing 3D Impedance Tomography for *In-Vitro* models
P19	Michaelis, S.	PEDOT:PSS as transparent, low-cost electrode material for impedance-based cell analysis
P20	Mozafari, M.	Impedance Flow Cytometry for Electrogenic Microorganisms

P21	Naber, T.	Impedance Spectroscopic Monitoring of indirectly co-cultured monolayers (CIS-TER)
P22	Paarvanova, B.	Application of Thermal Dielectrospectroscopy in Studying the Membrane of Human Erythrocytes
P23	Pliquett, U.	Concept for high channel systems for cell sensing
P24	Rafferty, C.	Biophysical Profiling of MASLD-MASH Disease Transition
P25	Rottbauer, L.C.	ECIS-O_2: Dual Sensor Approach to Monitor Metabolic Respiration and Cell Morphology
P26	Savova, G.	Electrochemical Impedance Analysis of Poly-phosphocholinated Liposomes Stability on Solid Electrode Surfaces
P27	Schaffer, M.	Dual Monitoring of Impedance-Based Barrier Function and NF-κB Reporter Signaling in a Caco-2 Intestinal Inflammation Model
P28	Schwenk, P.	Correlation between label-free impedance analysis and Ca^{2+} fluorescence *in vitro* imaging
P29	Tacheva, B.B.	Impedance-Based Analysis of Human Erythrocytes in Hereditary Spherocytosis
P30	Tacheva, B.B.	Effect of Hyperbranched Poly-L-lysine on Cell Adhesion to Surfaces
P31	Tang, B.	Smart Membrane: An On-Chip Cell Sensor for Monitoring Barrier Tissue Supported by an Artificial Neural Network
P32	Tang, D.	Impedance in real-time monitoring of trophoblast spheroid invasion dynamics and future applications
P33	Vachkova, E.G.	Age-related differences in renewal potential of equine ASCs
P34	Wiest, J.	Microphysiometric Organ-on-Chip System
P35	Chen, W.-L.	Development of a label-free method for measuring Transwell Matrigel cell invasion
P36	Chen, J.W.	Electrically Monitoring Osteogenic Differentiation of Human Dental Pulp Stem Cells Using Electric Cell-Substrate Impedance Sensing

Information for Participants

(1) Internet Access

(1a) You can use "Bayern WLAN" as free WLAN service. Once you are connected, open your browser and confirm.

(1b) "eduroam" is available everywhere on UR campus.

(2) Campus Map

See addendum

(3) Time tables for bus lines 6 and 11

Time tables *venue* ⇒ *city* or *city* ⇒ *venue* are available on the following pages. Both lines provide service to/from the main train station. To reach the venue of our conference dinner, you are better off using line 11. Bus stop "Thundorferstraße" is very close to the "Salzstadl".

(4) Bus Routing within City Limits

See addendum.

IBCA 2025

Line 6

University ⇒ City

Linie 6 — **Klinikum - Universität - Hauptbahnhof - Bismarckplatz - Clermont-Ferrand-Allee - Roter-Brach-Weg** — Bus

Montag - Freitag		5	6					7 - 8						9						10						11 - 13						14
VERKEHRSHINWEIS																																
Klinikum (A)		34	57	17	34	44	54	04	14	24	34	44	54	04	14	24	34	44	54	04	14	24	34	44	54	04	14	24	34	44	54	04
Neuprüll		35	58	18	35	45	55	05	15	25	35	45	55	05	15	25	35	45	55	05	15	25	35	45	55	05	15	25	35	45	55	05
An der Kreuzbreite		36	59	19	36	46	56	06	16	26	36	46	56	06	16	26	36	46	56	06	16	26	36	46	56	06	16	26	36	46	56	06
Universität (E)		**38**	**01**	**21**	**38**	**48**	**58**	**08**	**18**	**28**	**38**	**48**	**58**	**08**	**18**	**28**	**38**	**48**	**58**	**08**	**18**	**28**	**38**	**48**	**58**	**08**	**18**	**28**	**38**	**48**	**58**	**08**
Otto-Hahn-Straße		40	03	23	40	50	00	10	20	30	40	50	00	10	20	30	40	50	00	10	20	30	40	50	00	10	20	30	40	50	00	10
TechCampus/OTH		41	04	24	41	51	01	11	21	31	41	51	01	11	21	31	41	51	01	11	21	31	41	51	01	11	21	31	41	51	01	11
Haydnstraße		42	05	25	43	53	03	13	23	33	43	53	03	13	23	33	43	53	03	13	23	33	43	53	03	13	23	33	43	53	03	13
HBF Süd/Arcaden		43	06	26	45	55	05	15	25	35	45	55	05	15	25	35	45	55	05	15	25	35	45	55	05	15	25	35	45	55	05	15
Hauptbahnhof (B1)	an	**45**	**08**	**28**	**47**	**57**	**07**	**17**	**27**	**37**	**47**	**57**	**07**	**17**	**27**	**37**	**47**	**57**	**07**	**17**	**27**	**37**	**47**	**57**	**07**	**17**	**27**	**37**	**47**	**57**	**07**	**17**
Hauptbahnhof (B1)	ab	**45**	**08**	**28**	**48**	**58**	**08**	**18**	**28**	**38**	**48**	**58**	**08**	**18**	**28**	**38**	**48**	**58**		**18**		**38**		**58**		**18**		**38**		**58**		**18**
Justizgebäude		47	10	30	50	00	10	20	30	40	50	00	10	20	30	40	50	00		20		40		00		20		40		00		20
Bismarckplatz		50	13	33	53	03	13	23	33	43	53	03	13	23	33	43	53	03		23		43		03		23		43		03		23
Ostdeutsche Galerie		53	16	36	56	06	16	26	36	46	56	06	16	26	36	46	56	06		26		46		06		26		46		06		26
Gumpelzhaimerstraße		54	17	37	57	07	17	27	37	47	57	07	17	27	37	47	57	07		27		47		07		27		47		07		27
Albertus-Magnus-Gymnasium		55	18	38	58	08	18	28	38	48	58	08	18	28	38	48	58	08		28		48		08		28		48		08		28
Josef-Adler-Straße		56	19	39	59	09	19	29	39	49	59	09	19	29	39	49	59	09		29		49		09		29		49		09		29
Boessnerstraße		57	20	40	00	10	20	30	40	50	00	10	20	30	40	50	00	10		30		50		10		30		50		10		30
Clermont-Ferrand-Allee		58	21	41	01	11	21	31	41	51	01	11	21	31	41	51	01	11		31		51		11		31		51		11		31
Wernerwerkstraße		00	23	43	03	13	23	33	43	53	03	13	23	33	43	53	03	13		33		53		13		33		53		13		33
Hermann-Köhl-Straße		01	24	44	04	14	24	34	44	54	04	14	24	34	44	54	04	14		34		54		14		34		54		14		34
Sparkasse		02	25	45	05	15	25	35	45	55	05	15	25	35	45	55	05	15		35		55		15		35		55		15		35
Roter-Brach-Weg		**04**	**27**	**47**	**07**	**17**	**27**	**37**	**47**	**57**	**07**	**17**	**27**	**37**	**47**	**57**	**07**	**17**		**37**		**57**		**17**		**37**		**57**		**17**		**37**

Montag - Freitag		14					15						16 - 17						18						19				20		21
VERKEHRSHINWEIS																																
Klinikum (A)		14	24	34	44	54	04	14	24	34	44	54	04	14	24	34	44	54	04	14	24	34	44	54	04	16	31	45	00	15	45	
Neuprüll		15	25	35	45	55	05	15	25	35	45	55	05	15	25	35	45	55	05	15	25	35	45	55	05	17	32	46	01	16	46	
An der Kreuzbreite		16	26	36	46	56	06	16	26	36	46	56	06	16	26	36	46	56	06	16	26	36	46	56	06	18	33	47	02	17	47	
Universität (E)		**18**	**28**	**38**	**48**	**58**	**08**	**18**	**28**	**38**	**48**	**58**	**08**	**18**	**28**	**38**	**48**	**58**	**08**	**18**	**28**	**38**	**48**	**58**	**08**	**20**	**35**	**49**	**04**	**19**	**49**	
Otto-Hahn-Straße		20	30	40	50	00	10	20	30	40	50	00	10	20	30	40	50	00	10	20	30	40	50	00	10	22	37	51	06	21	51	
TechCampus/OTH		21	31	41	51	01	11	21	31	41	51	01	11	21	31	41	51	01	11	21	31	41	51	01	11	23	38	52	07	22	52	
Haydnstraße		23	33	43	53	03	13	23	33	43	53	03	13	23	33	43	53	03	13	23	33	43	53	03	13	25	40	53	08	23	53	
HBF Süd/Arcaden		25	35	45	55	05	15	25	35	45	55	05	15	25	35	45	55	05	15	25	35	45	55	05	15	27	42	55	10	25	55	
Hauptbahnhof (B1)	an	**27**	**37**	**47**	**57**	**07**	**17**	**27**	**37**	**47**	**57**	**07**	**17**	**27**	**37**	**47**	**57**	**07**	**17**	**27**	**37**	**47**	**57**	**07**	**17**	**29**	**44**	**57**	**12**	**27**	**57**	
Hauptbahnhof (B1)	ab		**38**		**58**	**08**	**18**	**28**	**38**	**48**	**58**	**08**	**18**	**28**	**38**	**48**	**58**	**08**	**18**	**28**		**48**		**08**		**30**	**45**	**00**		**30**	**00**	
Justizgebäude			40		00	10	20	30	40	50	00	10	20	30	40	50	00	10	20	30		50		10		32	47	02		32	02	
Bismarckplatz			43		03	13	23	33	43	53	03	13	23	33	43	53	03	13	23	33		53		13		35	50	05		35	05	
Ostdeutsche Galerie			46		06	16	26	36	46	56	06	16	26	36	46	56	06	16	26	36		56		16		38	53	08		38	08	
Gumpelzhaimerstraße			47		07	17	27	37	47	57	07	17	27	37	47	57	07	17	27	37		57		17		39	54	09		39	09	
Albertus-Magnus-Gymnasium			48		08	18	28	38	48	58	08	18	28	38	48	58	08	18	28	38		58		18		40	55	10		40	10	
Josef-Adler-Straße			49		09	19	29	39	49	59	09	19	29	39	49	59	09	19	29	39		59		19		41	56	11		41	11	
Boessnerstraße			50		10	20	30	40	50	00	10	20	30	40	50	00	10	20	30	40		00		20		42	57	12		42	12	
Clermont-Ferrand-Allee			51		11	21	31	41	51	01	11	21	31	41	51	01	11	21	31	41		01		21		43	58	13		43	13	
Wernerwerkstraße			53		13	23	33	43	53	03	13	23	33	43	53	03	13	23	33	43		03		23		45	00	14		44	14	
Hermann-Köhl-Straße			54		14	24	34	44	54	04	14	24	34	44	54	04	14	24	34	44		04		24		46	01	15		45	15	
Sparkasse			55		15	25	35	45	55	05	15	25	35	45	55	05	15	25	35	45		05		25		47	02	16		46	16	
Roter-Brach-Weg			**57**		**17**	**27**	**37**	**47**	**57**	**07**	**17**	**27**	**37**	**47**	**57**	**07**	**17**	**27**	**37**	**47**		**07**		**27**		**49**	**04**	**18**		**48**	**18**	

Montag - Freitag		21 - 23		0
VERKEHRSHINWEIS				FR
Klinikum (A)		**15**	**45**	**15**
Neuprüll		16	46	16
An der Kreuzbreite		17	47	17
Universität (E)		**19**	**49**	**19**
Otto-Hahn-Straße		21	51	21
TechCampus/OTH		22	52	22
Haydnstraße		23	53	23
HBF Süd/Arcaden		25	55	25
Hauptbahnhof (B1)	an	**27**	**57**	**27**
Hauptbahnhof (B1)	ab	**30**	**00**	
Justizgebäude		32	02	
Bismarckplatz		35	05	
Ostdeutsche Galerie		38	08	
Gumpelzhaimerstraße		39	09	
Albertus-Magnus-Gymnasium		40	10	
Josef-Adler-Straße		41	11	
Boessnerstraße		42	12	
Clermont-Ferrand-Allee		43	13	
Wernerwerkstraße		44	14	
Hermann-Köhl-Straße		45	15	
Sparkasse		46	16	
Roter-Brach-Weg		**48**	**18**	

ZEICHENERKLÄRUNG: FR= Nur freitags

Während Sommer- und Weihnachtsferien bitte Fahrplanänderung beachten

Gültig ab 01.08.2025

IBCA 2025

Line 6

City ⇒ University

Linie 6 — **Roter-Brach-Weg - Clermont-Ferrand-Allee - Bismarckplatz - Hauptbahnhof - Universität - Klinikum** — Bus

Montag - Freitag	5	6						7							8							9					10
VERKEHRSHINWEIS								U																			
Roter-Brach-Weg	17 37 57	07	17	27	37	47	57		07	17	27	37	47	57	07	17	27	37	47	57	07	17	27	37	47		
Sparkasse	17 37 57	07	17	27	37	47	57		07	17	27	37	47	57	07	17	27	37	47	57	07	17	27	37	47		
Hermann-Köhl-Straße	18 38 58	08	18	28	38	48	58		08	18	28	38	48	58	08	18	28	38	48	58	08	18	28	38	48		
Wernerwerkstraße	19 39 59	09	19	29	39	49	59		09	19	29	39	49	59	09	19	29	39	49	59	09	19	29	39	49		
Clermont-Ferrand-Allee	20 40 00	10	20	30	40	50	00		10	20	30	40	50	00	10	20	30	40	50	00	10	20	30	40	50		
Boessnerstraße	21 41 01	11	21	31	41	51	01		11	21	31	41	51	01	11	21	31	41	51	01	11	21	31	41	51		
Josef-Adler-Straße	22 42 02	12	22	32	42	52	02		12	22	32	42	52	02	12	22	32	42	52	02	12	22	32	42	52		
Albertus-Magnus-Gymnasium	23 43 03	13	23	33	43	53	03		13	23	33	43	53	03	13	23	33	43	53	03	13	23	33	43	53		
Gumpelzhaimerstraße	24 44 04	14	24	34	44	54	04		14	24	34	44	54	04	14	24	34	44	54	04	14	24	34	44	54		
Ostdeutsche Galerie	26 46 06	16	26	36	46	56	06		16	26	36	46	56	06	16	26	36	46	56	06	16	26	36	46	56		
Bismarckplatz	28 48 09	19	29	39	49	59	09		19	29	39	49	59	09	19	29	39	49	59	09	19	29	39	49	59		
Justizgebäude	30 50 12	22	32	42	52	02	12		22	32	42	52	02	12	22	32	42	52	02	12	22	32	42	52	02		
Fritz-Fend-Straße	31 51 13	23	33	43	53	03	13		23	33	43	53	03	13	23	33	43	53	03	13	23	33	43	53	03		
Hauptbahnhof West	32 52 14	24	34	44	54	04	14		24	34	44	54	04	14	24	34	44	54	04	14	24	34	44	54	04		
Hauptbahnhof (B4) an	| |	|	|	|	|	|	|		|	|	|	|	|	|	|	|	|	|	|	|	|	|		
Hauptbahnhof (B4) ab	| |	|	|	|	|	|	|		|	|	|	|	|	|	|	|	|	|	|	|	|		
Hauptbahnhof (B8) an	**35 55** **17**	**27**	**37**	**47**	**57**	**07**	**17**		**27**	**37**	**47**	**57**	**07**	**17**	**27**	**37**	**47**	**57**	**07**	**17**	**27**	**37**	**47**	**57**	**07**		
Hauptbahnhof (B8) ab	**35 55 08 18**	**28**	**38**	**48**	**58**	**08**	**18**	**21**	**28**	**38**	**48**	**58**	**08**	**18**	**28**	**38**	**48**	**58**	**08**	**18**	**28**	**38**	**48**	**58**	**08**		
HBF Süd/Arcaden	36 56 09 19	29	39	49	59	09	19	22	29	39	49	59	09	19	29	39	49	59	09	19	29	39	49	59	09		
Haydnstraße	38 58 11 21	31	41	51	01	11	21	24	31	41	51	01	11	21	31	41	51	01	11	21	31	41	51	01	11		
TechCampus/OTH	39 59 12 22	32	42	52	02	12	22	25	32	42	52	02	12	22	32	42	52	02	12	22	32	42	52	02	12		
Otto-Hahn-Straße	40 00 13 23	33	43	53	03	13	23	26	33	43	53	03	13	23	33	43	53	03	13	23	33	43	53	03	13		
Universität (A)	**42 02 15 25**	**35**	**45**	**55**	**05**	**15**	**25**	**28**	**35**	**45**	**55**	**05**	**15**	**25**	**35**	**45**	**55**	**05**	**15**	**25**	**35**	**45**	**55**	**05**	**15**		
An der Kreuzbreite	43 03 16 26	36	46	56	06	16	26	29	36	46	56	06	16	26	36	46	56	06	16	26	36	46	56	06	16		
Neuprüll	44 04 17 27	37	47	57	07	17	27	30	37	47	57	07	17	27	37	47	57	07	17	27	37	47	57	07	17		
Klinikum West	46 06 19 29	39	49	59	09	19	29	32	39	49	59	09	19	29	39	49	59	09	19	29	39	49	59	09	19		
Klinikum (A)	**48 08 21 31**	**41**	**51**	**01**	**11**	**21**	**31**	**34**	**41**	**51**	**01**	**11**	**21**	**31**	**41**	**51**	**01**	**11**	**21**	**31**	**41**	**51**	**01**	**11**	**21**		

Montag - Freitag	10 - 14					15							16 - 17						18			19		20 - 22		23	0
VERKEHRSHINWEIS																											
Roter-Brach-Weg	**07**	**27**	**47**		**07**	**17**	**27**	**37**	**47**	**57**		**07**	**17**	**27**	**37**	**47**	**57**		**07**	**27**	**47**	**07**	**39**	**09**	**39**	**09**	**39**	
Sparkasse	07	27	47		07	17	27	37	47	57		07	17	27	37	47	57		07	27	47	07	39	09	39	09	39	
Hermann-Köhl-Straße	08	28	48		08	18	28	38	48	58		08	18	28	38	48	58		08	28	48	08	40	10	40	10	40	
Wernerwerkstraße	09	29	49		09	19	29	39	49	59		09	19	29	39	49	59		09	29	49	09	41	11	41	11	41	
Clermont-Ferrand-Allee	10	30	50		10	20	30	40	50	00		10	20	30	40	50	00		10	30	50	10	42	12	42	12	42	
Boessnerstraße	11	31	51		11	21	31	41	51	01		11	21	31	41	51	01		11	31	51	11	43	13	43	13	43	
Josef-Adler-Straße	12	32	52		12	22	32	42	52	02		12	22	32	42	52	02		12	32	52	12	44	14	44	14	44	
Albertus-Magnus-Gymnasium	13	33	53		13	23	33	43	53	03		13	23	33	43	53	03		13	33	53	13	45	15	45	15	45	
Gumpelzhaimerstraße	14	34	54		14	24	34	44	54	04		14	24	34	44	54	04		14	34	54	14	46	16	46	16	46	
Ostdeutsche Galerie	16	36	56		16	26	36	46	56	06		16	26	36	46	56	06		16	36	56	16	47	17	47	17	47	
Bismarckplatz	19	39	59		19	29	39	49	59	09		19	29	39	49	59	09		19	39	59	19	50	20	50	20	50	
Justizgebäude	22	42	02		22	32	42	52	02	12		22	32	42	52	02	12		22	42	02	22	52	22	52	22	52	
Fritz-Fend-Straße	23	43	03		23	33	43	53	03	13		23	33	43	53	03	13		23	43	03	23	53	23	53	23	53	
Hauptbahnhof West	24	44	04		24	34	44	54	04	14		24	34	44	54	04	14		24	44	04	24	54	24	54	24	54	
Hauptbahnhof (B4) an	|	|		|	|	|	|	|	|		|	|	|	|	|		|	|	|	|	**57**	**27**	**57**	**27**	**57**	
Hauptbahnhof (B4) ab	|	|		|	|	|	|	|	|		|	|	|	|	|		|	|	|	|	**00**	**30**	**00**	**30**	**00**	
Hauptbahnhof (B8) an	**27**	**47**		**07**	**27**	**37**	**47**	**57**	**07**	**17**		**27**	**37**	**47**	**57**	**07**	**17**		**27**	**47**	**07**	**27**	**00**	**30**	**00**	**30**	**00**	
Hauptbahnhof (B8) ab	**18 28 38 48**	**58**	**08**	**18**	**28**	**38**	**48**	**58**	**08**	**18**	**28**	**38**	**48**	**58**	**08**	**18**	**28**	**38**	**48**	**08**	**28**	**00**	**30**	**00**	**30**	**00**	
HBF Süd/Arcaden	19 29 39 49	59	09	19	29	39	49	59	09	19	29	39	49	59	09	19	29	39	49	09	29	01	31	01	31	01	
Haydnstraße	21 31 41 51	01	11	21	31	41	51	01	11	21	31	41	51	01	11	21	31	41	51	11	31	03	33	03	33	03	
TechCampus/OTH	22 32 42 52	02	12	22	32	42	52	02	12	22	32	42	52	02	12	22	32	42	52	12	32	04	34	04	34	04	
Otto-Hahn-Straße	23 33 43 53	03	13	23	33	43	53	03	13	23	33	43	53	03	13	23	33	43	53	13	33	05	35	05	35	05	
Universität (A)	**25 35 45 55**	**05**	**15**	**25**	**35**	**45**	**55**	**05**	**15**	**25**	**35**	**45**	**55**	**05**	**15**	**25**	**35**	**55**	**15**	**35**	**07**	**37**	**07**	**37**	**07**		
An der Kreuzbreite	26 36 46 56	06	16	26	36	46	56	06	16	26	36	46	56	06	16	26	36	56	16	36	08	38	08	38	08		
Neuprüll	27 37 47 57	07	17	27	37	47	57	07	17	27	37	47	57	07	17	27	37	57	17	37	09	39	09	39	09		
Klinikum West	29 39 49 59	09	19	29	39	49	59	09	19	29	39	49	59	09	19	29	39	59	19	39	11	41	11	41			
Klinikum (A)	**31 41 51 01**	**11**	**21**	**31**	**41**	**51**	**01**	**11**	**21**	**31**	**41**	**51**	**01**	**11**	**21**	**31**	**41**	**01**	**21**	**41**	**13**	**43**	**13**	**43**			

Line 11

University ⇒ City

Linie 11 — **Burgweinting - Universität - OTH - Hauptbahnhof - Arnulfsplatz - Wernerwerkstraße** — Bus

Montag - Freitag	5			6					7					8				9			10 - 18			19		20 - 22		23	0
Burgw. Herm.-Höcherl-Str.	16		41		01		21	41	01		21		41	01		21	41	01	21	41	01	21	41	16	46	16	46	16	
Burgw. Sophie-Scholl-Str.	17		42		02		22	42	02		22		42	02		22	42	02	22	42	02	22	42	17	47	17	47	17	
Burgw. Langer Weg	18		43		03		23	43	03		23		43	03		23	43	03	23	43	03	23	43	18	48	18	48	18	
Burgw. Droste-Hülshoff-Weg	19		44		04		24	44	04		24		44	04		24	44	04	24	44	04	24	44	19	49	19	49	19	
Burgw. Kurzer Weg	20		45		05		25	45	05		25		45	05		25	45	05	25	45	05	25	45	20	50	20	50	20	
Burgw. Fr.-Viehbacher-Allee	21		46		06		26	46	06		26		46	06		26	46	06	26	46	06	26	46	21	51	21	51	21	
Burgweinting Kirche	22		48		08		28	48	08		28		48	08		28	48	08	28	48	08	28	48	22	52	22	52	22	
Benzstraße	24		50		10		30	50	10		30		50	10		30	50	10	30	50	10	30	50	24	54	24	54	24	
Schöneberger Straße	25		51		11		31	51	11		31		51	11		31	51	11	31	51	11	31	51	25	55	25	55	25	
Schwabenstraße	27		53		13		33	53	13		33		53	13		33	53	13	33	53	13	33	53	27	57	27	57	27	
Johann-Hösl-Straße	28		55		15		35	55	15		35		55	15		35	55	15	35	55	15	35	55	28	58	28	58	28	
Franz-Hartl-Straße	29		56		16		36	56	16		36		56	16		36	56	16	36	56	16	36	56	29	59	29	59	29	
Am Biopark	30		57		17		37	57	17		37		57	17		37	57	17	37	57	17	37	57	30	00	30	00	30	
Otto-Hahn-Straße	32		59		19		39	59	19		39		59	19		39	59	19	39	59	19	39	59	32	02	32	02	32	
Universität (B) an	**34**		**01**		**21**		**41**	**01**	**21**		**41**		**01**	**21**		**41**	**01**	**21**	**41**	**01**	**21**	**41**	**01**	**34**	**04**	**34**	**04**	**34**	
Universität (B) ab	**34**		**02**		**22**		**42**	**02**	**22**		**42**		**02**	**22**		**42**	**02**	**22**	**42**	**02**	**22**	**42**	**02**	**34**	**04**	**34**	**04**	**34**	
OTH Regensburg	35		03		23		43	03	23		43		03	23		43	03	23	43	03	23	43	03	35	05	35	05	35	
Oberer kath Friedhof	36		05		25		45	05	25		45		05	25		45	05	25	45	05	25	45	05	36	06	36	06	36	
Evang. Zentralfriedhof	37		06		26		46	06	26		46		06	26		46	06	26	46	06	26	46	06	37	07	37	07	37	
HBF Süd/Arcaden	39		08		28		48	08	28		48		08	28		48	08	28	48	08	28	48	08	39	09	39	09	39	
Hauptbahnhof (A5) an	**42**		**11**		**31**		**51**	**11**	**31**		**51**		**11**	**31**		**51**	**11**	**31**	**51**	**11**	**31**	**51**	**11**	**42**	**12**	**42**	**12**	**42**	
Hauptbahnhof (A5) ab	**42**		**12**		**32**		**52**	**12**	**32**		**52**		**12**	**32**		**52**	**12**	**32**	**52**	**12**	**32**	**52**	**12**	**45**	**15**	**45**	**15**	**45**	
Dachauplatz	44		14		34		54	14	34		54		14	34		54	14	34	54	14	34	54	14	47	17	47	17	47	
Thundorferstraße	47		17		37		57	17	37		57		17	37		57	17	37	57	17	37	57	17	50	20	50	20	50	
Fischmarkt	48		18		38		58	18	38		58		18	38		58	18	38	58	18	38	58	18	51	21	51	21	51	
Keplerstraße	49		19		39		59	19	39		59		19	39		59	19	39	59	19	39	59	19	52	22	52	22	52	
Arnulfsplatz	**51**		**21**		**41**		**01**	**21**	**41**		**01**		**21**	**41**		**01**	**21**	**41**	**01**	**21**	**41**	**01**	**21**	**54**	**24**	**54**	**24**	**54**	
Ostdeutsche Galerie	53		23		43		03	23	43		03		23	43		03	23	43	03	23	43	03	23	56	26	56	26	56	
Hans-Sachs-Straße	54		24		44		04	24	44		04		24	44		04	24	44	04	24	44	04	24	57	27	57	27	57	
Obermaierstraße	55		26		46		06	26	46		06		26	46		06	26	46	06	26	46	06	26	58	28	58	28	58	
Dornierstraße	56		28		48		08	28	48		08		28	48		08	28	48	08	28	48	08	28	59	29	59	29	59	
Boessnerstraße	58		30		50		10	30	50		10		30	50		10	30	50	10	30	50	10	30	01	31	01	31	01	
Weinweg	59		31		51		11	31	51		11		31	51		11	31	51	11	31	51	11	31	02	32	02	32	02	
Westheim	00		32		52		12	32	52		12		32	52		12	32	52	12	32	52	12	32	03	33	03	33	03	
Westbad	02		34		54		14	34	54		14		34	54		14	34	54	14	34	54	14	34	05	35	05	35	05	
Wernerwerkstraße	**04**	**08**	**36**	**48**	**56**	**08**	**16**	**36**	**56**	**08**	**16**	**28**	**36**	**56**	**08**	**16**	**36**	**56**	**16**	**36**	**56**	**16**	**36**	**07**	**37**	**07**	**37**	**07**	
Hermann-Köhl-Straße		09		49		09				09		29			09														
Sparkasse		10		50		10				10		30			10														
Roter-Brach-Weg		11		51		11				11		31			11														
St. Bonifaz		12		52		12				12		32			12														
Deiningerstraße		13		53		13				13		33			13														
Rennplatz		**15**		**55**		**15**				**15**		**35**			**15**														

Gültig ab 15.04.2024

Bus stop „Thundorferstraße“ is close to site of conference dinner.

Line 11

City ⇒ University

Linie 11 — **Wernerwerkstraße - Arnulfsplatz - Hauptbahnhof - OTH - Universität - Burgweinting** — Bus

Montag - Freitag	5	6				7	8			9			10 - 17			18			19	20		21		22		23	0
Rennplatz			15		55	15			15	35		15															
Lilienthalstraße			17		57	17			17	37		17															
Heinkelstraße			18		58	18			18	38		18															
Wernerwerkstraße	**07**	**35**	**00**	**20**	**40**	**00**	**20**	**40**	**00**	**20**	**40**	**00**	**20**	**40**	**00**	**20**	**40**	**00**	**20**	**50**	**20**	**50**	**20**	**50**	**20**	**50**	**20**	
Wernerwerkstraße	07	35	00	20	40	00	20	40	00	20	40	00	20	40	00	20	40	00	20	50	20	50	20	50	20	50	20	
Westbad	08	36	01	21	41	01	21	41	01	21	41	01	21	41	01	21	41	01	21	51	21	51	21	51	21	51	21	
Westheim	09	37	02	22	42	02	22	42	02	22	42	02	22	42	02	22	42	02	22	52	22	52	22	52	22	52	22	
Weinweg	10	38	03	23	43	03	23	43	03	23	43	03	23	43	03	23	43	03	23	53	23	53	23	53	23	53	23	
Boessnerstraße	11	39	04	24	44	04	24	44	04	24	44	04	24	44	04	24	44	04	24	54	24	54	24	54	24	54	24	
Dornierstraße	13	41	06	26	46	06	26	46	06	26	46	06	26	46	06	26	46	06	26	56	26	56	26	56	26	56	26	
Obermaierstraße	14	42	08	28	48	08	28	48	08	28	48	08	28	48	08	28	48	08	28	58	28	57	27	57	27	57	27	
Hans-Sachs-Straße	15	43	09	29	49	09	29	49	09	29	49	09	29	49	09	29	49	09	29	59	29	58	28	58	28	58	28	
Ostdeutsche Galerie	16	44	11	31	51	11	31	51	11	31	51	11	31	51	11	31	51	11	31	01	31	59	29	59	29	59	29	
Arnulfsplatz	**19**	**47**	**14**	**34**	**54**	**14**	**34**	**54**	**14**	**34**	**54**	**14**	**34**	**54**	**14**	**34**	**54**	**14**	**34**	**04**	**34**	**02**	**32**	**02**	**32**	**02**	**32**	
Keplerstraße	20	48	15	35	55	15	35	55	15	35	55	15	35	55	15	35	55	15	35	05	35	03	33	03	33	03	33	
Fischmarkt	21	49	16	36	56	16	36	56	16	36	56	16	36	56	16	36	56	16	36	06	36	04	34	04	34	04	34	
Thundorferstraße	23	51	18	38	58	18	38	58	18	38	58	18	38	58	18	38	58	18	38	08	38	06	36	06	36	06	36	
Dachauplatz	26	54	21	41	01	21	41	01	21	41	01	21	41	01	21	41	01	21	41	11	41	09	39	09	39	09	39	
Hauptbahnhof (B4) an	|	|	|	|	|	|	|	|	|	|	|	|	|	|	|	|	|	|	**12**	**42**	**12**	**42**	**12**	**42**	
Hauptbahnhof (B4) ab	|	|	|	|	|	|	|	|	|	|	|	|	|	|	|	|	|	|	**15**	**45**	**15**	**45**	**15**	**45**	
Hauptbahnhof (B8) an	**29**	**56**	**23**	**43**	**03**	**23**	**43**	**03**	**23**	**43**	**03**	**23**	**43**	**03**	**23**	**43**	**03**	**23**	**43**	**13**	**43**	**15**	**45**	**15**	**45**	**15**	**45**	
Hauptbahnhof (B8) ab	**32**	**56**	**24**	**44**	**04**	**24**	**44**	**04**	**24**	**44**	**04**	**24**	**44**	**04**	**24**	**44**	**04**	**24**	**44**	**14**	**44**	**15**	**45**	**15**	**45**	**15**	**45**	
HBF Süd/Arcaden	33	57	25	45	05	25	45	05	25	45	05	25	45	05	25	45	05	25	45	15	45	16	46	16	46	16	46	
Evang. Zentralfriedhof	34	58	27	47	07	27	47	07	27	47	07	27	47	07	27	47	07	27	47	17	47	17	47	17	47	17	47	
Oberer kath Friedhof	36	00	29	49	09	29	49	09	29	49	09	29	49	09	29	49	09	29	49	19	49	18	48	18	48	18	48	
OTH Regensburg	37	01	30	50	10	30	50	10	30	50	10	30	50	10	30	50	10	30	50	20	50	19	49	19	49	19	49	
Universität (D)	**39**	**02**	**32**	**52**	**12**	**32**	**52**	**12**	**32**	**52**	**12**	**32**	**52**	**12**	**32**	**52**	**12**	**32**	**52**	**22**	**52**	**21**	**51**	**21**	**51**	**21**	**51**	
Otto-Hahn-Straße	41	04	34	54	14	34	54	14	34	54	14	34	54	14	34	54	14	34	54	24	54	23	53	23	53	23	53	
Am Biopark	42	05	36	56	16	36	56	16	36	56	16	36	56	16	36	56	16	36	56	26	56	24	54	24	54	24	54	
Franz-Hartl-Straße	43	06	37	57	17	37	57	17	37	57	17	37	57	17	37	57	17	37	57	27	57	25	55	25	55	25	55	
Johann-Hösl-Straße	44	07	39	59	19	39	59	19	39	59	19	39	59	19	39	59	19	39	59	29	59	26	56	26	56	26	56	
Schwabenstraße	45	08	40	00	20	40	00	20	40	00	20	40	00	20	40	00	20	40	00	30	00	27	57	27	57	27	57	
Schöneberger Straße	46	09	41	01	21	41	01	21	41	01	21	41	01	21	41	01	21	41	01	31	01	28	58	28	58	28	58	
Benzstraße	47	10	42	02	22	42	02	22	42	02	22	42	02	22	42	02	22	42	02	32	02	29	59	29	59	29	59	
Burgweinting Kirche	49	12	44	04	24	44	04	24	44	04	24	44	04	24	44	04	24	44	04	34	04	31	01	31	01	31	01	
Burgw. Fr.-Viehbacher-Allee	50	13	46	06	26	46	06	26	46	06	26	46	06	26	46	06	26	46	06	36	06	32	02	32	02	32	02	
Burgw. Kurzer Weg	51	14	48	08	28	48	08	28	48	08	28	48	08	28	48	08	28	48	08	38	08	33	03	33	03	33	03	
Burgw. Droste-Hülshoff-Weg	52	15	49	09	29	49	09	29	49	09	29	49	09	29	49	09	29	49	09	39	09	34	04	34	04	34	04	
Burgw. Langer Weg	53	16	50	10	30	50	10	30	50	10	30	50	10	30	50	10	30	50	10	40	10	35	05	35	05	35	05	
Burgw. Sophie-Scholl-Str.	54	17	51	11	31	51	11	31	51	11	31	51	11	31	51	11	31	51	11	41	11	36	06	36	06	36	06	
Burgw. Herm.-Höcherl-Str.	**56**	**19**	**53**	**13**	**33**	**53**	**13**	**33**	**53**	**13**	**33**	**53**	**13**	**33**	**53**	**13**	**33**	**53**	**13**	**43**	**13**	**38**	**08**	**38**	**08**	**38**	**08**	

Bus stop „Thundorferstraße“ is close to site of conference dinner.

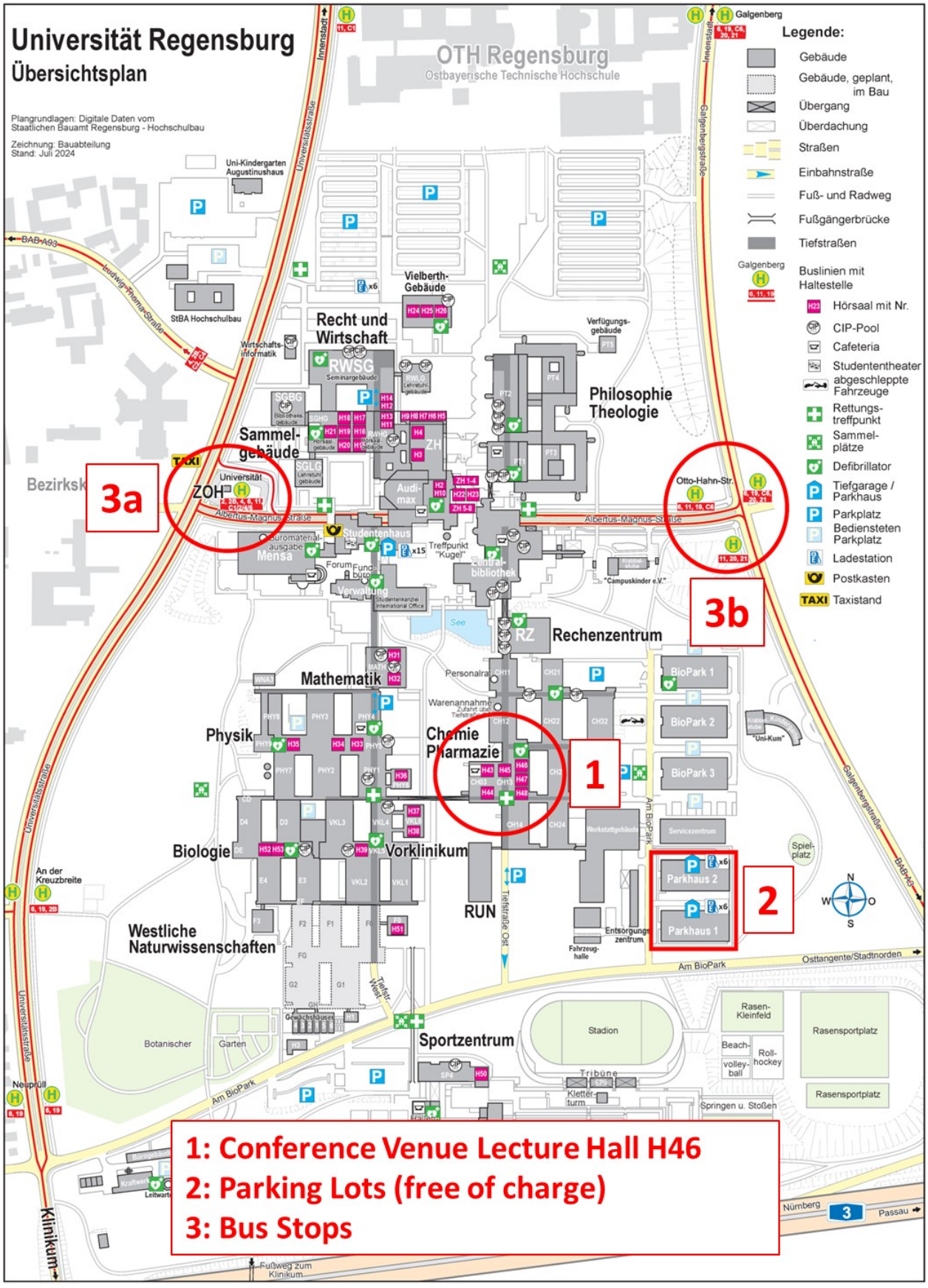
Universität Regensburg
Übersichtsplan
Plangrundlagen: Digitale Daten vom Staatlichen Bauamt Regensburg - Hochschulbau
Zeichnung: Bauabteilung
Stand: Juli 2024
OTH Regensburg
Ostbayerische Technische Hochschule
Legende:
Gebäude
Gebäude, geplant, im Bau
Übergang
Überdachung
Straßen
Einbahnstraße
Fuß- und Radweg
Fußgängerbrücke
Tiefstraßen
Buslinien mit Haltestelle
Hörsaal mit Nr.
CIP-Pool
Cafeteria
Studententheater
abgeschleppte Fahrzeuge
Rettungs-treffpunkt
Sammel-plätze
Defibrillator
Tiefgarage / Parkhaus
Parkplatz
Bediensteten Parkplatz
Ladestation
Postkasten
Taxistand
Recht und Wirtschaft
RWSG
Vielberth-Gebäude
Philosophie Theologie
Sammel-gebäude
ZH
ZOH
Universität
Audi-max
Mensa
Studentenhaus
Zentral-bibliothek
RZ
Rechenzentrum
Mathematik
Physik
Chemie Pharmazie
Biologie
Vorklinikum
RUN
Westliche Naturwissenschaften
Sportzentrum
Stadion
Rasen-Kleinfeld
Rasensportplatz
Beach-volley-ball
Roll-hockey
Springen u. Stoßen
BioPark 1
BioPark 2
BioPark 3
Parkhaus 1
Parkhaus 2
Servicezentrum
Entsorgungszentrum
Fahrzeug-halle
Werkstattgebäude
Uni-Kindergarten Augustinushaus
StBA Hochschulbau
Wirtschafts-informatik
Verfügungs-gebäude
Otto-Hahn-Str.
Albertus-Magnus-Straße
Universitätsstraße
Innerstadt
Galgenbergstraße
Ludwig-Thoma-Straße
BAB A93
BAB A3
An der Kreuzbreite
Neuprüll
Klinikum
Am BioPark
Osttangente/Stadtnorden
Nürnberg
Passau
Fußweg zum Klinikum
Botanischer Garten
Gewächshäuser
Tiefstr. West
Tiefstraße Ost
Spiel-platz
3a
3b
1
2
1: Conference Venue Lecture Hall H46
2: Parking Lots (free of charge)
3: Bus Stops